



LONG-TERM MORPHOLOGY OF THE EASTERN SCHELDT



Auteur: C. de Bok

Werkdocument RIKZ/2002.108x

Cover: The Eastern Scheldt Storm Surge Barrier during a storm surge
(photograph courtesy of RWS-Meetskundige Dienst)



LONG-TERM MORPHOLOGY OF THE EASTERN SCHELDT

Auteur: C. de Bok

werkdokument RIKZ/2002.108x

augustus 2001

Preface

.....

This study is done within the framework of my final thesis for my study Applied Earth Sciences at the Delft University of Technology. From November 2000 to August 2001 this study was performed at the National Institute for Coastal and Marine Management/RIKZ in the Hague. This study is a part of the project K2005*voordelta led by dr. Ir. J.M.T. Stam.

I would like to thank my Examination Committee, Prof. dr. A.K. Turner, dr. Ir. J.M.T. Stam, P.M. Maurenbrecher M.Sc, dr. H.R.G.K. Hack and dr. Ir. J. van de Graaff, with special thanks to dr. Ir. J.M.T. Stam for her daily support. I would also like to thank E.J. Biegel for his crash course GIS. I would like to thank P. van der Weijde and I. Schep for their help in finding the discharge data buried deep within the attic of the "Meetdienst Zeeland" Flushing. I would like to thank J. Cleveringa for his creativity with graphics. I would like to thank S.C. Vardy for his support with the English language. Last but not least, all the people on my floor at RIKZ the Hague who patiently answered all my small and big questions.

Abstract

The purpose of this work is to increase our understanding of the long-term morphological consequences of major human interventions in the coastal area. This will enable better predictions of the consequences of large-scale future interventions in tidal basins and estuaries.

This study focuses on the effects of the closure of a tidal inlet in the southwestern part of The Netherlands: the Eastern Scheldt, during 1972-1986. An analysis of morphological and hydrodynamic parameters have been carried out to see if the Eastern Scheldt system has reached morphological stability after the closure works.

For this the development of the following morphological and hydrodynamic parameters has been evaluated and compared:

- tidal volume
- tidal prism
- cross-sectional area of the inlet
- basin volume
- volume of the outer tidal delta

Discharge data and bathymetric soundings between 1960 and 1996 have been used for a reconstruction of the evolution of the parameters.

Equilibrium relationships between tidal prism and inlet cross-sectional area, and tidal prism and sand volume of the outer tidal delta present the final situation of the parameters.

The comparison of the parameters shows that the basin volume does not change, but redistribution of the sediment in the basin results in sedimentation in the channels and erosion in the inter-tidal area, until equilibrium velocities are reached. It will take more than 11 years before the outer tidal delta of the Eastern Scheldt reaches equilibrium.

The equilibrium relationship between tidal prism and cross-sectional area shows that the tidal volume and tidal prism should decrease with 77 %. This means that the final equilibrium situation in the inlet at the storm surge barrier location will only be reached after a very long period. The equilibrium relationship for the sand volume of the outer tidal delta cannot be used, due to a large difference in sand volumes caused by the different calculation methods of the sand volumes.

Without human interference (decreasing the basin area by building dams) the system will never reach equilibrium, because the inlet will never reach an equilibrium situation. The other parameters already have reached an equilibrium or will reach an equilibrium within 20 years or more.

Future studies with more digital bathymetric data of the basin can give more insight and enable predictions on the equilibrium situation of the basin.

Contents

Preface	1
Abstract	3
1 Introduction	9
2 Description of Study Area	11
2.1 The History of the Southwest Part of The Netherlands	11
2.1.1 Natural Coastal Evolution from the Pleistocene to 200 AD	13
2.1.2 Human Intervention from 200 AD to 1953 AD	15
2.1.3 The Delta Project from 1953 to present	17
2.1.4 The Eastern Scheldt Storm Surge Barrier	19
2.2 The Geological Characteristics of the Eastern Scheldt Outer Tidal Delta	21
2.3 Hydrodynamics of the Eastern Scheldt Tidal Basin	23
2.3.1 Tide	23
2.3.2 Waves	27
2.3.3 River Discharges	27
3 Study Method	29
3.1 Data Description	31
3.1.1 Hydrodynamic Data	31
3.1.2 Bathymetric Data	31
3.2 Data Preparation	33
3.2.1 Grids Covering the Outer Tidal Delta and Inlet	33
3.2.2 Grids Covering the tidal basin	33
3.3 Calculations with the Data	33
3.3.1 Computing the Tidal Volumes Passing Through the Eastern Scheldt Inlet	35
3.3.2 Computing the Tidal prism	35
3.3.3 Computing the Cross-sectional Area of the Eastern Scheldt Inlet	35
3.3.4 Calculating the Volume of the Eastern Scheldt Basin	35
3.3.5 Calculating the Volume of Outer Tidal Delta	37
3.4 Evaluation of the Data	37
3.4.1 Evaluation of Development Over Time	39
3.4.2 Evaluation Using Empirical Equilibrium Relationships	39
4 Theoretical Large-scale Relationships for Tidal Basins and Estuaries	41
4.1 Definitions and Conceptual System	41
4.2 Empirical Relationships	45
4.2.1 Tidal Prism and Cross-sectional Area of the Inlet	45
4.2.2 Tidal Prism and Sand Volume of the Outer Tidal Delta	49

5	Application to the Eastern Scheldt	51
5.1	Expected Changes of the System During the Delta Project	51
5.1.1	Changes Prior to 1969	51
5.1.2	Changes in the Period 1969 - 1977	51
5.1.3	Changes in the Period 1977 - 1986	53
5.1.4	1986 - future; equilibrium	55
5.2	Development of Tidal Volume	61
5.2.1	Tidal Volumes through the Individual Channels	61
5.2.2	Tidal Volume through the Total Inlet	63
5.3	Development of the Tidal Prism	65
5.3.1	Tidal Amplitude	65
5.3.2	Computing the Tidal Prism	67
5.4	Computing the Cross-sectional Area of the Eastern Scheldt Inlet	69
5.4.1	Comparison with Cross-sectional Areas Calculated by Haring (1978)	69
5.4.2	Other Profiles	71
5.4.3	The Dam Location	71
5.5	Calculation of the Volume of the Eastern Scheldt Basin	73
5.6	Calculation of the Volume of the Outer Tidal Delta	75
5.6.1	Haring's (1948) Standard Compartments	75
5.6.2	Morphological Boundaries	77
5.6.3	Discussion on the Calculation Boundaries	79
5.6.4	Resulting Volume Calculations	81
6	Discussion of Results	83
6.1	Development of Eastern Scheldt; 1820 - Equilibrium Situation	83
6.1.1	Natural Development of the Tidal Volume between 1820 and 1969	85
6.1.2	Effects of an Increasing Tidal Volume in the Period 1969 - 1977	87
6.1.3	Effect of a Decreasing of Tidal Volume in the Period 1977 - 1986	89
6.1.4	Changes after Completion of the Delta Works (1986 – present)	91
6.2	Equilibrium Relationships	93
6.2.1	Tidal Prism Versus Cross-sectional Area of the Inlet	93
6.2.2	Tidal Prism versus Sand Volume of the Outer Tidal Delta	95
7	Conclusions and Recommendations	97
7.1	Conclusions	97
7.2	Recommendations	99
8	References	101

1 Introduction

Several large structures in the southwestern coastal area of The Netherlands, including the various dams of the Delta Project, have been erected. These have radically changed the coastal morphology. Several other projects, such as land reclamation for industrial purposes and the reopening of closed tidal inlets, are still under discussion. Assessment of such projects requires good predictions of the morphological and hydrological changes caused by large coastal engineering structures. Studies of the hydrological and morphological effects caused by large coastal engineering structures constructed in the past will contribute to a better understanding of these effects, and they will in turn, result in better predictions of the consequences of large future interventions.

The Eastern Scheldt area is a good example of an altered coastal environment, due to the construction of large dams. Of all the closed tidal estuaries in the southwest of The Netherlands, the Eastern Scheldt is the only tidal basin that remains in contact with the North Sea. A study on the Eastern Scheldt system will improve our understanding of tidal systems.

This study focuses on the development of the coastal morphology of the Eastern Scheldt system, the changes in morphology due to the Delta Project, its present morphological state, and the development of the coastal morphology in the future.

The main question is whether the system has reached large-scale equilibrium and what time scales and driving forces are involved.

To be able to answer these questions, several methods based on bathymetric data covering a time span of 38 years are used. These methods include:

- a) Volumetric calculations of the basin and outer tidal delta
- b) Determination of empirical relations between morphological units (such as outer tidal delta, inlet cross-section and basin volume), and
- c) Analysis of sea bed profiles.

Chapters 2, 3 and 4 contains the information available in the literature necessary for this study. Chapter 5 discusses the available data, such as tidal volume, tidal prism, volume of basin, cross-section of the inlet and volume of the outer tidal delta. In Chapter 6 these data are used to determine the equilibrium state of the separate units using the empirical relationships. The fourth section (Chapter 7) discusses the results of Chapter 6 to derive an answer to the main question.

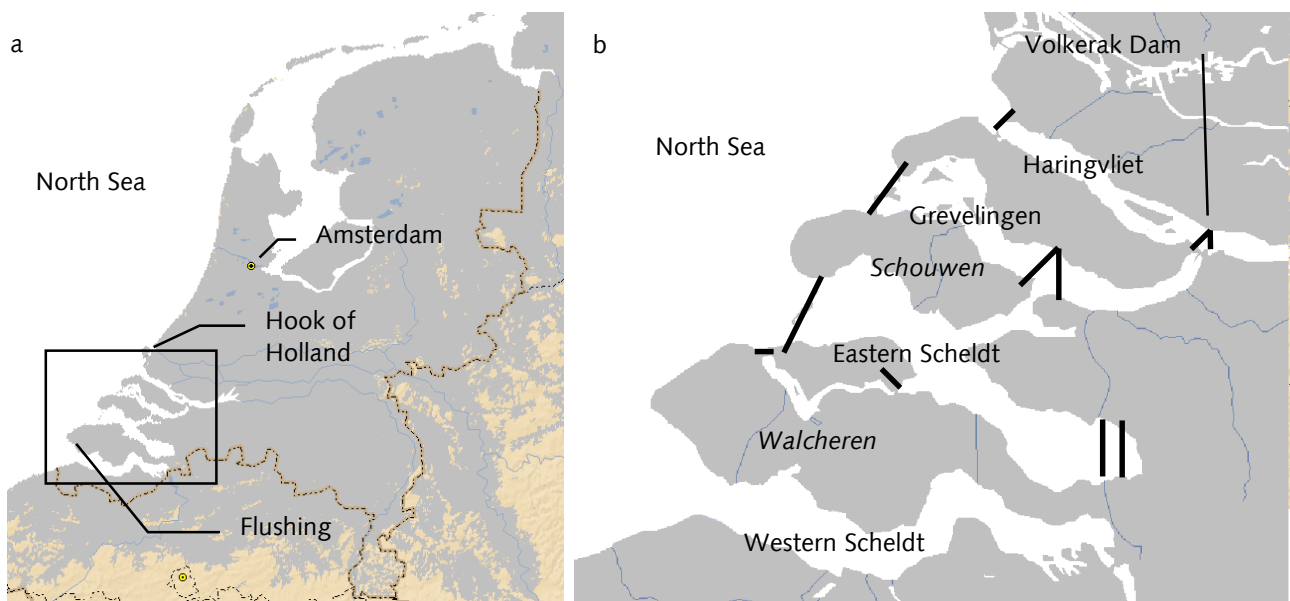


Figure 2.1: Location maps. (a) The Netherlands, (b) province of Zeeland with the dams of the Delta Works.

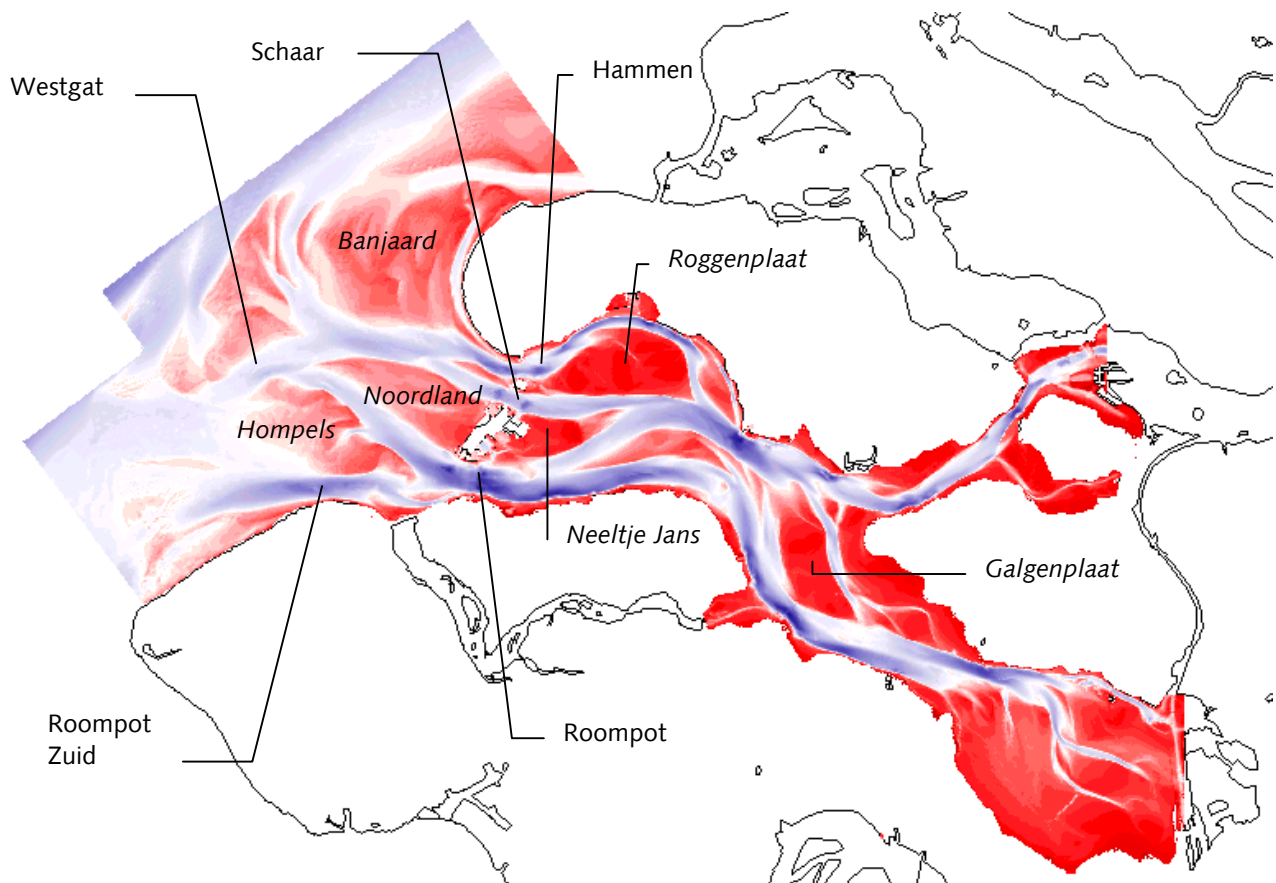


Figure 2.2: The study area the Eastern Scheldt. (channel names are in normal type and the sandy shoal names are in italics.)

2 Description of Study Area

The study area is situated in the southwest of The Netherlands (Figure 2.1a). The Netherlands is bordered by Germany to the east, Belgium to the south, and the North Sea to the west and north. The southwestern Netherlands is characterised by three tidal basins and one estuary separated by series of former islands (Figure 2.1b). The coastline of these islands is made up of narrow sandy beaches, protected by groins, behind which dikes have been raised to protect the hinterland. Most parts of the former islands lie beneath sea level. The North Sea offshore from the southwestern Netherlands is relatively shallow, with a maximum depth of approximately 35 m, and the seabed is covered with sandy sediment. The actual study area consists of the Eastern Scheldt area, which comprises the Eastern Scheldt basin and outer tidal delta (Figure 2.2).

A major storm surge in 1953 flooded a large part of the southwest of the Netherlands, and caused much damage and several deaths. In response to this catastrophe the Delta Project was developed, which ultimately closed three of the four inlets. The Delta Project will be discussed in detail in Section 2.1.3.

Originally the Eastern Scheldt was a tidal estuary, transporting the river discharges from the Rhine/Maas and the Scheldt to the North Sea. In 1867 one of the remaining two connection between the Eastern and Western Scheldt was closed, cutting of the Scheldt from its northern connection with the open sea. In 1969, when the Volkerak Dam was finished, the Rhine discharge was also cut off from the Eastern Scheldt and the flow became regulated by sluices. The Eastern Scheldt was turned into a tidal basin.

The basin is now confined by several islands and two compartmentalisation dams. The Eastern Scheldt Storm Surge Barrier is situated across the inlet of the Eastern Scheldt. The Eastern Scheldt basin contains meandering channels and tidal flats and is approximately 50 km long (measured from the location of the Eastern Scheldt Barrier). Before closure, the basin was 55 km long. The inlet width of the Eastern Scheldt is 7.5 km and at its widest point the basin is 10.5 km. The channels at the inlet are 21 to 31 m deep.

The outer tidal delta consists of a network of ebb and flood dominated channels and sandy shoals that extend up to 15 km into the North Sea. The channels in the outer tidal delta can reach a depth of 37 meters below NAP. The tops of the tidal flats are typically located between 1 and 3 meters below NAP.

2.1 The History of the Southwest Part of The Netherlands

Over a period of 11000 years the southwestern part of The Netherlands changed from a polar desert to a marine tidal-flat area around 4400 BC, and then to a swampy area around 2500 BC, and finally reverted to a tidal area again around 350 AD. This evolution in the first 9200 years was caused by natural phenomena, but since 200 AD the development became increasingly affected by human interference.

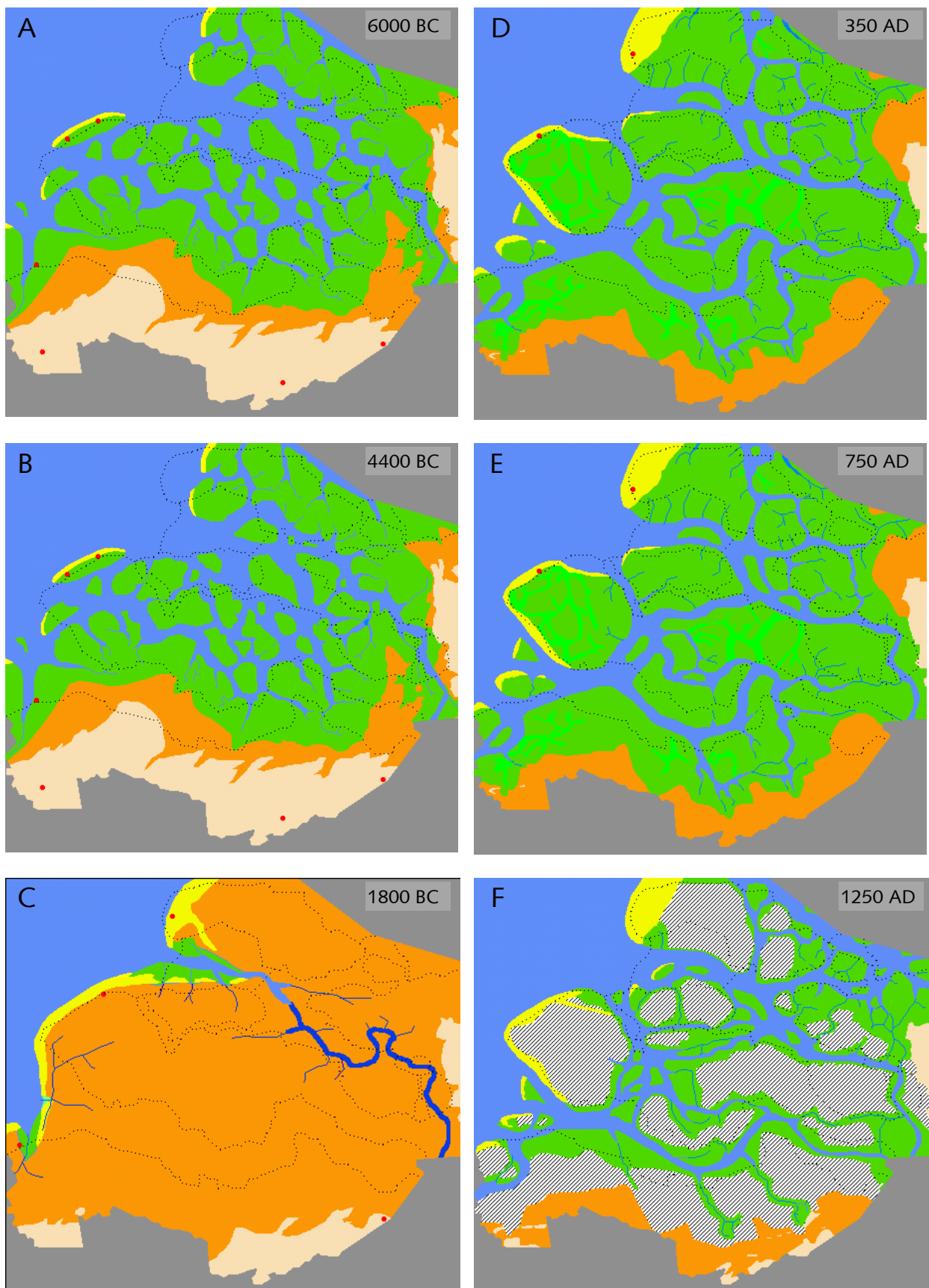


Figure 2.3: The development of the Southwest of the Netherlands from 6000 BC to 1950 AD and the sealevel rise graph (9000 BP is 7000 BC) (NITG-TNO, 1997). Figure continues on page 6.

The following sections first describe the natural evolution to the swampy conditions of 2500 BC, then the coastal evolution back to a tidal delta area as a result of human interference is discussed. These two sections are mainly based on "De ontstaansgeschiedenis van het Zeeuwse kustlandschap" (NITG-TNO, 1997).

Subsequent sections describe the overall Delta Project and the construction of the Eastern Scheldt storm surge barrier. These section are mainly based on the series "drie maandelijks bericht Deltawerken".

Figure 2.3 illustrates nine evolutionary stages of this coastal region up to the present day. The letters in the text refer to the letters defining these nine maps of Figure 2.3. Figure 2.3 also shows a graph with the development of the water level from 8000 BC to 2000 AD.

2.1.1 Natural Coastal Evolution from the Pleistocene to 200 AD

The situation in the Weichselien (110,000 - 9000 BC), at the end of the Pleistocene, was very different from the present situation. During the last Ice Age, the present North Sea basin was dry and consisted of either exposed frozen tundra or continental ice sheets. The southwestern parts of The Netherlands were a polar desert. After the last Ice Age, the Earth's temperature rose again, causing the glaciers and frozen ground to melt. At this time, due to glacial loading, the land surface around the Eastern Scheldt inlet and outer tidal delta lay more than 8 meters below the current elevations in the south and more than 12 meters below the current levels in the North.

Melting of the continental ice sheets caused a global sea level rise. Due to the fact that this sea-level rise occurred much more rapidly than the eustatic rebound of the land surface due to glacial unloading, a complex cycle of marine transgressions occurred. By 9000 BC (the beginning of the Holocene), the shoreline of the North Sea had reached the western part of Schouwen. The river the Scheldt joined the Rhine/Maas river system more to the north than it does now. This was partly due to a barrier.

By 6700 BC, the southwestern portions of The Netherlands were characterised by an extensive tidal area containing a lagoon and coastal swamps. Extensive tidal flats and a low tidal range of 1 meter resulted in a low sedimentation rate that could not keep up with the rate of sea level rise, so lagoons could form (A). The course of the Scheldt remained fairly stable during the period 9000 - 6700 BC.

Due to further rise in sea level, the river Scheldt channel migrated so that it flowed directly into the sea after 6700 BC, through a brackish estuary surrounded by lagoons and tidal areas. The lagoons disappeared following 5500 BC, due to a slower rise in sea level.

In 4400 BC the transgression reached its maximum. Almost all of the southwestern portions of The Netherlands were a tidal area ringed with coastal peat swamps (B).

A period of regression started around 3100 BC because sedimentation rates increased and were sufficient to cause the land surface to increase more rapidly than the rise in sea level. By 2500 BC the whole area had changed into a swamp area (C) protected by sand dunes, with the Scheldt river flowing through the area directly into the North Sea. The main inlet of the Scheldt was situated at the present location of the inlet of the Eastern Scheldt and it has stayed at this location until the present.

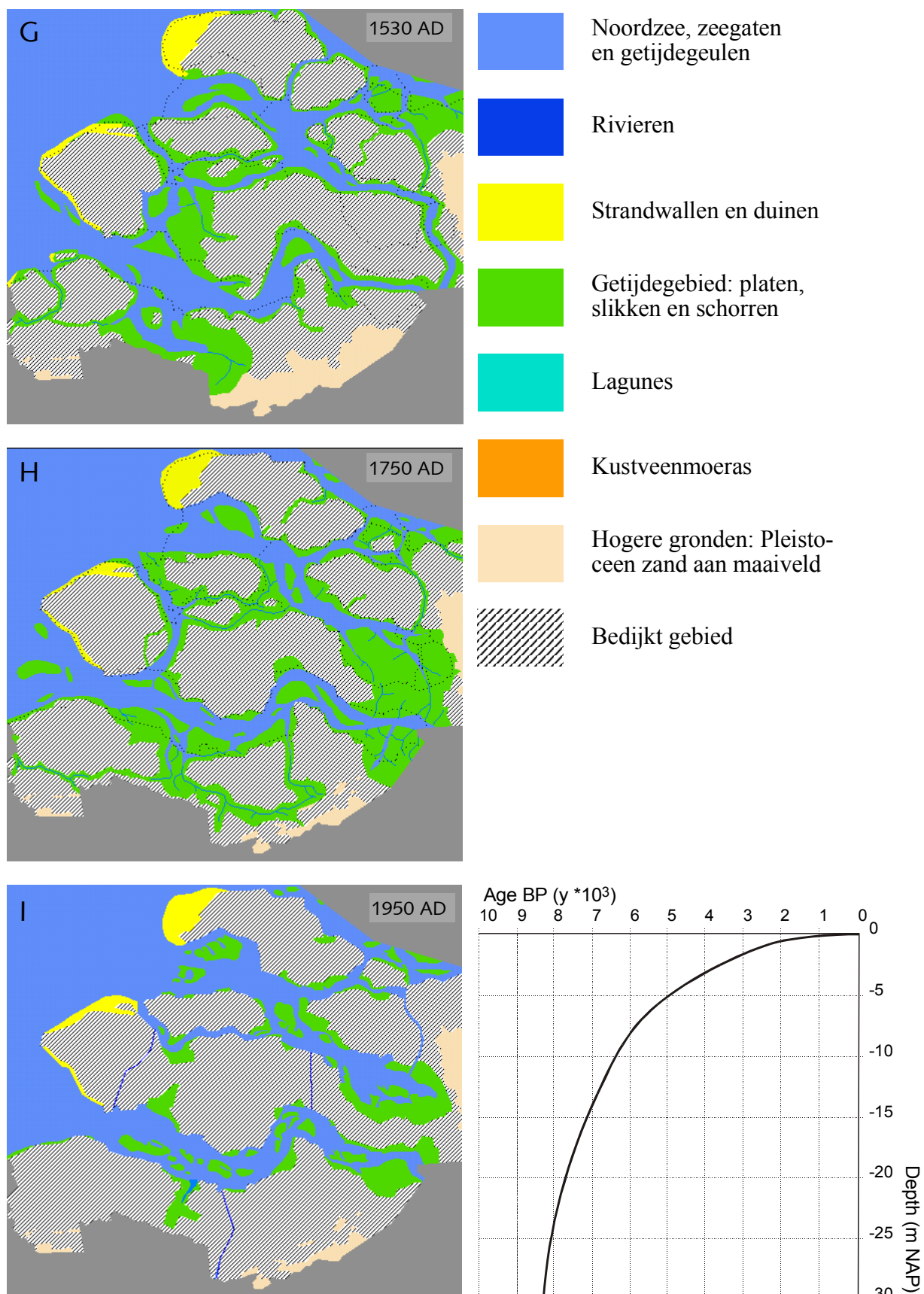


Figure 2.3: The development of the Southwest of the Netherlands from 6000 BC to 1950 AD and the sealevel rise graph (9000 BP is 7000 BC) (NITG-TNO, 1997).

The area did not change significantly in the following centuries. Beginning around 500 BC the first noticeable increases in marine influence occurred with the formation of small tidal areas at the mouth of the Scheldt and behind the sand dunes.

2.1.2 Human Intervention from 200 AD to 1953 AD

Beginning around 200 AD, the Romans settled in the peat swamps of this region. They drained the land to make it inhabitable. This caused the area to settle. After 300 AD the process of peat consolidation caused the land surface settlement to become great enough to cause the swamps to revert into a tidal area with flats and channels. By about 350 AD (D) the tidal regime was well established and the inlet of the Eastern Scheldt had become wider.

In the period from 350 AD to about 1000 AD, the channels slowly migrated as old channels silted up and new channels were formed and the region changed again slowly into a marsh area.

Around 1000 AD people started to live on the salt marshes. In the 11th and 12th centuries the inhabitants started to build dikes to protect themselves against floods. Within about 100 years all the salt marshes were surrounded by dikes (E).

In the following periods the inhabitants started to exploit large peat areas and also to drain areas. Both these actions caused renewed land surface subsidence. Continuing rising sea levels and storm surges caused the poorly maintained dikes to break. A large part of Zeeuws Vlaanderen was lost during storms in 1375, 1376 and 1404.

In 1531 the eastern part of Zuid-Beveland was flooded (G and H). This caused the tidal divide between the Eastern and Western Scheldt to shift to the North and changed the course of the Scheldt so that it flowed mainly through the Western Scheldt instead of the Eastern Scheldt.

The tidal divide between the Eastern and Western Scheldt silted up and was closed in 1867 with the Kreekrak Dam. The last hydraulic connection between the Eastern and Western Scheldt was closed in 1871 with the completion of the railway embankment along the Sloe Dam (Figure 2.4).

**Figure 2.4**

The locations of the dams in the southwest of The Netherlands. The names of the dams with the corresponding numbers are given in Table 2.1.

Number	Date of completion	Dam Name
1	1867	Kreekrak Dam
0	1871	Sloe Dam
2	1960	Zandkreek Dam
3	1961	Veerse Gat Dam
4	1965	Grevelingen Dam
5	1969	Volkerak Dam
6	1970	Haringvliet Dam
7	1971	Brouwers Dam
10	1983	Markiezaats quay
8	1986	Eastern Scheldt Storm Surge Barrier
9	1986	Philips Dam
11	1986	Oester Dam

Table 2.1

The year of completion of the works in the Southwest of the Netherlands. The location is indicated with the corresponding number in Figure 2.4.

2.1.3 The Delta Project from 1953 to present

The great storm, which raged during the night of the 31st of January, 1953 and into the 1st of February, 1953, left large parts of the southwestern Netherlands flooded. This catastrophe marked the birth of the Delta Project. The Delta Project was aimed at increasing the safety of the area by protecting it against flooding. To this purpose, several options were considered. Raising all the dikes was one option, but this was very expensive and would have to be repeated if the water level continued to rise. The best option was to shorten the coastal length by closing three of the four tidal inlets (the Haringvliet, the Grevelingen, and the Eastern Scheldt) leaving only the southernmost inlet (the Western Scheldt) open as a harbour entrance to Antwerp. The closure of inlets would shorten the coastline from more than 700 km to just 25 km, avoiding expensive dike adaptations. The law establishing the Delta Project was accepted by the Dutch -parliament on the 5th of November 1957.

The Delta Project began with the closure of the Veerse Gat by constructing the Zandkreek Dam (2) and Veerse Gat Dam (3). This left a fresh water basin in its place.

The next step was the construction of the Grevelingen Dam (4), completed in 1965. This dam was built on a tidal divide in the Grevelingen estuary, and so the dam cut off Rhine/Maas river discharge through the Grevelingen, turning the Grevelingen estuary into a tidal basin.

In 1969 the Haringvliet estuary was also changed into a tidal basin by the construction of the Volkerak Dam (5). The Volkerak Dam contains sluices to allow regulated water discharges from the Rhine/Maas.

Closure of the inlets to the two northern tidal basins with the Haringvliet Dam (6) in 1970 and the Brouwers Dam (7) in 1971, changed the Haringvliet and Grevelingen tidal basins into fresh water lakes.

During the 1970's, public pressure and the growing environmental awareness caused the redesign of the proposed Eastern Scheldt Dam, the last dam to be constructed in Zeeland. The new design involved a "Storm Surge Barrier", that would only be closed during periods of high water. To preserve specified important ecological environments, the tidal amplitude had to be substantially maintained. It was recognised that the storm surge barrier, even when open, would cause a restriction in tidal volumes, and hence a reduction in the tidal amplitudes within the basin, unless countermeasures were undertaken.

Accordingly two compartmentalisation dams were built, the Philips Dam (9) in 1986 and the Oester Dam (11) in 1986. These served to reduce the volume of the basin and so partially compensate for the reduced tidal volumes passing through the storm surge barrier, and so maintain most of the tidal amplitude within the basin. The Eastern Scheldt Storm Surge Barrier (8) was finished in 1986.

The Delta project was finished with an additional storm surge barrier across the New Waterway in 1997. Figure 2.4 shows the locations of all these dams. Table 2.1 defines the dams and provide their dates of completion.

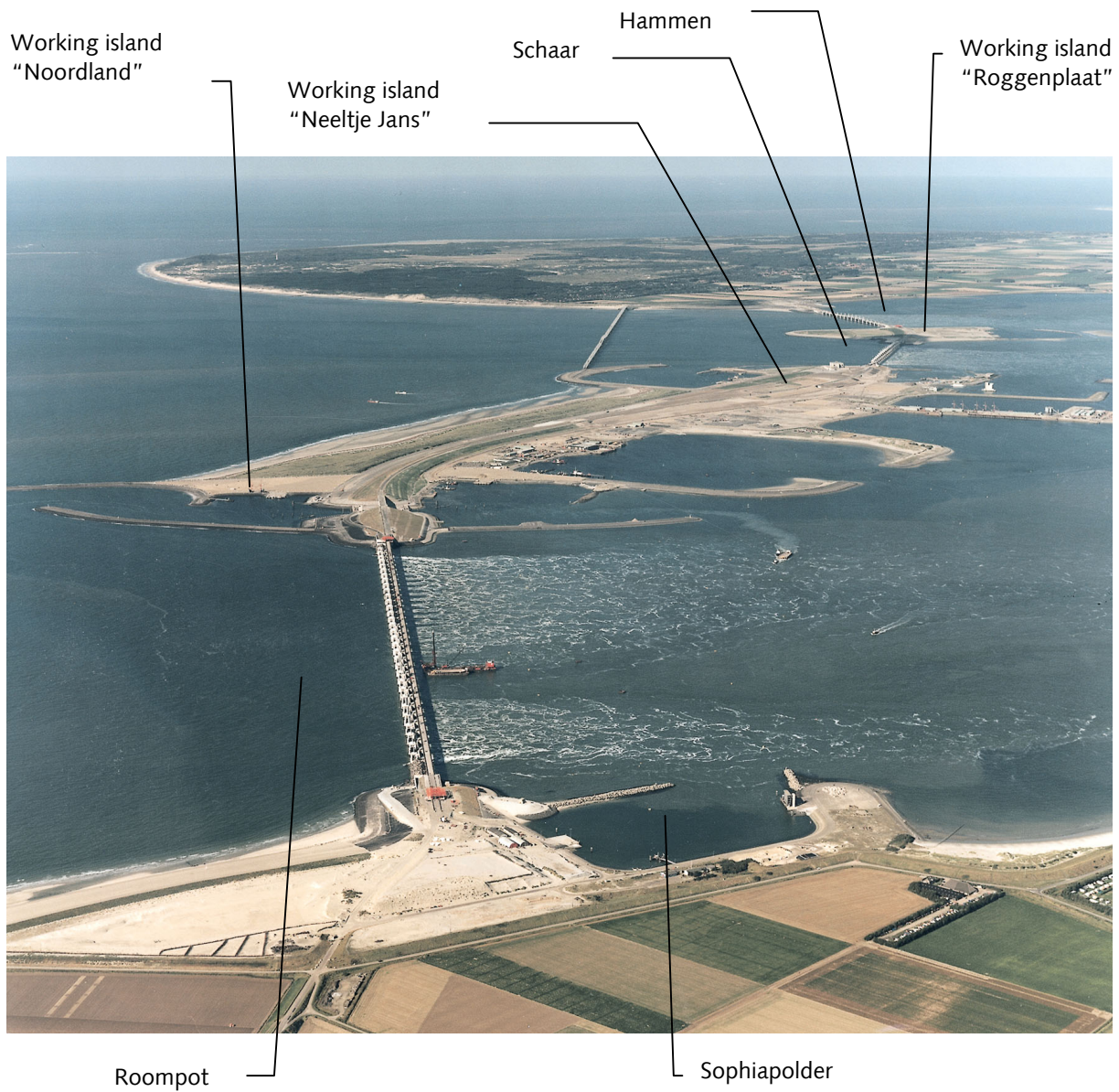


Figure 2.5: An aerial photograph of the Eastern Scheldt storm surge barrier with the channel "Roompot" in the front and in the back the channels "Schaar" and "Hammen" (photograph courtesy of RWS-Meetskundige Dienst).

2.1.4 The Eastern Scheldt Storm Surge Barrier

The Eastern Scheldt Storm Surge Barrier was the last dam to be built in Zeeland. Because of the large tidal volumes that flow through the selected location, this dam was the most difficult one to close and was left to the last. The tidal volume at the inlet to the Eastern Scheldt is 1100 million cubic meters. This is almost four times as great as the 300 million cubic meters of the Grevelingen. The experience gained with the construction of the previous dams was used during the construction of the storm surge barrier. With such a structure, the closure of the Eastern Scheldt inlet was to start in 1969 and was to have been finished in 1978. However, as discussed below, increasing public awareness of environmental consequences of a traditional dam, caused the proposed design to be withdrawn and a new storm surge barrier to be designed instead.

The research necessary to construct the original dam started immediately after the acceptance of the law providing the Delta Project in 1957. Since 1959 preparatory work was carried out, including hydraulic measurements and the collection of soil samples. The first two working harbours were constructed -- the Schelphoek (1967-1968) and the Sophia-polder (1968-1969) (Figure 2.5).

Meanwhile a location for the dam was chosen. The location had to be suitable for first building the dam on the shallow parts and then in the channels. This had to be done without changing the flow velocities, as higher velocities and different flow directions would make the closure of the channels more difficult. Other aspects involved were the stability of nearby shorelines, the wave height (for the working ships), the length of coast protected after construction, soil mechanics considerations, costs and feasibility. The location of the dam was officially accepted on the 22nd of January of 1969.

After having established the location of the dam the construction of the dam could start. The first construction steps were (see locations on Figure 2.5):

- Development of a "working island" on the tidal flat "Roggeplaat" (April 1969 to April 1970)
- Development of a "working island" and "working harbour" called "Neeltje Jans" (March 1970 to the beginning of 1971)
- Development of the "working island" called "Noordland" (April 1971 to the beginning of 1972)
- Closure of the Geul channel with sand (June 1972 to September 1972)

Due to the increasing awareness of environmental issues a committee was formed in August 1973 to find a better solution for the closure of the Eastern Scheldt -a solution that would better satisfy the interests of both safety and environment. During this time, work continued on stabilising and protecting the seabed across the inlet, especially in the channels Roompot, Hammen and Schaar van Roggeplaat (further referred to as "Schaar"). At the end of 1974 work on the Eastern Scheldt ceased, because the debate concerning the merits of an open or closed Eastern Scheldt estuary had not been concluded. In March 1974 the parliamentary committee proposed a semi-closed dam (or storm surge barrier) as the best way to fulfil both environmental and safety requirements. This also included two compartmentalisation dams. The Dutch Parliament agreed on the semi-closed dam with two compartmentalisation dams, one, the Oester Dam in the back of the basin and one the Philips Dam at the location of the Grevelingen Dam.

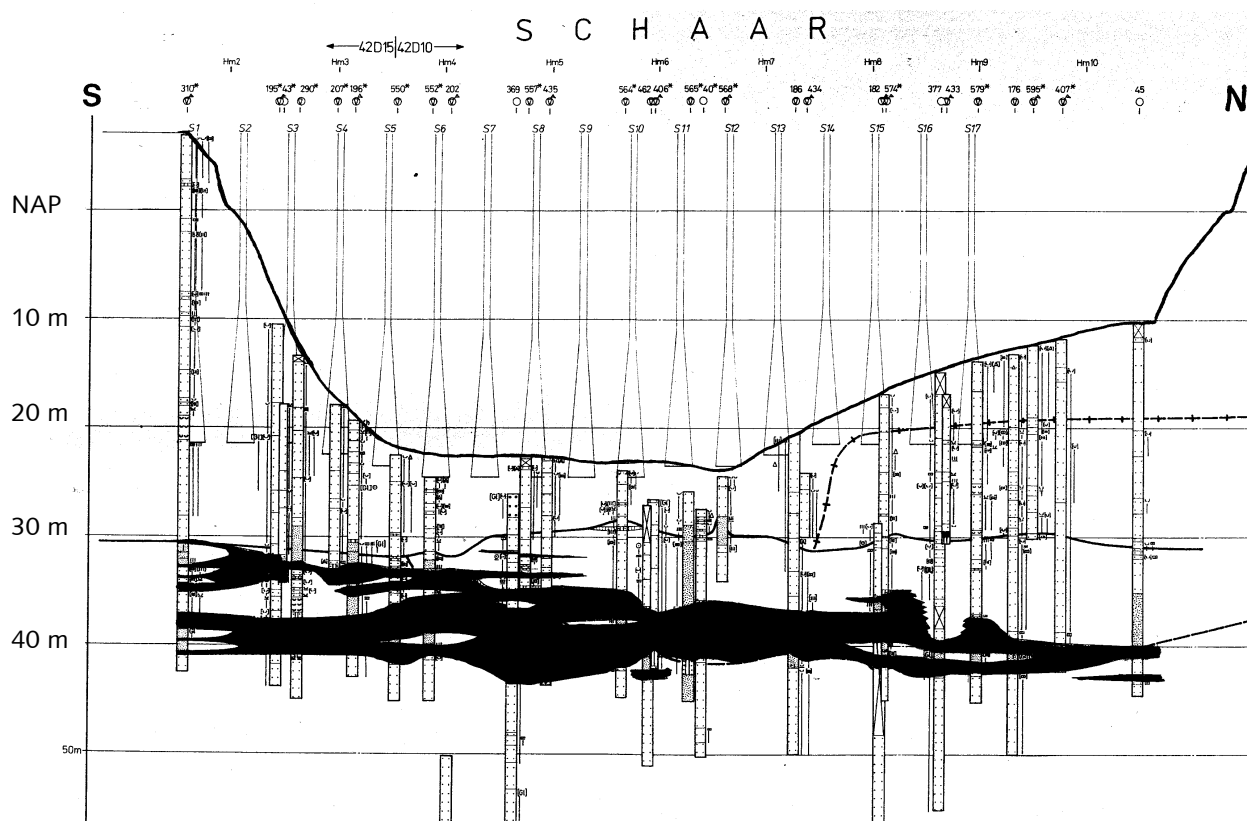


Figure 2.6: The geological cross-section of the Schaar (Figure 2.2), with clay layers in black and sand layers in white (Rijks Geologische Dienst, 1980)

The new storm surge barrier design consisted of piers with gates in between, which would provide storm protection, while also maintaining the tidal character of the Eastern Scheldt basin. This design required a totally different construction method and required new research on soil mechanics, hydraulics and constructional aspects. The previously installed seabed protection had to be removed at the pier locations to allow construction of foundation pits for the piers. This removal started on 7 September 1976. Meanwhile, seabed protection continued at other locations.

The first piers were placed in the Hammen in August 1983, starting from the middle of the channel and proceeding toward the shores. By mid November 1983, all the piers were placed in the Hammen. The piers in the Schaar were placed from the end of February 1984 to mid April 1984. The placing of the piers in the Roompot channel followed immediately, and the last pier was placed on 19 September 1984.

The gates in the Hammen were placed from the end of August to the end of November, 1984. Some of the gates in the Schaar were also placed during this period. Due to a production problem, the placing of the remaining gates was delayed, but this was finally completed in early 1986.

On 6 October 1986, Her Majesty, Queen Beatrix, officially opened the Eastern Scheldt Storm Surge Barrier.

2.2 The Geological Characteristics of the Eastern Scheldt Outer Tidal Delta

A careful review of the geological evolution of the southwestern parts of the Netherlands reveals that the Eastern Scheldt outer tidal delta has specific geological characteristics that distinguish it from the other outer tidal deltas in Zeeland. The most important difference is that the Eastern Scheldt inlet is located on the lowest point of the Pleistocene relief. This is the reason the outflow of the River Scheldt has been located here since 4400 BC. None of the other inlets in Zeeland have existed for nearly such long time. As a consequence, the Eastern Scheldt outer tidal delta and inlet contains mainly sand, with only thin clay and peat layers found in the deepest channels (Figure 2.6).

Unlike the Western Scheldt (Spek, 1997) dominant clay or peat layers that can be used to determine the morphological development of the delta are absent.

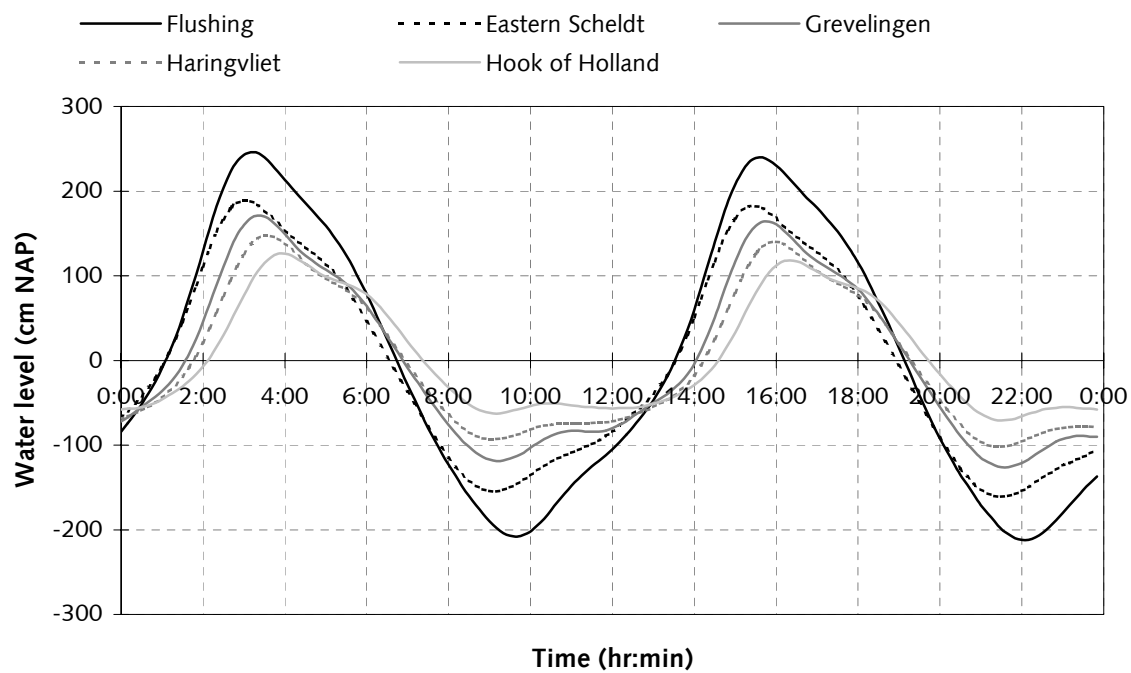


Figure 2.7: The decrease of tidal range from Flushing to Hook of Holland

Table 2.2: Mean tidal range and mean tidal amplitude of 1991 (Rijkswaterstaat, 1994)

Location	mean tidal range (m)	mean amplitude (m)
Roompot Buiten (outside)	2.88	1.44
Roompot Binnen (inside)	2.54	1.27
Stavenisse	2.97	1.49
Bergse diepsluis west	3.46	1.73
Krammersluizen west	3.08	1.54

2.3 Hydrodynamics of the Eastern Scheldt Tidal Basin

The southern North Sea is generally a mixed energy environment dominated by both tide and waves (Hayes, 1979). Beyond the mouth of the Eastern Scheldt estuary there is a tidal delta, created by tide-related inflow and outflow currents. The hydrodynamic aspects of these tidal effects are discussed here and the concepts are utilised in the analysis described in Section 5.2. The effects of waves and river discharge are also briefly discussed below.

In the following discussions, terms “flood tide” and “ebb tide”, and equivalent modifier terms, are used. The flood tide is the period when the water level is rising, the ebb tide is the period when the water level is dropping.

2.3.1 Tide

The southern North Sea is characterised by a semi-diurnal tide, with a tidal period of 12 hours and 25 minutes. Due to the shape of the North Sea the tidal wave travels through the North Sea as a Kelvin wave. This results in a flood tidal current that flows toward the north and an ebb tidal current that flows toward the south along the same coast.

Tidal Amplitude and Tidal Range

The average tidal range, the average height difference between low and high water level, in the southeastern North Sea varies from 3.86 meters near Flushing to 1.74 meters at Hook of Holland (Rijkswaterstaat, 1994).

The shape of the tidal wave in the Eastern Scheldt basin is determined by several factors, including:

- basin geometry,
- ocean tide characteristics,
- bed roughness characteristics, and
- fresh water flow.

The length of the basin (l) and the tidal wave length (λ) determine what type of tidal wave will occur.

In a long basin, where $l \gg \frac{\lambda}{4}$ the tidal wave will propagate and damp at the inland side of the basin.

In a short basin, where $l < \frac{\lambda}{4}$ the tidal wave will be reflected at the end of the basin, because the tidal wave will not be damped.

The wave length formula for shallow water can be used to define which conditions are represented by the Eastern Scheldt basin. The formula is

$$\lambda = \sqrt{gdT}$$

where:

- λ = tidal wave length (m)
- g = gravity parameter (m/s^2)
- d = mean depth of basin (m)
- T = tidal period (s)

Table 2.3: Maximum tidal velocities at the North Sea in front of the Eastern Scheldt and in the inlet of the Eastern Scheldt measured on 27-6-1967 (Rijkswaterstaat, 1967).

	North Sea			Eastern Scheldt inlet		
distance from coast	6 km	16 km	30 km	roompot	schaar	hammen
ebb velocity (m/s)	0.54	0.70	0.70	1.23	0.67	1.09
flood velocity (m/s)	0.52	0.84	0.75	0.98	0.62	0.84

With a mean water depth (d) of 10 and 15 meters and a tidal period (T) of 12.42 hours, the tidal wave length for the Eastern Scheldt basin lies between 443 km and 542 km. Since the actual basin length is 50 km, which is much less than one quarter of the tidal wave length, the Eastern Scheldt basin is a short basin and the tidal wave will be reflected.

The water level equation for short basins is:

$$\eta(x,t) = a \frac{\cos(k(x-l))}{\cos kl} \cos \omega t, \text{ with } k = \frac{\omega}{\sqrt{gh}} \text{ and } \omega = \frac{2\pi}{T}$$

Where:

a = amplitude at the inlet (x = 0) (m)

k = wave number

l = length of basin (m)

ω = surface wave frequency (s^{-1})

x = distance from the inlet (x = 0)

This equation is based on an idealised uniform basin and on one dimensional water movement. The equation is derived from the shallow water equation, where friction is negligible.

To analyse the water levels in the Eastern Scheldt estuary, the following values should be used:

a = 1.27 meters (Table 2.2)

l = 50,000 meters

T = 44700 seconds

These values produce a value for $\omega = 1.41 \cdot 10^{-4} s^{-1}$,

Furthermore:

If the typical average depth (d) is 10 meters, then $k = 1.42 \times 10^{-5}$ and if the typical average depth (d) is 15 meters, then $k = 1.16 \times 10^{-5}$

The maximum amplitude (t = 0) is then:

in the inlet: $\eta_{\max}(x=0) = a \cos(\omega t) = 1.27 \text{ meters}$

at the back of the basin: $\eta_{\max}(x=l) = a \frac{\cos(\omega t)}{\cos(kl)} = 1.67 \text{ meters}$ for

h = 10 meters

$\eta_{\max}(x=l) = a \frac{\cos(\omega t)}{\cos(kl)} = 1.52 \text{ meters}$ for

h = 15 meters

Thus, due to the reflecting wave, the amplitude of the tidal wave at the back of the basin can be in the order of 0.25 to 0.40 meters higher than in the inlet.

Current Velocities

Along the Dutch coast, measurements have shown that the maximum flood tidal current velocity is larger than the maximum ebb tidal current velocity at distances of 16 and 30 km out of the coast (Rijkswaterstaat, 1967 and Schaap, 1971). The flood current is thus dominant in this part of the North Sea, except relatively near the shore where the two currents are about equal (Table 2.3). At the inlet to the Eastern Scheldt, however, the maximum ebb velocity is larger than the maximum flood velocity (Table 2.3).

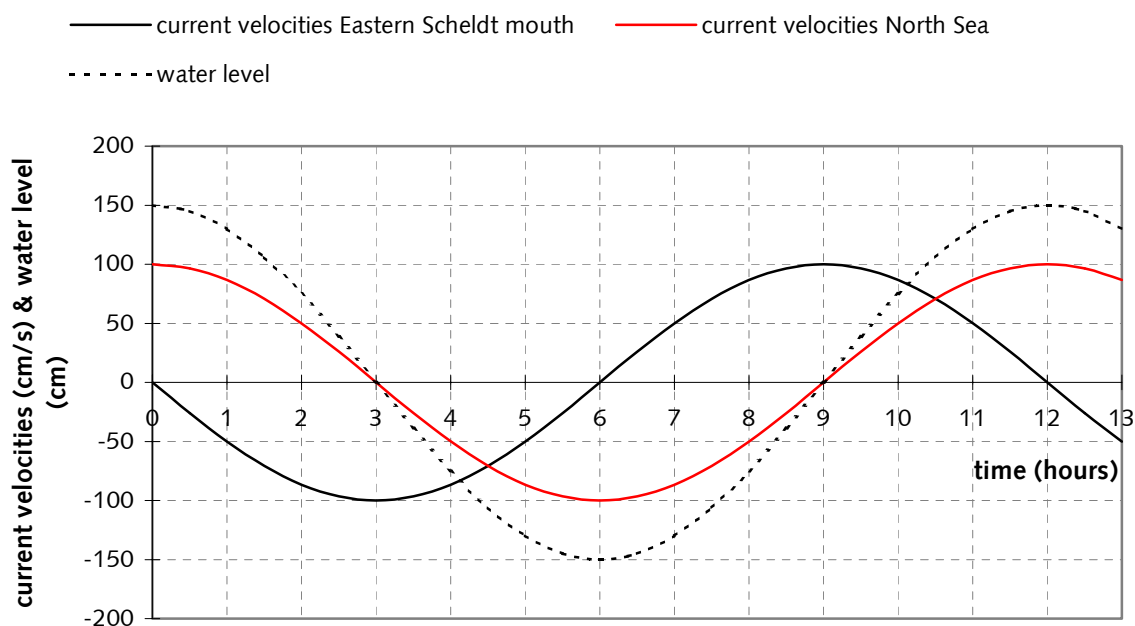


Figure 2.8: The water level in the inlet and the current velocity at the North Sea and in the inlet of the Eastern Scheldt.

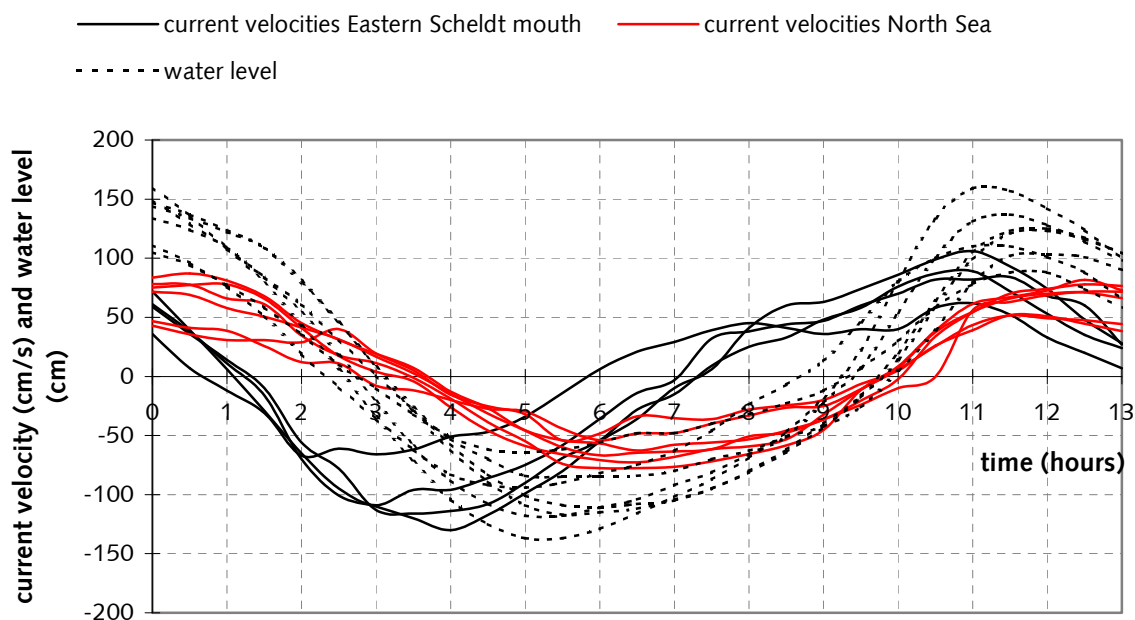


Figure 2.9: Water levels and current velocities at several locations at the North Sea and in the Eastern Scheldt inlet measured on 27 June 1967.

Tidal Amplitude and Current Velocity

The amplitude and current velocity of a reflecting wave is 90° out of phase, for a travelling wave the phase difference is less than 90°.

The North Sea tidal wave along the coast of the southwestern Netherlands is a travelling wave with no phase difference (Vriend et al., 1998). In the Eastern Scheldt basin a reflecting wave occurs, as shown by earlier computations, and, friction is negligible, the tidal amplitude and current velocity are 90° out of phase. Figure 2.8 shows the theoretical phase differences between tidal amplitudes and tidal velocities for the North Sea and at the inlet to the Eastern Scheldt. Figure 2.9 shows amplitudes and current velocities measured in 1967 at the Eastern Scheldt inlet. These measurements confirm more or less the theoretical values shown in Figure 2.8.

Ebb and Flood Tidal Volume

The ebb tidal volume is the volume of water passing through a particular area during outgoing tide and the flood tidal volume is the volume of water passing through a particular area during incoming tide.

Table 2.4 shows the ebb and flood tidal volumes in the North Sea just outside the Eastern Scheldt estuary. These were calculated for an area stretching 30 km into the sea using flow rate measurements obtained in 1967 and 1969 (before closure).

Table 2.4

The ebb and flood tidal volumes at the North Sea near the Eastern Scheldt Rijkswaterstaat, 1967 and Schaap, 1971).

	South of mouth Eastern Scheldt		North of mouth Eastern Scheldt	
Measurement date	27-06-1967	9-9-1969	27-06-1967	9-9-1969
volume ebb (10^9 m^3)	-6.68	-5.78	-5.34	-5.71
volume flood (10^9 m^3)	6.81	6.53	6.32	6.69
difference (10^9 m^3)	0.13	0.75	0.99	0.98

2.3.2 Waves

The wind regime is seasonal and varies considerably. The wind directions control the wave directions, however the resulting main energy flux component for waves is from the southwest. Occasional storms can produce long-period waves travelling from the northwest. The average significant wave height is 1.2 meters at a water depth of 21 meters (Louters et. al., 1991).

2.3.3 River Discharges

The Eastern Scheldt is a tidal basin, since discharges from both the Rhine and the Scheldt rivers have been diverted. Since the completion of the Kreekrakdam (1867) and the closure of the Sloe (1872) the river Scheldt discharges into the Western Scheldt. The discharges from the combined Rhine and Maas rivers has been controlled since the completion of the Volkerak Dam in 1969. Some fresh water from the Rhine and Maas is now passed through the sluices on regular basis. After 1987, this fresh water discharge was decreased from 50 m^3/s (for the period 1969 to 1986) to only 20 m^3/s .

3 Study Method

The main research questions of this thesis are:

- Has the morphology of the coastal system reached large-scale equilibrium?
- What time scales are involved?
- What driving forces are responsible for defining the coastal morphology?

When the morphology of the coastal system has achieved large-scale equilibrium, the system is in fact in a state of dynamic equilibrium because changes during a tidal period, such as the transport of sediment back and forth during a tidal period, are ignored.

It can be assumed that normally natural changes in hydrodynamics or morphology occur slowly enough to allow the coastal system morphology to adapt gradually. Therefore, the coastal system morphology exhibits a state of large-scale equilibrium. However, major changes due to human interventions may have larger and more rapid effects and can bring the system out of equilibrium.

The interactions between hydrodynamics and morphology are important. If the morphology undergoes major changes, the hydrodynamics will be affected, which in turn will affect the morphology until a new equilibrium is reached. Similarly, changes in the hydrodynamics regime may initiate a series of morphological and hydrodynamic adjustments.

The equilibrium state represents a delicate balance between processes, such as tides, waves, and currents, which apply energy to the system and the ability of the system to absorb or dissipate the energy being applied. Balanced energy absorption and dissipation is achieved by adjustments to the geometry of the coastal features. These geometrical adjustments reflect the characteristics of the materials forming the coastal landforms, as well as the energy regime. A stable coastal morphology results when the net volume of the transported material is minimised. While very slow morphologic changes suggest the establishment of system equilibrium, a true equilibrium may never exist.

Analysis of hydraulic and morphological data collected over time can possibly establish if the equilibrium state is reached. When the system is not yet in equilibrium, observations of the evolutionary development of the coastal morphology over time can provide an estimate of how long it will take before the system is in equilibrium. Empirical equilibrium relationships can be used to determine the characteristics of a long-term equilibrium situation for the coastal system.

The following morphological units and hydrodynamic parameters may be used to establish the state of equilibrium:

- tidal volume
- tidal prism
- cross-sectional area of the inlet
- volume of the basin
- volume of the outer tidal delta

The following empirical equilibrium relationships may be used to establish the state of equilibrium:

- tidal prism and cross-sectional area of the inlet to the tidal basin or estuary
- tidal prism and sand volume of the outer tidal delta

The analysis procedure involves the following steps:

- An inventory of the discharge and bathymetric data has to be made and the data has to be tracked over time to reveal trends.
- Then the data has to be prepared for calculations. For example, bathymetric data grids must be constructed to cover the internal basin (estuary/tidal) area, the outer tidal delta, and inlet region.
- Then calculations can be undertaken to quantify the tidal volume, tidal prism, cross-sectional area of the inlet, volume of the basin, and the volume of the outer tidal delta.
- Then the data are plotted to show changes between time periods. To check the data for errors, the calculation results are compared with the expected calculation results.
- Then the equilibrium state of the calculated data is determined.
- If equilibrium is not yet reached, an estimate of the time to reach equilibrium may be made and an estimate of the equilibrium end state of the parameters may be made with the use of empirical relationships.
- Finally the conclusions of the last two steps are compared and discussed to come with an overall answer to the main research question.

3.1 Data Description

As an initial step, an inventory was made of the hydrodynamic data, including the current velocities and tidal volumes and the bathymetric data.

3.1.1 Hydrodynamic Data

Several measurement locations existed in the Eastern Scheldt basin where water levels had been measured over long periods. These measurement locations and measurement periods are defined in Appendix C1. The measured water levels were used to calculate, among other things, the mean high water level (MHWL) and the mean low water level (MLWL) for each year for which measurements had been made. These values were collected in the books "tienjarig overzicht" (RIKZ, Rijkswaterstaat).

Since 1933 velocity measurements were undertaken at the Eastern Scheldt inlet to calculate the discharge through the different channels in the inlet. The measurement methods used in this period are described in Appendix B1. The discharge volumes passing through each channel in the inlet were calculated by multiplying the measured velocities by the cross-sectional area of the individual channels. An overview of these data can be seen in Appendix B2. The original data is found and stored in the libraries of RIKZ in Middelburg and The Hague, in "Het Zeeuws archief" in Middelburg and in the "Meetdienst Zeeland" in Vlissingen. The addresses for these institutes and the storage locations of all the data can be seen in Appendix B3.

3.1.2 Bathymetric Data

Within the bathymetric data, a distinction is made between coastal measurements and marine soundings. The measurement methods for these coastal measurements and the marine soundings are described in Appendix A1.

The coastal measurements are carried out along the entire coast between the shoreline and offshore for a distance of 1 km from the coast. These measurements are executed every year and have been undertaken in the study area since 1965. The measurements are performed using sounding techniques and laser altimetry, introducing a maximum estimated vertical error of 10 cm (Appendix A4). The coastal measurement data is stored in the database "DONAR" at RIKZ in The Hague.

The entire coastal area of The Netherlands is divided into sections, and every section is measured on a frequent basis using sounding techniques. The measurement frequency depends on the dynamics of the area. The maximum vertical measurement error introduced by the sounding technique is estimated at 10 cm (Appendix A4). The bathymetric data for each of these sections is available either as digital grids or as maps and covers the period 1959 to 2000. The digital grids are available at RIKZ office in Middelburg, while the maps are stored at the "Meetdienst Zeeland" in Vlissingen. An overview of the available grids and maps, as well as the locations of the sections, are provided in Appendix A2.

3.2 Data Preparation

The preparation of the data implies making digital grids covering the whole outer tidal delta and Eastern Scheldt inlet and making digital grids covering the Eastern Scheldt basin area.

3.2.1 Grids Covering the Outer Tidal Delta and Inlet

The available grids (Appendix A2) between 1959 and 2000 have to be combined, or merged, to form grids that cover both the outer tidal delta and the inlet. For the period 1960 to 1980 maps for the outer tidal delta were digitised once every four years, so complete grids of the years 1960, 1964, 1968, 1972, 1976, 1980 could be constructed. After 1984 more digital grids are available. The trend once in four years is continued and complete grids of 1984, 1988 and 1992 were also made. After 1992, the frequency of measurements changed to once in three years, so complete grids of the years 1995 and 1998 were made. The year 2001 survey data was not yet available. The process used to create and complete grids covering entire the outer tidal delta and Eastern Scheldt inlet is described in Appendix A3.

3.2.2 Grids Covering the tidal basin

Similar digital data defining the interior of the Eastern Scheldt tidal basin is scarce and incomplete. Three grids were found that covered the basin and defined the situation in the years 1968, 1983 and 1994. The grids for the years 1968 and 1983 were developed for use in computer models to predict the changes in hydrodynamics due to the construction of the Eastern Scheldt storm surge barrier. The grid of 1994 is currently being used in a computer model for wave prediction. The conversion of these data to grids is described in Appendix A3.

3.3 Calculations with the Data

The bathymetric and hydrodynamic data was used in this study to calculate:

- tidal volumes,
- tidal prisms,
- cross-sectional areas of the inlet,
- volumes of the Eastern Scheldt tidal basin, and
- volumes of the outer tidal delta.

GIS methods were used with the prepared bathymetric grid data to calculate the volumes of the tidal prisms, cross-sectional areas of the inlet, the volumes of the Eastern Scheldt tidal basin, and the volumes of the outer tidal delta for each possible time period.

The calculations of the desired volumes above the grids were undertaken with the program "Vakgis" (Bogaard, **). With this program the surface area of every depth in the grid is calculated within a defined boundary. The volume is calculated by multiplying the surface areas with the depth of the surface areas. The summation of these volumes is the total volume.

The cross-sections were calculated by the program "Geoprof" (Biegel, 1998). This program calculates the area of a given profile with the trapezium calculation method and also draws the seabed profiles.

3.3.1 Computing the Tidal Volumes Passing Through the Eastern Scheldt Inlet

The tidal volumes flowing through the inlet were calculated by multiplying the discharge measurements obtained across the various channels in the inlet by the appropriate cross-sectional areas.

The tidal volumes passing through individual channels were calculated by adding up the ebb and flood discharge volumes. The tidal volumes for the total inlet are calculated by adding the tidal volumes of the individual channels that are measured simultaneously or in a close time range.

These data are not corrected for tidal variations, weather conditions, measurement errors, etc. The error of the tidal volumes may be estimated by comparing measurements obtained on consecutive days. The differences in such daily tidal volumes estimates is divided by the lowest tidal volume to give an error percentage. Typically a sequence of six daily measurements are made on consecutive days.

3.3.2 Computing the Tidal prism

The tidal prisms of the Eastern Scheldt tidal basin were calculated using the constructed basin bathymetry grids. The area of the basin is subdivided into 7 sections. For each of these sections, the mean high water level (MHWL) and the mean low water level (MLWL) for each time period was determined by using the mean tidal amplitude data from surrounding measurement locations. The locations of these measurements and the calculation method used is described in Appendix C1 and C2. The tidal prism for the entire basin is calculated by adding the calculated volumes of the individual sections.

The introduced absolute error is estimated by multiplying the estimated elevation error of the grids (Appendix A4) by the appropriate surface area of the basin. For this purpose the area of the basin was defined by the area enclosed by the mean tidal elevation, so NAP was used. The relative error was estimated by dividing the absolute error volume by the tidal prism.

3.3.3 Computing the Cross-sectional Area of the Eastern Scheldt Inlet

The cross-sectional area of the Eastern Scheldt inlet is calculated for 9 locations in and around the inlet, including the dam location using "Geoprof".

The absolute error introduced is estimated by multiplying the width of the cross-section at NAP with the estimated vertical error of the grids (Appendix A4). The relative error is estimated by dividing the relative error by the cross-sectional area.

3.3.4 Calculating the Volume of the Eastern Scheldt Basin

The volume the basin was calculated with "Vakgis" program. This calculation was performed using the maximum area of the basin that is covered by the available bathymetric data.

The absolute error in this volume estimate was estimated by multiplying the surface area at NAP by the estimated vertical error of 10 cm (Appendix A4). The relative error is estimated by dividing the computed absolute error by the volume of the basin.

3.3.5 Calculating the Volume of Outer Tidal Delta

The volume of the outer tidal delta has been calculated in two ways.

The first method defines the calculation area using several arbitrarily defined straight-lined areas (or zones) and calculates a volume for each of these sections. The sum of these section volumes is the volume of the outer tidal delta. This approach was used when calculations were done by hand (Haring, 1948), and is still used.

The second method defines the calculation area to reflect the shape of the morphological boundary of the outer tidal delta. Because the shape and location of this morphological boundary changes over time, a new defined area is made for each individual study date, and hence the volumes may vary from time period to time period as the delta migrates. The volume calculations are referenced to the changing morphological boundaries over time and to the largest and smallest calculated areas within the morphological boundaries.

The expected absolute error is calculated by multiplying the surface area at NAP by the estimated vertical error of the grids of 10 cm (Appendix A4). The relative error is estimated by dividing the absolute error by the volume of the outer tidal delta.

3.4 Evaluation of the Data

The calculated values are now used to evaluate whether or not the coastal system morphology has reached equilibrium. The state of equilibrium may be determined using several methods. First, the development over time of the following parameters were evaluated:

- The tidal volume flowing through the inlet,
- The tidal prism,
- The cross-sectional area of the inlet,
- The volume of the tidal basin, and
- The volume of the outer tidal delta.

This evaluation allows an estimate to be made of the time scale involved in reaching equilibrium.

Subsequently, the equilibrium state was estimated by using equilibrium relationships. This allows an estimate to be made concerning the magnitudes of the system parameters (i.e. cross-sectional area of the inlet, sand volume of the outer tidal delta, etc.) when large-scale equilibrium is achieved.

3.4.1 Evaluation of Development Over Time

The development of the tidal volumes passing through the inlet, the tidal prism, the cross-sectional area of the inlet, and the volume of the outer tidal delta are plotted as a time-series in a series of graphs. The trend shown by these curves are evaluated.

Because a natural system will adapt faster in the beginning and will slow down over time, an exponential fit would be a good approach for the development in time. The classical exponential function used is:

$$V_t = V_\infty (1 - e^{-\frac{t}{T}})$$

WHERE:

t = time

T = adaptation time

V_t = volume at t

V_∞ = equilibrium volume at $t = \infty$

3.4.2 Evaluation Using Empirical Equilibrium Relationships

Published equilibrium relationships between the tidal prism and the cross-sectional area of the inlet, and between the volumes of the tidal prism and the volume of sand in the outer tidal delta may be used to see if the system is approaching equilibrium and what the end state of the system might be. Graph made with the calculated data are compared to published empirical equilibrium relationships.

The sand volume of the outer tidal delta is the extra amount of sand due to the delta, compared to the expected coastal area without an outer tidal delta. It is difficult to determine the bathymetry of the expected coast without outer tidal delta for the Eastern Scheldt, because it is surrounded by other outer tidal deltas. Bathymetries of surrounding coasts cannot be used. As coastal bathymetry a horizontal coast at NAP –15 m will be used to calculate the extra sand volume of the outer tidal delta of the Eastern Scheldt.

These calculated changes in delta volume can be used to calculate the amount of erosion or sedimentation occurring within the delta. To calculate the natural sedimentation/erosion this volume has to be adjusted for known human-induced sand extraction or nourishment.

4 Theoretical Large-scale Relationships for Tidal Basins and Estuaries

.....

If we want to define the characteristics of the equilibrium situation along a section coast and determine what forces affect the system dynamics, the interactions between hydrodynamics processes and resulting morphology must be understood.

In this study, the large-scale coastal equilibrium referred to is a dynamic equilibrium. It can therefore be assumed that natural changes in hydrodynamics or morphology are slow enough for the system to adapt gradually and therefore remain in a constant dynamic equilibrium. Sudden changes, such as those caused by human intervention, however, may cause the system no longer remain in its dynamic equilibrium state. Such changes act as a clear driving force to which the system adapts until it has returned to dynamic equilibrium (i.e. stability).

The large scale hydrodynamics of a tidal basin system can be simply described as follows:

- During rising tide the tidal wave enters the basin, causing a certain volume of water to flow through the inlet.
- The basin will be filled up until the tidal wave starts to leave the basin. This is the high water level.
- The water level in the open sea or ocean will lower again and the water will flow out of the basin into the sea, until the low water level is reached.
- This cycle will repeat itself, changing and influencing the morphology by causing sediment erosion, transport and deposition.

Hydrodynamic parameters are expressed in tidal range and tidal volume. The morphological parameters are tidal prism, the smallest cross-section of the inlet, basin volume and volume of the outer tidal delta.

4.1 Definitions and Conceptual System

In this study the tidal prism is defined as the amount of water necessary to fill up the basin between ebb tidal water level and flood tidal water level. This means that the tidal prism is directly related to the area of the basin and therefore the change in basin area is a measure for the change in tidal prism. The tidal prism determines the amount of water that should flow into the basin during a flood (rising) tide or should flow out of the basin during an ebb (lowering) tide.

In this study the tidal volume is defined as the amount of water that flows through the inlet during an ebb and flood period together. The tidal prism should equal one half of the tidal volume. This is not always the case due to measurement and calculation errors.

A large change in either the hydrodynamic situation or the coastal morphology may bring the system out of equilibrium and result in the adjustment of both the hydrodynamics and morphology, until a new equilibrium is reached.

Three cases of human interventions resulting in a change in hydrodynamics or/and morphology relevant for this study will now be discussed, based on physical considerations:

1) **Decrease in basin area**

A decrease in basin area, for example by “reclaiming” part of a basin with dikes, will cause a decrease in the tidal prism and consequently in tidal volume

Consequence for the inlet

The decrease in tidal volume will initially be obtained by decreasing the velocities in the inlet. This causes sedimentation in the inlet and on longer time span the cross-sectional area of the inlet will decrease, so the velocities in the inlet will increase. In other words, in response to a decrease in the size of the basin and its tidal prism, the tidal volume decreases and thus the velocities in the inlet also decreases. This results in sedimentation in the channels through the inlet. As the inlet cross-sectional area is reduced, flow velocities increase and may return to approximately their original values.

Consequences for the basin

Due to the decreased tidal volume in the inlet, the velocities in the basin also decrease. This results in sedimentation in the channels of the basin. The build up of the sandy shoals may also decrease, due to the lower velocities in the basin. As the channel cross-sections of the basin is reduced, flow velocities increase and may return to approximately their original values. As a result, the build up of the sandy shoals may increase as well.

Consequences for the outer tidal delta

The decrease in tidal volume reduces the tidal current force that extended the outer tidal delta. The waves may have more influence and erosion on the outer tidal delta may occur.

2) **Increase in basin area**

A large increase in basin area will cause an increase in the tidal prism and consequently of the tidal volume.

Consequences for the inlet

This increase in tidal volume will initially require increased velocities in the inlet. If the inlet configuration is such that frictional and turbulence losses prevent sufficient velocities being reached, a reduction in the tidal range within the basin will occur. The higher velocities may initiate erosion at the inlet, increasing its cross-sectional area and resulting in an increase in the tidal volumes. This increase may cause the tidal range within the basin to gradually increase as the tidal volume increases again. As the inlet enlarges, the flow velocities drop and erosion rates may become negligible. The inlet may have new equilibrium tidal flow velocities as well as a new morphology.

Consequences for the basin

Due to the increased tidal volumes in the inlet, the velocities within the basin will increase as well. The increased velocities may result in erosion within the basin channels. The increased velocities in the channels may cause a faster build up of the sandy shoals, so sedimentation may take place in the inter-tidal areas. This sedimentation may result in a slow decrease in tidal prism. In this way a new equilibrium state will evolve, incorporating morphological and hydrodynamic adjustments.

Consequences for the outer tidal delta

The increased tidal volume cause larger tidal current force that can extend the outer tidal delta. The waves may have less influence and sedimentation on the outer tidal delta may occur.

3) Decrease in cross-sectional area of the inlet and consequences for the inlet

A decrease in cross-sectional area of the inlet, for example by installation of a storm surge barrier with control gates, will result in higher velocities in the inlet to maintain the tidal volumes to some extent. If the maximum possible velocity is insufficient to maintain the original tidal volumes, reduction of the tidal range within the basin will result. The increased velocities in the inlet may result in erosion of the adjacent channels. Properly designed gate structures should resist the currents, but erosion of nearby channels may be significant.

Consequences for the basin

The smaller tidal volume will lead to decreased velocities in the basin, and sedimentation within the channels in the basin will occur. The build up of the sandy shoals may decrease, due to the lower velocities in the basin. As the channel cross-sections of the basin is reduced, flow velocities increase and may return to approximately their original values. As a result, the build up of the sandy shoals may increase as well.

Consequences for the outer tidal delta

The decrease in tidal volume reduces the tidal current force that extended the outer tidal delta. The waves may have more influence and erosion on the outer tidal delta may occur.

4.2 Empirical Relationships

Several authors have formulated empirical equilibrium relationships between hydrodynamics and morphology. Generally these define empirical equilibrium relationships between the hydrodynamic parameters, such as the tidal prism or tidal volume, and morphological units, such as cross-sectional area of the inlet, sand volume of the outer tidal delta, and volume of the channels of the basin. The report "Empirical relationships for tidal inlets, basins and deltas" (Kleef, 1991) gives an overview of the empirical relationships.

The most widely published empirical relationship is between the tidal prism and cross-sectional area of the inlet.

In the equations below:

- The tidal prism (P) is measured in m³
- The cross-sectional area of the inlet (A) is measured in m². This is usually defined as below mean sea level (msl) at the narrowest point of the inlet.
- The volume of the outer tidal delta (V) is measured in m³

4.2.1 Tidal Prism and Cross-sectional Area of the Inlet

- The earliest known published relation between tidal prism and cross-sectional area of the inlet was given by LeConte in 1905 (in Jarret, 1976). LeConte found the following relationship for unprotected harbour entrances on the Pacific coast:

$$A = 1.08 \cdot 10^{-4} P$$

WHERE P is the tidal prism at spring range.

- O'Brien (1931) calculated the tidal prism by multiplying the spring or diurnal tidal range in the inlet with the tidal area of the basin at high water. He published the following relationship between tidal prism and cross-sectional area of the inlet, mainly based on Pacific coast data for jettied and unjettied inlets.

$$A = 1.54 \cdot 10^{-3} P^{0.85}$$

WHERE P is the product of the tidal area at high water times the diurnal or spring range in the inlet.

- This relationship was subsequently reviewed by O'Brien (1969). He concluded that his calculation method would not be suitable for the basins with a large tidal range difference throughout the basin. He suggested that the tidal prism calculation should be based upon a detailed summation of the surface area, tidal range and phase relationships. O'Brien stated "When the tidal range in the bay is markedly less than at the entrance, accurate determination of the tidal prism must be based upon a detailed summation of the surface area, tidal range and phase relationships or upon flow measurements at the entrance". The revised O'Brien relationship for inlets without jetties that includes new data from the Pacific and Atlantic coasts is:

$$A = 6.56 \cdot 10^{-5} P$$

O'Brien (1969) also concluded that "Estuaries of large rivers follow the same flow area-tidal prism relationship as tidal lagoons and bays".

- Johnson (1972) used O'Brien's original (1931) method, but calculated the mean tidal prism using the mean or diurnal tidal range. He simply averaged the P_m/A data, because there seemed to be no relationship. He found the following relationship for unimproved inlets on the Pacific coast.

$$A = 5.97 \cdot 10^{-5} P_m$$

WHERE P_m is the mean tidal prism, calculated by multiplying the bay surface area with the mean or diurnal tidal range.

Jarret (1976) used O'Brien's suggestion on the calculation method of the tidal prism and calculated the tidal prism with his invented "cubature" method. This involves the segmenting of the bay in subareas that have approximately the same "phase range" and calculating the volume change of the subarea with the phase range of that subarea during the interval of time between succeeding slack water in the inlet. The tidal prism is then calculated by summing the volume changes of each subarea. Jarret found the following equation for all the inlets used for the Gulf, Pacific and Atlantic coast.

$$A = 1.88 \cdot 10^{-4} P^{0.95}$$

He also found the following equation for inlets with no or one jetty for the Gulf, Pacific and Atlantic coast.

$$A = 3.41 \cdot 10^{-5} P^{1.03}$$

- For the inlet in The Netherlands Haring (1967) established similar relationships, as follows:

$$A = 4.13 \cdot 10^{-5} TV,$$

WHERE TV is the tidal volume, calculated with measured velocities in the inlet (tidal volume / 2 = tidal prism).

The Eastern Scheldt basin has a large tidal range difference of about 1.2 meters throughout the basin. Therefore it appears that the cubature method proposed by Jarret (Jarret, 1976) would give a better result than the more simple calculation methods originally proposed by O'Brien (O'Brien, 1931) or those proposed by Johnson (Johnson, 1972). Accordingly the "cubature method" was adopted for the calculations undertaken in this study.

4.2.2 Tidal Prism and Sand Volume of the Outer Tidal Delta

Walton and Adams (1976) established equilibrium relationships between tidal prism and sand volume in the outer tidal delta. They found the following relationships:

Highly exposed coasts	$V = 5.33 \cdot 10^{-3} P^{1.23}$, for $H^2T^2 > 28$
Moderately exposed coasts	$V = 6.44 \cdot 10^{-3} P^{1.23}$, for $2.8 < H^2T^2 < 28$
Mildly exposed coasts	$V = 8.46 \cdot 10^{-3} P^{1.23}$, for $H^2T^2 < 2.8$
All inlets	$V = 6.56 \cdot 10^{-3} P^{1.23}$	

Where H is the wave height in meters and T is the wave period in seconds.

The sand volume of the outer tidal delta is determined by calculating the volume enclosed by a coast line without an outer tidal delta and one with an outer tidal delta.

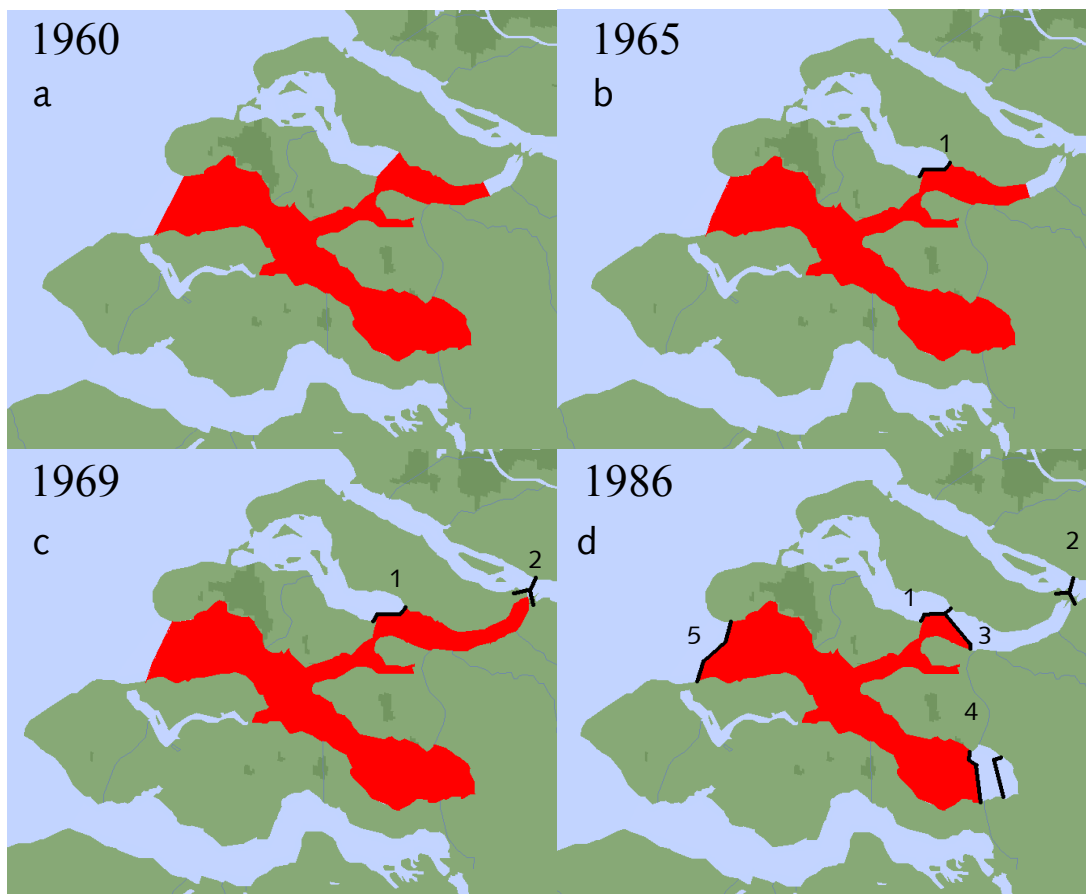


Figure 5.1: Development of the Eastern Scheldt basin area due to the Delta Works.

1. Grevelingen Dam
2. Volkerak Dam
3. Philips Dam
4. Oester Dam
5. Eastern Scheldt Storm Surge Barrier

Table 5.1: An overview of the works of the Delta project that influence the Eastern Scheldt.

	Basin area	inlet of the Eastern Scheldt
1965	Grevelingen Dam was finished	
1967		Start construction Eastern Scheldt storm surge barrier
1969	Volkerak Dam was finished	
1972		Closure of the channel "Geul"
1983 - 1986		Placement of the piers and gates in the inlet
1986	Philips Dam and Oester Dam finished	
1986		Eastern Scheldt Storm Surge Barrier finished

5 Application to the Eastern Scheldt

In this chapter the tidal volumes through the inlet, the tidal prisms, the cross-sectional areas of the inlet, the volumes of the basin, and the volumes of the outer tidal delta are calculated according to the methods described in Chapter 3. The results of these computations are evaluated by applying our knowledge of what the expected changes to the Eastern Scheldt system might be. These expected changes are described in Section 5.1 below. The comparisons between the theoretical and measured (calculated) responses described in this chapter will help to identify any major errors in the data.

5.1 Expected Changes of the System During the Delta Project

Major changes in basin area, and therefore to the tidal prism and to the inlet cross-section, and thus to the tidal volumes, will result in changes in the system hydrodynamics and the coastal morphology. These changes can be predicted by applying the same logic and principles as described for the theoretical cases in Chapter 4.

The Delta Project caused major changes to both the basin area and inlet geometry of the Eastern Scheldt. Table 5.1 summarises the major construction events of the Delta Project. Often changes to the basin area and the size of the cross-section of the inlet occurred simultaneously. This created complex changes to both the hydrodynamics and morphology.

The expected changes are discussed in the following sections and are illustrated in the theoretical graphs shown in Figure 5.2. The letters between brackets in the text refer to the pictures of the schematic presentation of the changes shown in Figure 5.3.

5.1.1 Changes Prior to 1969

Originally the Eastern Scheldt basin was limited by land boundaries and by two tidal divides (see Figure 5.1.a). One tidal divide was located between the Eastern Scheldt and the Haringvliet, while the second tidal divide was located between the Eastern Scheldt and the Grevelingen. The Grevelingen Dam was completed in 1965, but because this dam was built on the tidal divide between the Eastern Scheldt and the Grevelingen (Figure 5.1.b), it did not change the basin area, and so had no effect on the tidal prism or other system dynamics. Thus no measurable changes to the hydrodynamics and morphology of the Eastern Scheldt system are expected.

5.1.2 Changes in the Period 1969 - 1977

During this period, the Volkerak Dam was completed in 1969 and the "Geul" channel within the Eastern Scheldt inlet was closed in 1972. Some seabed stabilisation work also influenced (generally increased) the stability of the inlet during this period. The net effect of these activities was an increased tidal prism, and consequently an increased tidal volume through the inlet, because the tidal prism is one half of the tidal volume. The increased tidal volume was partially controlled by construction in the Eastern Scheldt inlet. The expected changes are:

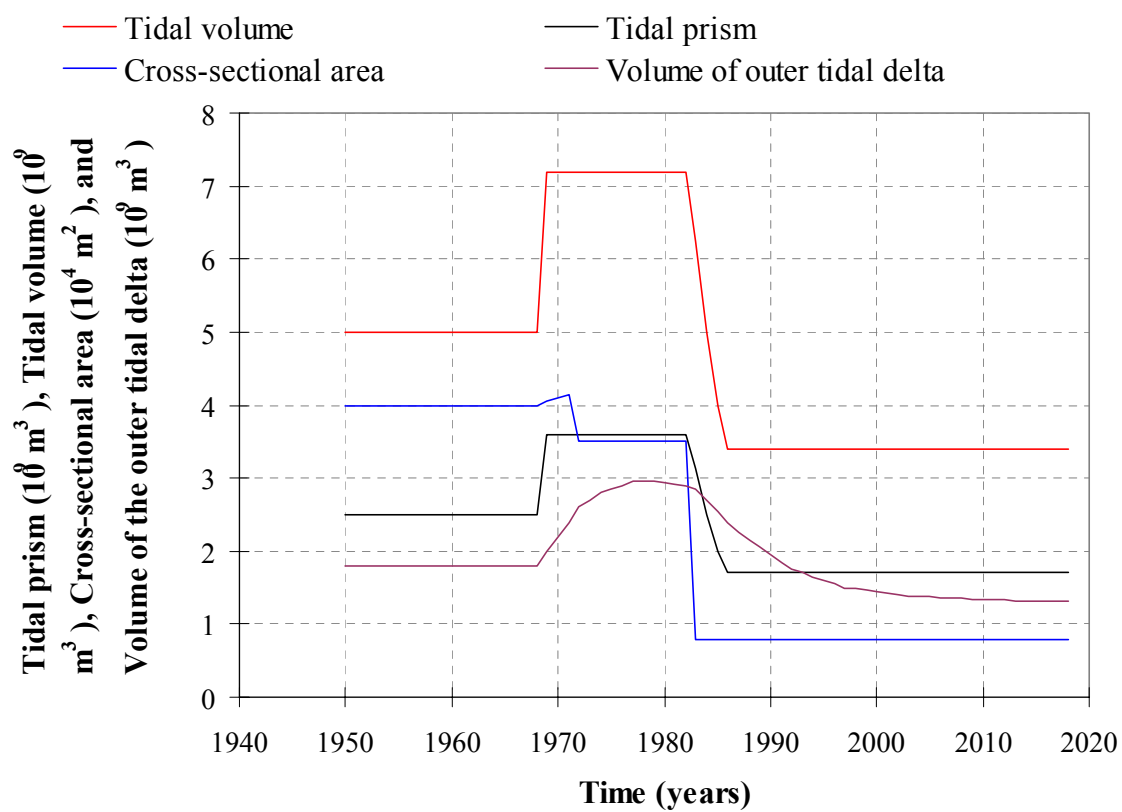


Figure 5.2: The expected developments of the tidal prism, tidal volume, cross-section of the inlet and water volume of the outer delta.

Basin area

Completion of the Volkerak Dam in 1969 caused an enlargement of the Eastern Scheldt basin area. The original (natural) tidal divide between the Eastern Scheldt and the Haringvliet was replaced by the dam which was located further to the North than the tidal divide (see Figure 5.1.c).

Tidal Prism and Tidal Volume

The enlargement of the Eastern Scheldt basin area due to the completion of the Volkerak Dam should result in an increase in tidal prism, and thus an increase in tidal volume. If the inlet is large enough, the tidal current velocities through the inlet can increase, thereby allowing the tidal volumes to increase enough to maintain the original tidal range in the basin. If the inlet is not large enough, or the tidal currents cannot increase enough, the tidal volume will be too small to maintain the original tidal range.

Inlet

The increase of the tidal volume would normally result in an increase of the cross-sectional area of the inlet. However, placement of seabed protection within the inlet starting in 1974 would prevent further erosion of the inlet at the protected locations. Furthermore, closure of the "Geul" channel in 1972 resulted in a decrease in cross-sectional area. The closure of the "Geul" channel might interfere with the tendency for the tidal volume to increase enough to maintain the original tidal range. The stabilisation measures effectively interfered with the tendency for the current velocities to decrease due to an enlarged inlet cross-sectional area.

Basin

The increased tidal volume should result in erosion in the channels within the basin and should cause sedimentation in the inter-tidal area, which will result in a slow decrease of the tidal prism.

Outer Tidal Delta

The sand volume of the outer tidal delta should increase as the tidal volume increases.

5.1.3 Changes in the Period 1977 - 1986

The final stages of construction of the Eastern Scheldt Storm Surge Barrier, Philips Dam and, Oester Dam occurred in this period. These construction works tended to cause a gradual reduction in the tidal volumes. This reduction resulted from a combination of decreased basin area, caused by closure of portions of the Eastern Scheldt basin by the Oester Dam and Philips Dam, and by a marked reduction in the cross-sectional area of the Eastern Scheldt inlet during construction and completion of the storm surge barrier. The anticipated changes during this period are:

Basin Area

Completion of the Oester Dam and the Philips Dam in 1986, caused a decrease in basin area because they isolated two portions of the former Eastern Scheldt basin (see Figure 5.1d).

Tidal Prism and Tidal Volume

Construction of the Philips Dam and Oester Dam from 1977 to 1986 could influence the tidal volume. An observed decrease in tidal range in those sections of the basin located behind these dams would indicate that not enough water was able to flow through these dam sites.

Furthermore, construction activities for the storm surge barrier caused a progressive decrease in the cross-sectional area of the inlet from 1983 to 1986 (c). Following completion of the storm surge barrier in 1986, this reduction reached about 80 % of the original area (Rijkswaterstaat, 1994). Such a marked reduction in the inlet cross-sectional area should result in a decrease in tidal volumes. Consequently a decrease in tidal range is expected to keep the tidal prism equal to half of the tidal volume.

The decrease in basin area after 1986 should result in an increase in tidal range. If the former tidal range is not reached (d1), the maximum possible tidal volume, and thus maximum tidal current velocities through the inlet will be reached. If the tidal range reaches its former level (d2 and d3) equilibrium current velocities or even tidal current velocities lower than the equilibrium velocities can occur.

Inlet

The placement of the storm surge barrier piers and gates across the inlet from 1983 to 1986 decreased the cross-sectional area of the inlet. This should cause an increase in tidal flow current velocities through and near the inlet during this period. However, erosion cannot occur within or adjacent to the storm surge barrier due to the seafloor protection measures. In contrast, those unprotected areas near the dam may.

This situation will not change after 1986. The inlet is still not expected to be large enough, so the tidal current velocities in the inlet will still be larger than the equilibrium velocities and the tidal range will still be smaller than the former tidal range. But if the tidal range has reached its former magnitude, the velocities in the inlet can be less than the maximum possible tidal current velocities.

Basin

The decreased tidal volume after 1983 should result in sedimentation in the channels within the basin and erosion in the inter-tidal zones within the basin. After 1986, after the decrease in tidal basin area, sedimentation in the basin will occur if the tidal range is smaller than its former level. If the tidal range is returned to its original tidal range, the basin volume might not change, because equilibrium velocities are reached (d2 and d3).

Outer Tidal Delta

The decreased tidal volume in the inlet after 1983 should result in a decrease in the sand volume of the outer tidal delta, thus erosion will occur.

5.1.4 1986 - future; equilibrium

Following completion of the Philips Dam, Oester Dam, and the Eastern Scheldt Storm Surge Barrier in 1986, it is expected that the Eastern Scheldt system will gradually achieve large-scale equilibrium. A series of morphologic adjustments, caused by erosion and sedimentation within and outside the Eastern Scheldt basin, will cause the entire system to reach equilibrium. Two possible routes to achieving this equilibrium can be described.

1)

Lower tidal ranges in the basin after 1986 compared to the original tidal ranges in the basin before 1983 indicate that the maximum possible tidal volume is flowing through the inlet. This also implies maximum possible velocities in the inlet.

Inlet

The larger velocities in the inlet should result in erosion in the inlet at the locations without seabed protection, until equilibrium velocities are reached. The cross-sectional areas at the protected locations cannot increase. At these locations maximum tidal current velocities will occur, unless the tidal prism is reduced even more.

Basin

The smaller tidal volume should result in sedimentation in the channels within the basin and erosion in the inter-tidal area, until equilibrium velocities are reached.

The outer tidal delta will undergo erosion, until a new equilibrium between the building and eroding forces (i.e. waves, tidal currents, etc.) of the outer tidal delta is found.

2)

Equal tidal ranges after 1986 to the tidal ranges before 1983 imply that the inlet is large enough. The tidal current velocities in the inlet will be equal or smaller than the maximum possible velocities.

Inlet

This implies that erosion will take place at the unprotected locations of the inlet, if the velocities are larger than the equilibrium velocities (d2), and sedimentation will take place, if the tidal current velocities are smaller than the equilibrium velocities (d3).

Basin

Within the basin the velocities might be reached. The volume of the basin is not expected to change significantly.

The outer tidal delta will undergo erosion, until a new equilibrium between the building and eroding forces (i.e. waves, tidal currents, etc.) of the outer tidal delta is found.

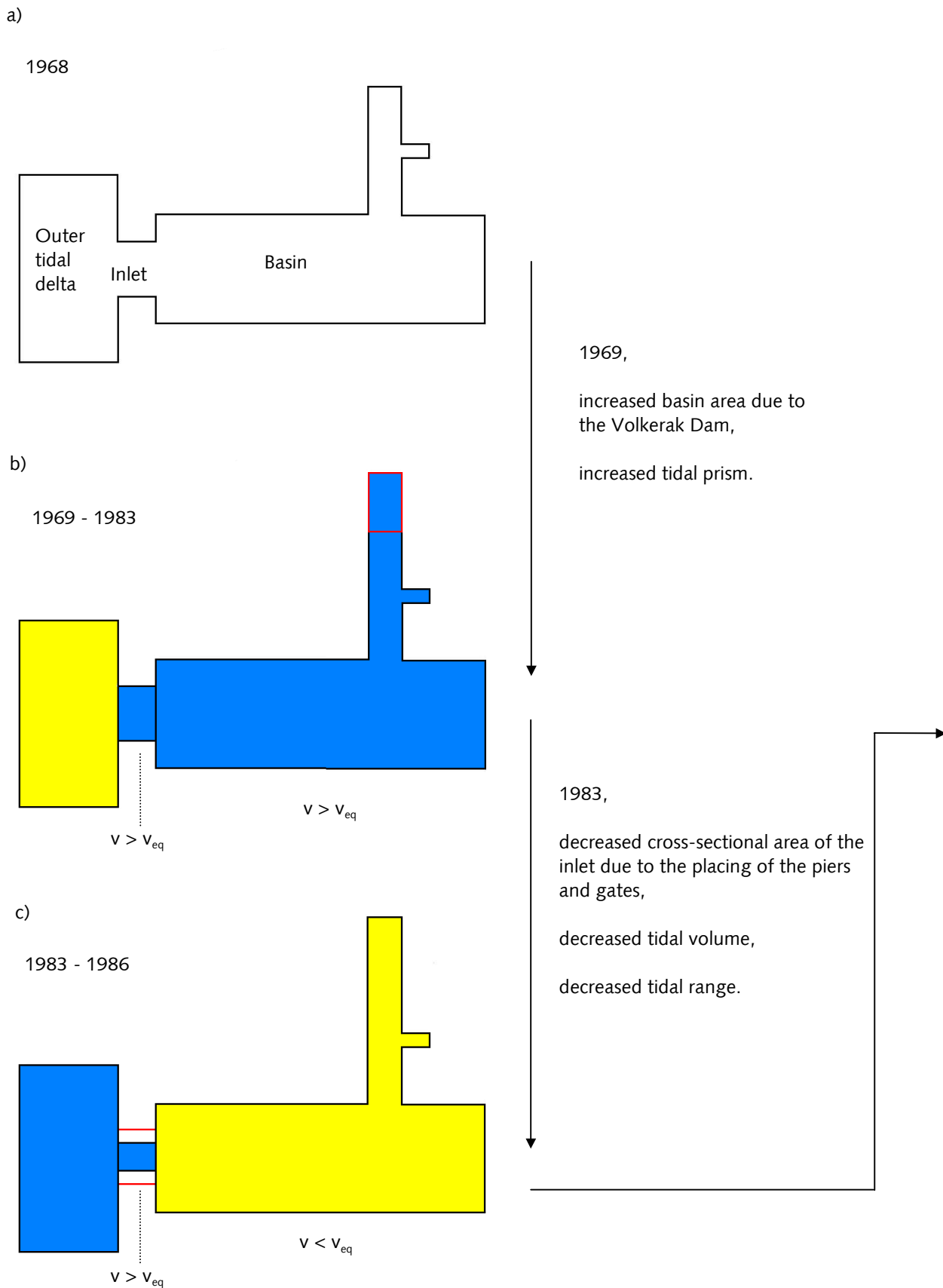
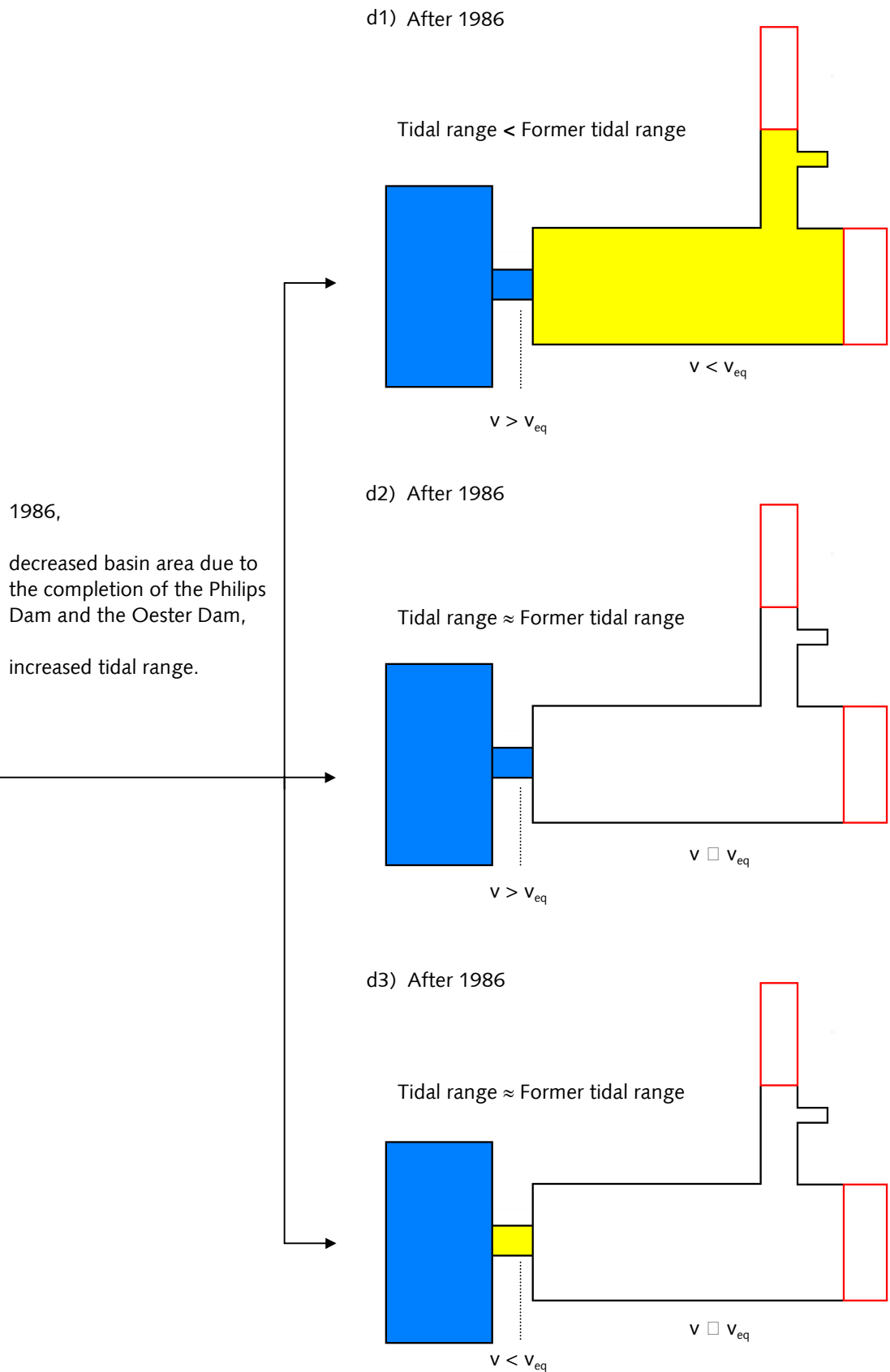


Figure 5.3: The schematical development of the Eastern Scheldt system (v = velocity, v_{eq} = equilibrium velocity, blue = erosion, yellow = sedimentation and red = changed parts)



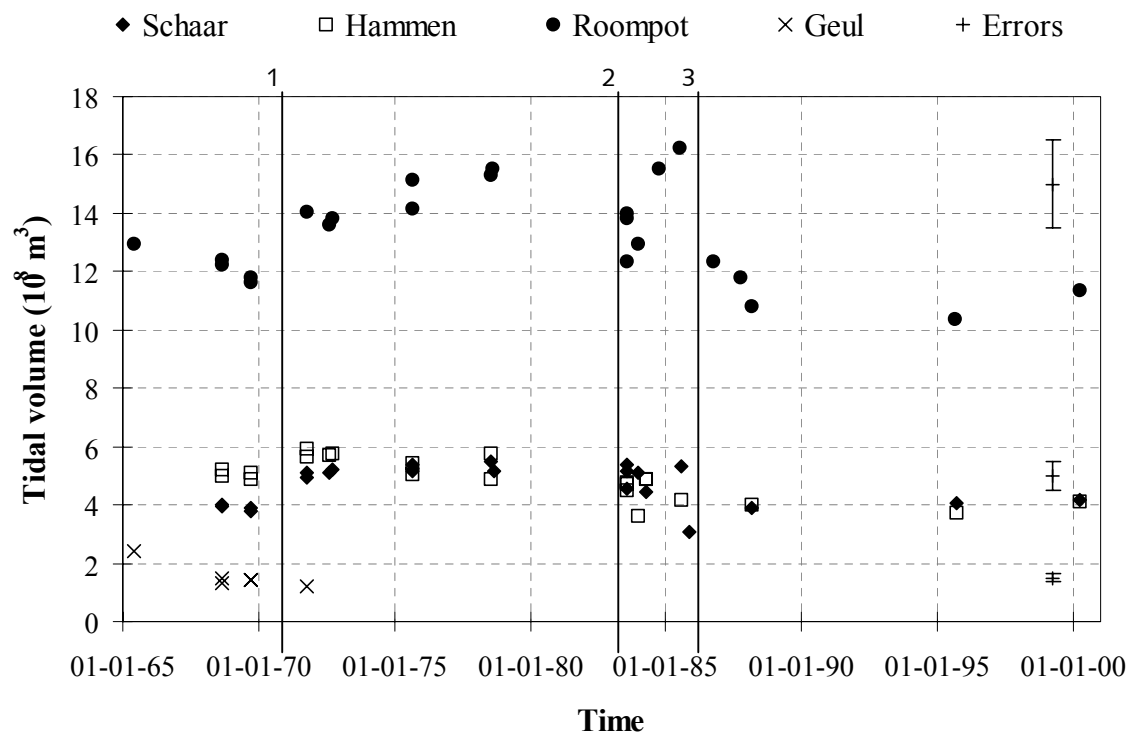


Figure 5.4: The tidal volumes of the individual channels; Roompot, Hammen, Schaar and Geul channels. The error of 11 % is indicated for different tidal volume values. (1. Construction working island, 2. Start placing piers in Hammen, 3. Construction of dam finished).

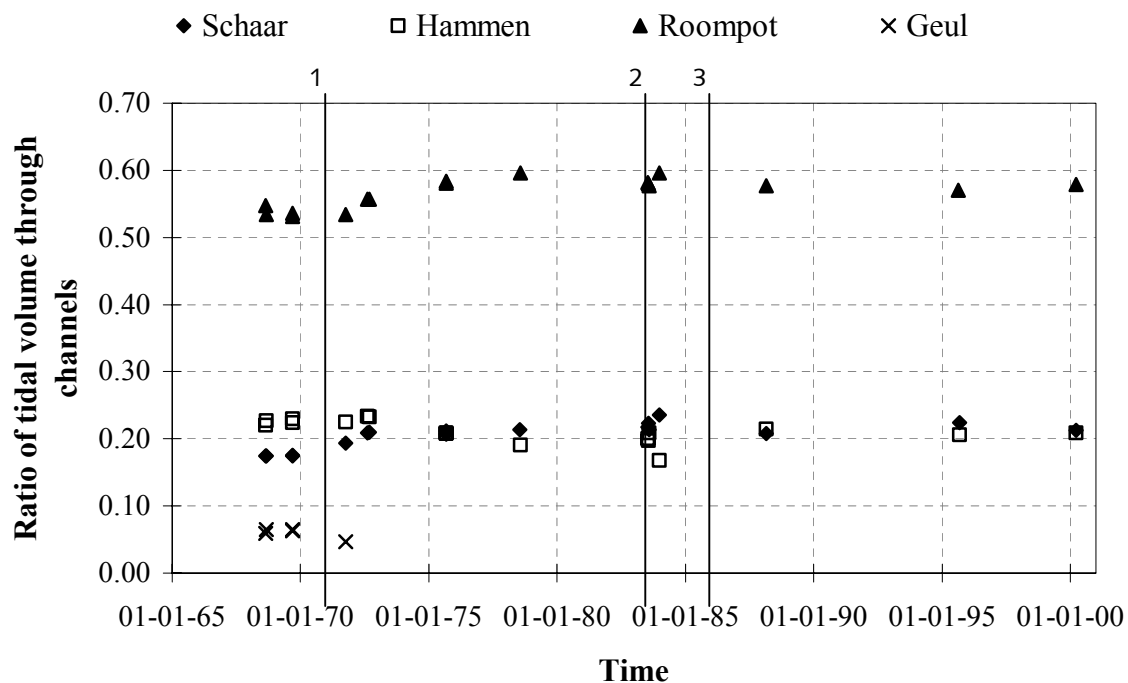


Figure 5.5: Ratio of tidal volumes of the individual channels (1. Construction working island, 2. Start placing piers in Hammen, 3. Construction of dam finished)

5.2 Development of Tidal Volume

The tidal volume is defined as the amount of water flowing through the inlet during both ebb and flood tides. The tidal volume of the entire inlet is calculated by adding the tidal volumes of the individual channels. The tidal volumes of the individual channels are calculated by adding up the ebb and flood discharge volumes of each channel. Appendix B2 shows the available discharge data and the calculated tidal volumes. The discharge data is not corrected for tidal variations, weather conditions, measurement errors, etc. The error of the data is estimated by comparing the tidal volumes of consecutive days. The calculated errors are provided in Table 5.2 and Appendix B4. The maximum error is 11 % and is taken as error of the tidal volume data.

Table 5.2: Calculated errors of the tidal volumes.

Year	Schaar	Hammen	Roompot	Geul	Total inlet
1967					9%
1968	1%	4%	1%	11%	1%
1969	3%	5%	1%	1%	2%
1971	3%	5%			
1971	4%	10%			
1975	4%	6%	7%		6%

5.2.1 Tidal Volumes through the Individual Channels

Figure 5.4 shows the tidal volumes for the individual channels forming the Eastern Scheldt inlet.

As discussed in Section 5.1, an increase in tidal volumes was expected following completion of the Volkerak Dam in 1969. Figure 5.4 shows increases in the tidal volumes for all the channels, especially the "Roompot" channel. These increases are larger than the tidal volumes that passed through the "Geul" channel, prior to its closing. Thus it can be concluded that both the closure of the "Geul" channel and the completion of the Volkerak Dam contributed to the increased tidal volumes.

A decrease of the tidal volumes after 1983 was expected due to the placing of the piers and gates in the channels. Because the piers and the gates were not simultaneously placed in all channels, the various channels show a relatively complex adjustment of individual tidal volumes. Figure 5.4 shows that after 1986, when all the piers and gates were placed, the tidal volumes of all the channels have decreased.

The reaction of the individual channels to the construction of the dam can best be evaluated by examining the ratio of the tidal volumes of the separate channels to the total tidal volume for the entire inlet. These data are presented in Figure 5.5.

In 1972 the "Geul" channel was closed and its discharge was diverted over the channels "Roompot", "Schaar" and "Hammen".

The placing of the piers beginning in 1983 also caused a change in the ratios of tidal volume among the remaining channels. The piers were first placed in the "Hammen" channel, resulting in a lower ratio of tidal volume passing through the "Hammen" channel and higher ratios of volumes passing through both the "Schaar" and the "Roompot" channels. As the piers were

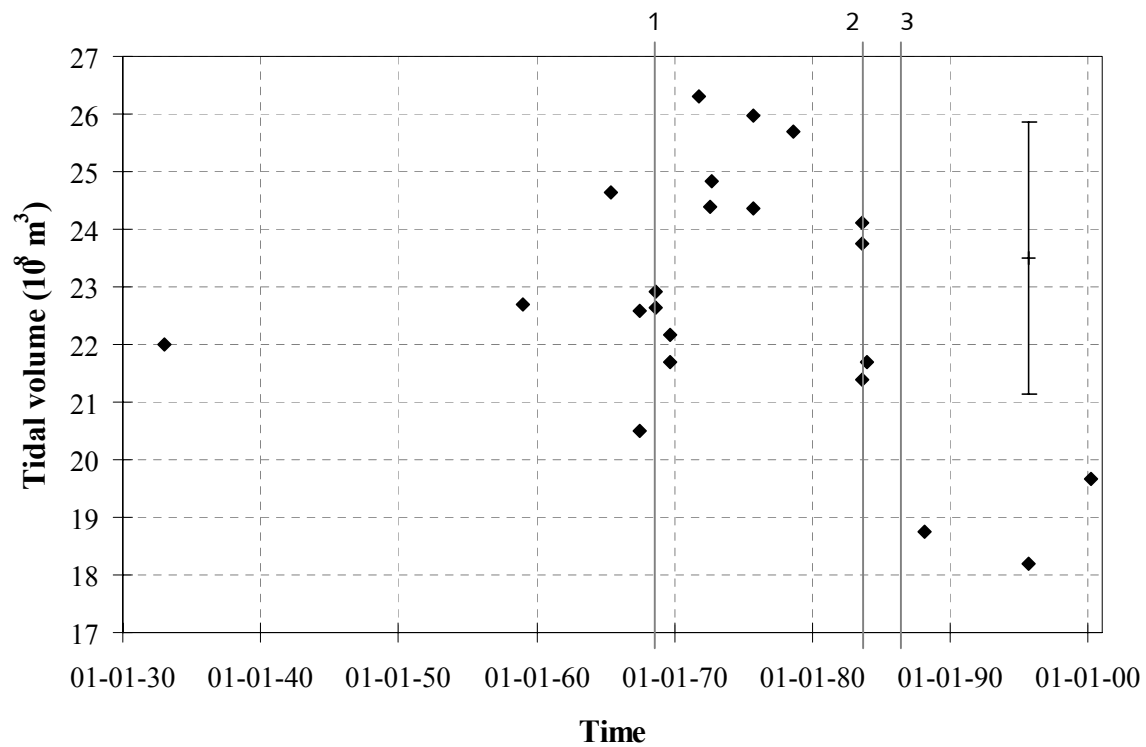


Figure 5.6: Development of tidal volume in the Eastern Scheldt. (1. Completion of the Volkerak Dam, 1969; 2. Placement of piers in inlet, 1983; 3. Completion of Philips Dam and Oester Dam, 1986)

subsequently placed in the "Schaar" channel, a lower flow ratio for the "Schaar" channel and an increased flow ratio for the "Roompot" channel as can be seen in Figure 5.5

After the completion of the Eastern Scheldt compartmentalisation dams in 1986 the flow ratios for the "Roompot", "Schaar" and "Hammen" channels are respectively, 58 : 21 : 21. This seems to be a stable situation. These ratios are essentially the same as existed in the pre-construction period of 1975.

5.2.2 Tidal Volume through the Total Inlet

Figure 5.6 shows the tidal volume for the entire inlet. The tidal volume of the total inlet is calculated by adding up the tidal volumes of the individual channels.

Despite the inherent variability of the measured and computed tidal volumes, and the error of 11 % a trend in the tidal volume measurements can be seen. The expected increase in tidal volume due to the building of the Volkerak Dam in 1969 is clearly visible in Figure 5.6. The increase is about $3.4 \times 10^8 \text{ m}^3$ from 1969 to 1972; This is an increase of 15 % compared to the tidal volume before completion of the Volkerak Dam. Figure 5.6 also shows the reaction of the tidal volumes to the placing of the piers from 1983 to 1986 across the various channels forming the Eastern Scheldt inlet. The tidal volumes decreased over this 5-year period by $6.8 \times 10^8 \text{ m}^3$. This is a decrease of 26 % compared to the total tidal volume of 1978. Thus it can be concluded that the measurements and calculations support the concepts proposed in Section 5.1 concerning the development of the tidal volumes.

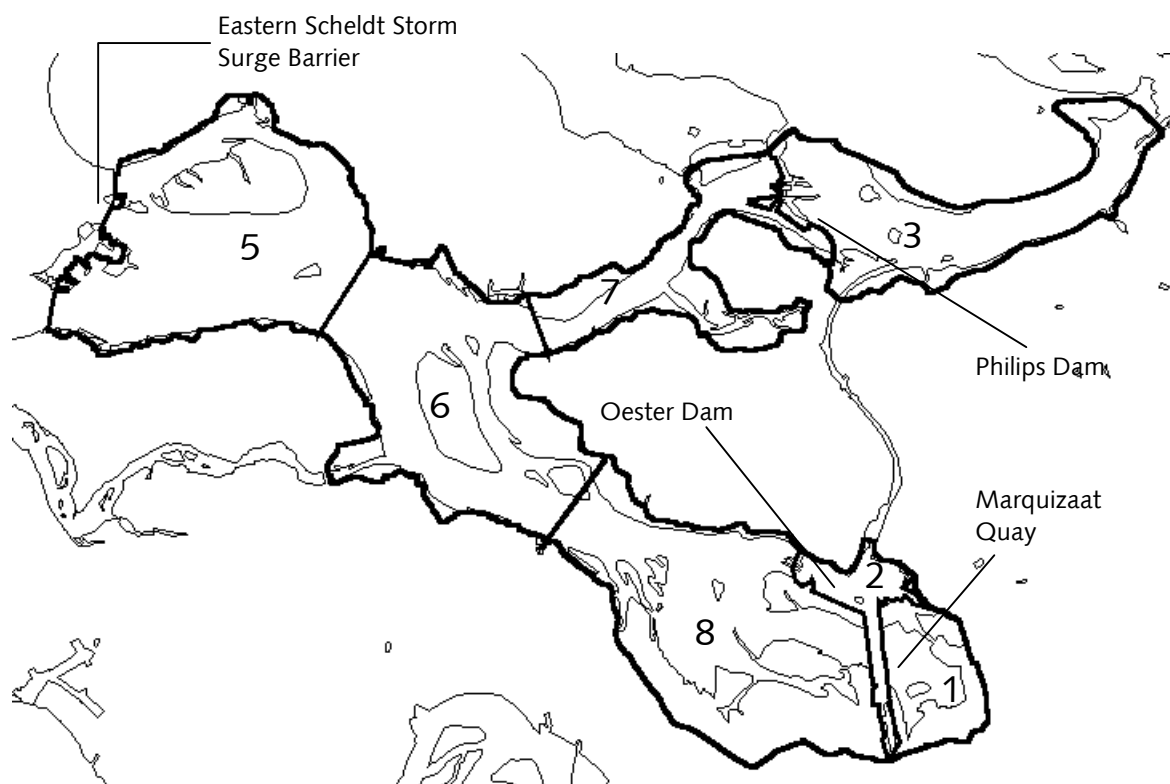


Figure 5.7: The calculation sections of the basin

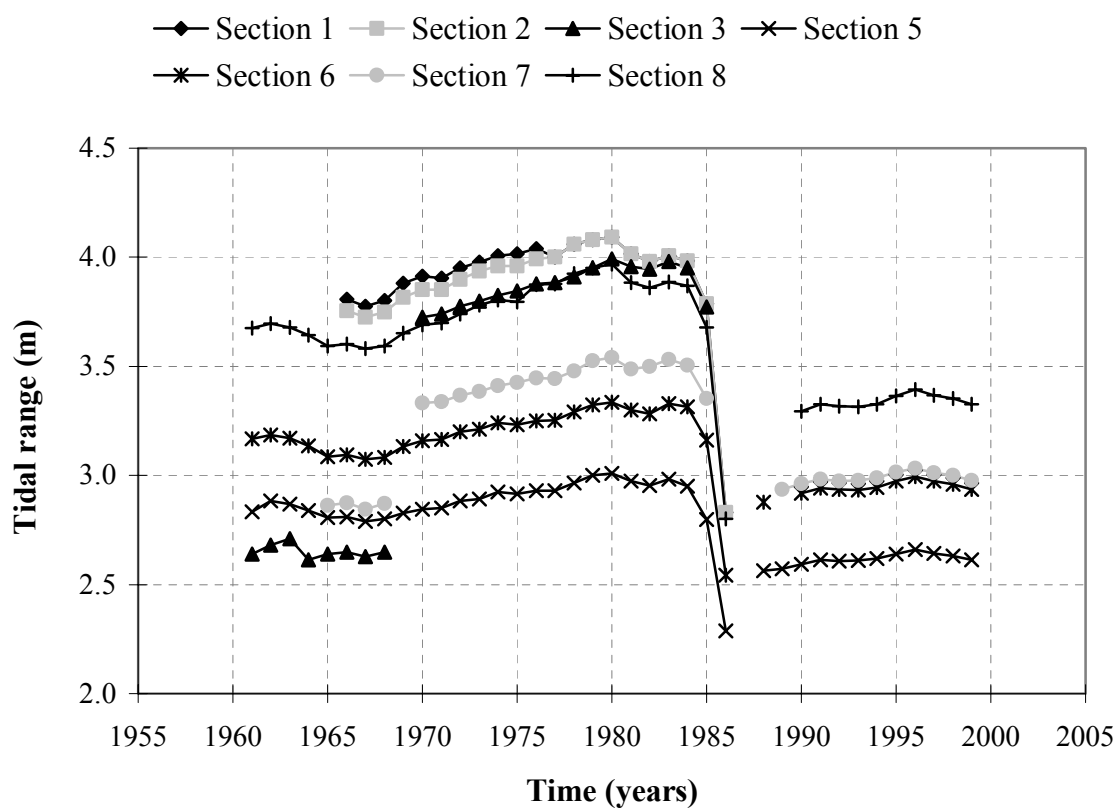


Figure 5.8: The tidal range of the calculation sections of the basin (Rijkswaterstaat RIKZ, 1985, Rijkswaterstaat RIKZ, 1989, and Rijkswaterstaat RIKZ, 1994).

5.3 Development of the Tidal Prism

The tidal prism is defined as the amount of water necessary to fill up the basin between the ebb tidal water level and the flood tidal water level.

By using current computer technology and GIS methods, the exact volume between a given water level and the seafloor defined by bathymetric data can be calculated. This will give better results than the original method of manual calculation that simply multiplied the basin surface area by the tidal range. In the Eastern Scheldt basin, observations of the mean high water levels (MHWL) and mean low water levels (MLWL) are available at numerous locations over a long time span (Appendix C1). Thus, these observations of the MHWL and MLWL were used to calculate the tidal prisms. The process was made more accurate by subdividing the entire Eastern Scheldt basin into a series of seven sections that had distinctive tidal ranges and/or phases. These values were then summed to compute the volume of the tidal prism for the entire basin. The following sections discuss these computations in more detail.

5.3.1 Tidal Amplitude

Figure 5.7 shows the several locations around the basin where water levels are measured. The mean high water (MHW) and mean low water (MLW) levels for each of the calculation sections were determined by analysing these water level observations. Appendix C1 provides the water levels of the measurement locations. Appendix C3 provides the MHW and MLW levels for each of the calculation sections.

The effect of the completion of the Volkerak Dam in 1969 is clearly visible in the large increase in tidal amplitudes (shown in Figure 5.8). For example, the tidal range increased by 0.4 m in Section 7 and 1 m in Section 3. These large increases are believed to be caused by the reflection of the tidal wave against the Volkerak Dam.

Figure 5.8 also shows a sudden drop in tidal amplitudes in 1985. For example, the tidal range decreased by 0.7 m in Section 5, by 0.8 m in Section 6, and by 1.1 m in Section 8. After 1986, the tidal amplitudes increase. The tidal range increases by 0.3 m in Section 5, by 0.35 m in Section 6, and by 0.5 m in Section 8. The decrease in tidal range after 1985 is caused by the decrease of the cross-sectional area of the inlet. The tidal current velocities in the inlet cannot increase enough to let enough water through the inlet during rising tide to maintain the original tidal range. After 1986 the basin area decreased, so less water is necessary to fill the basin and the tidal ranges can rise again.

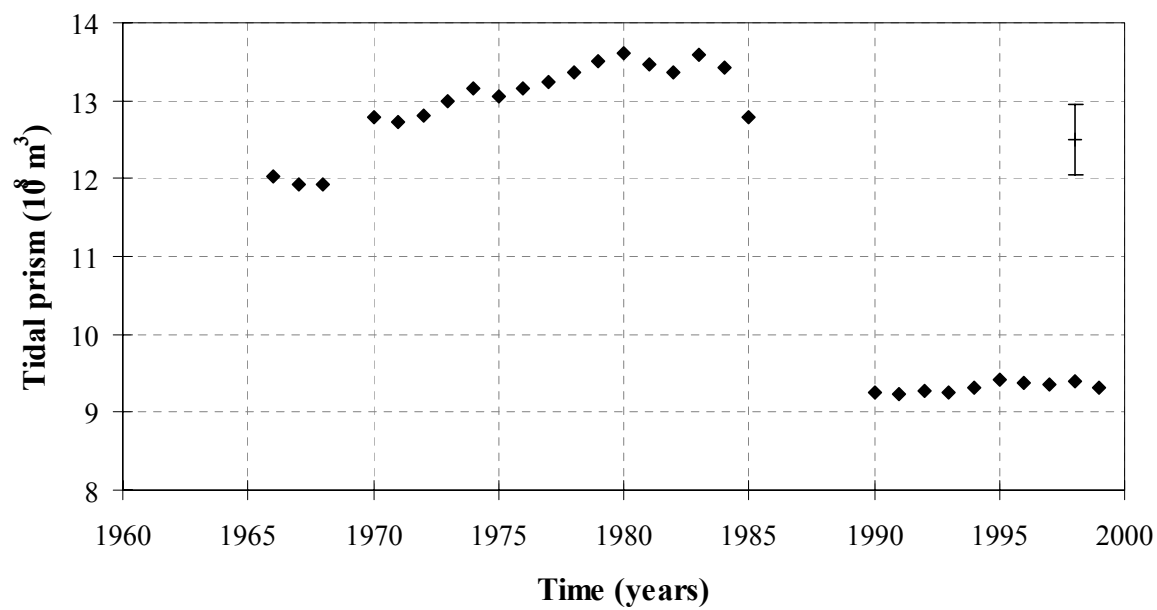


Figure 5.9: The mean tidal prism plotted against time.

Table 5.3: The volume and volume difference of the total basin between NAP -2 and 2 m.

year	Volume between NAP -2 m and NAP 2 m in 10^9 m^3
1968	1.22
1983	1.18
1994	1.19
year	difference between years
1968 – 1983	-3.39 %
1983 - 1994	1.48 %

5.3.2 Computing the Tidal Prism

The water levels used for the tidal prism calculations are provided in Appendix C3.

Grids covering the entire Eastern Scheldt basin are available only for the years 1968, 1983, and 1994. Only the grid of 1968 was used for the tidal prism calculations in this study, because of the following assumptions:

- changes in the tidal prism are primarily caused by changes in basin area.
- changes in tidal prism due to adaptation of the inter-tidal area (i.e. volume changes between NAP -2 and +2 m) are of second order and can be neglected. As has been shown in Table 5.3, the difference between the basin volumes contained between elevations NAP +2 m. (maximum high water) and NAP -2 m. (maximum low water) for the years 1968, 1983, and 1994 is less than 4 %.

The tidal prisms for each section of the basin shown in Figure 5.7 are calculated separately. The total volume of the tidal prism for the entire basin is computed by adding the calculated volumes for the different sections. For the years 1966 to 1986 the volumes of all seven the sections are added, because the basin area was not reduced yet by dams. However, after completion of the Oester Dam and Philips Dam in 1986, the tidal basin included only sections 5, 6, 7, and 8. The volume of each section was calculated between the relevant MHW and MLW levels given in Appendix C3. The calculated volumes for each section are provided in Appendix C4.

The absolute error in the tidal prism is calculated by multiplying the surface area of the basin at elevation NAP +2 m by the estimated vertical error of 10 cm. These error values for each section are tabulated in Appendix C5. The absolute error for the entire basin (sections 1, 2, 3, 5, 6, 7, 8), valid for the period prior to 1986, is estimated at $4.53 \times 10^7 \text{ m}^3$, while the absolute error for the smaller basin consisting of only sections 5, 6, 7, and 8, and valid for the period after 1986, is estimated as $3.54 \times 10^7 \text{ m}^3$.

The relative error is calculated by dividing the absolute error by the calculated volumes or tidal prisms. The relative error values are tabulated in Appendix C5. The relative error is estimated at 3.5 % for the original large basin and 3.8 % for the smaller basin.

Figure 5.9 shows the calculated tidal prisms and their errors. The expected increase of the tidal prism between 1969 and 1986 is clearly seen. This increase is caused only by the increase in the tidal range, because no adjustments on the area of the basin for the moved tidal divide (Figure 5.1) have yet occurred. The increase is $8 \times 10^7 \text{ m}^3$. This is 7 % of the 1986 tidal prism. After 1986, and the completion of the Oester Dam and the Philips Dam, the tidal prism decreases $4.2 \times 10^8 \text{ m}^3$ due to the decreased basin area. This corresponds to 31 % of the previous tidal prism. After 1986 the tidal prism remains fairly stable.

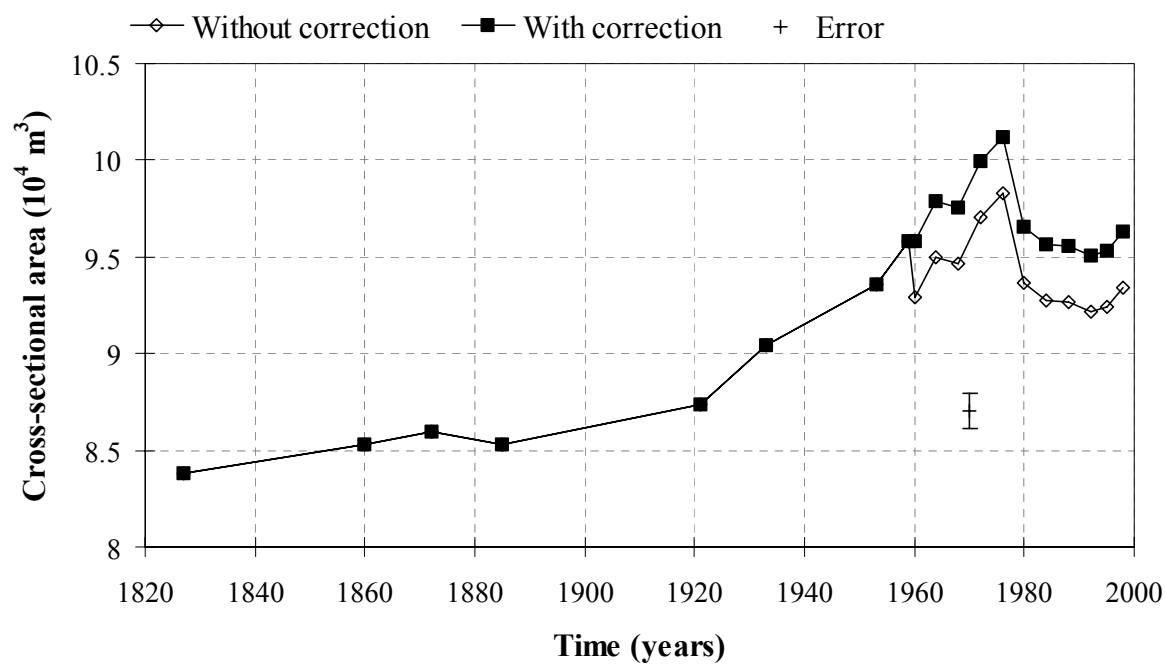


Figure 5.10: The cross-sectional area of the inlet at Harings cross-section location without and with correction for the different calculation methods used.

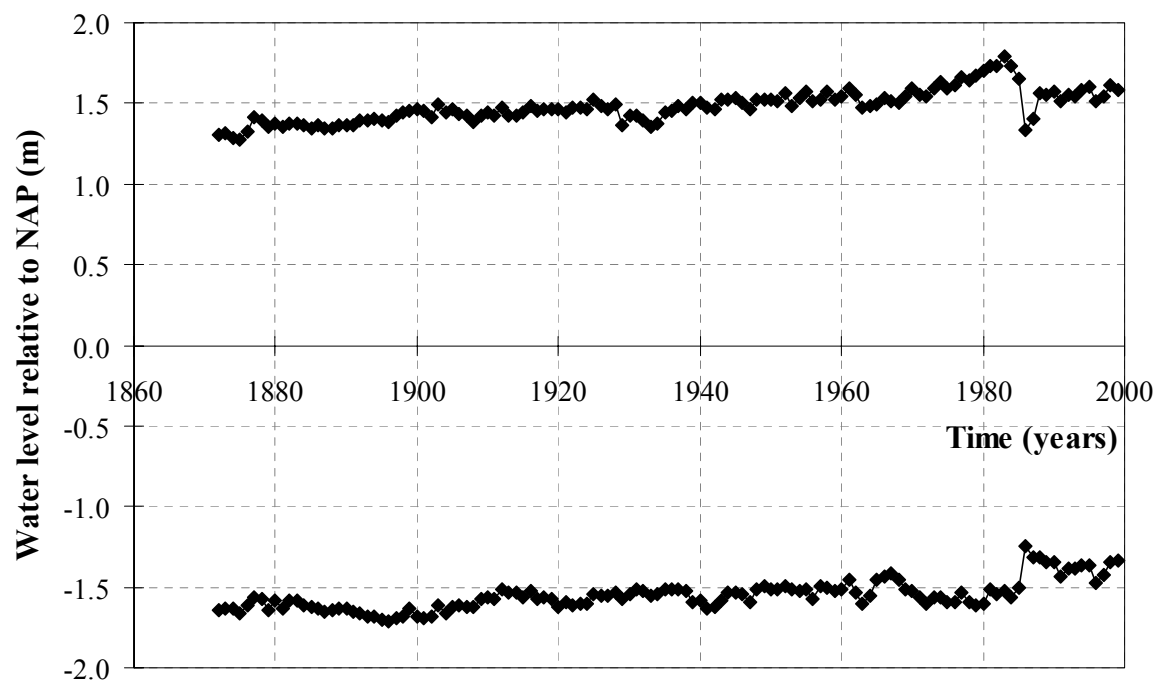


Figure 5.11: The mean annual high and low water level at the location "Stavenisse".

5.4 Computing the Cross-sectional Area of the Eastern Scheldt Inlet

The cross-sectional area was calculated along several locations across the Eastern Scheldt inlet (see Figure 5.12). One of these profiles matches the location of a profile used by Haring to calculate the cross-sectional area for data from 1827 and 1959. By continuing calculations at the same location during this study allows the tracking of cross-section development in the Eastern Scheldt inlet over a time span of almost 170 years. Additional calculations were made along a number of other profiles, including one that follows the storm surge barrier location (Figure 5.12).

The maximum absolute error of these cross-sectional areas is determined by multiplying the width of the cross-sections by the estimated vertical error of 10 cm. Table 5.4 defines the absolute errors of the different profiles. These errors are also indicated in Figures 5.10 and 5.13. The relative error is calculated by dividing the absolute error by the cross-sectional areas.

Table 5.4: The absolute errors of the cross-sectional areas

Profile	Inlet width at NAP (m)	Maximum absolute error (m ²)
0	9100	910
1	16000	1600
2	11150	1115
3	10410	1041
4	10090	1009
5	9800	980
6	9300	930
7	8550	855
8	8630	863

5.4.1 Comparison with Cross-sectional Areas Calculated by Haring (1978)

Figure 5.10 plots the cross-sectional area at Haring's location against time. The sea bed profile can be seen in Appendix D1.

The cross-sectional area along this profile generally increased from 1827 to 1976, although it decreased slightly in 1876. The increase in cross-sectional area indicates that velocities through the inlet generally exceeded the equilibrium velocity for the inlet. It appears likely that the tidal prism probably increased during this period. Increases in the tidal prism could be caused by an enlargement of the basin or by an increase in tidal range. An increase in the tidal range could be related to the sea level rise. Figure 5.11 shows this possibility using the MHW and MLW levels and the tidal range at Stavenisse. The small decrease in cross-sectional area observed in 1876 could have been caused by the construction of the Kreekrakdam in 1867 (see Section 2.1.2), that could have caused a small decrease in tidal prism (see Figure 5.11).

A decrease in cross-section can be observed after 1976. This decrease is believed to be mainly caused by the construction of the working island Neeltje Jans. The small increase in cross-

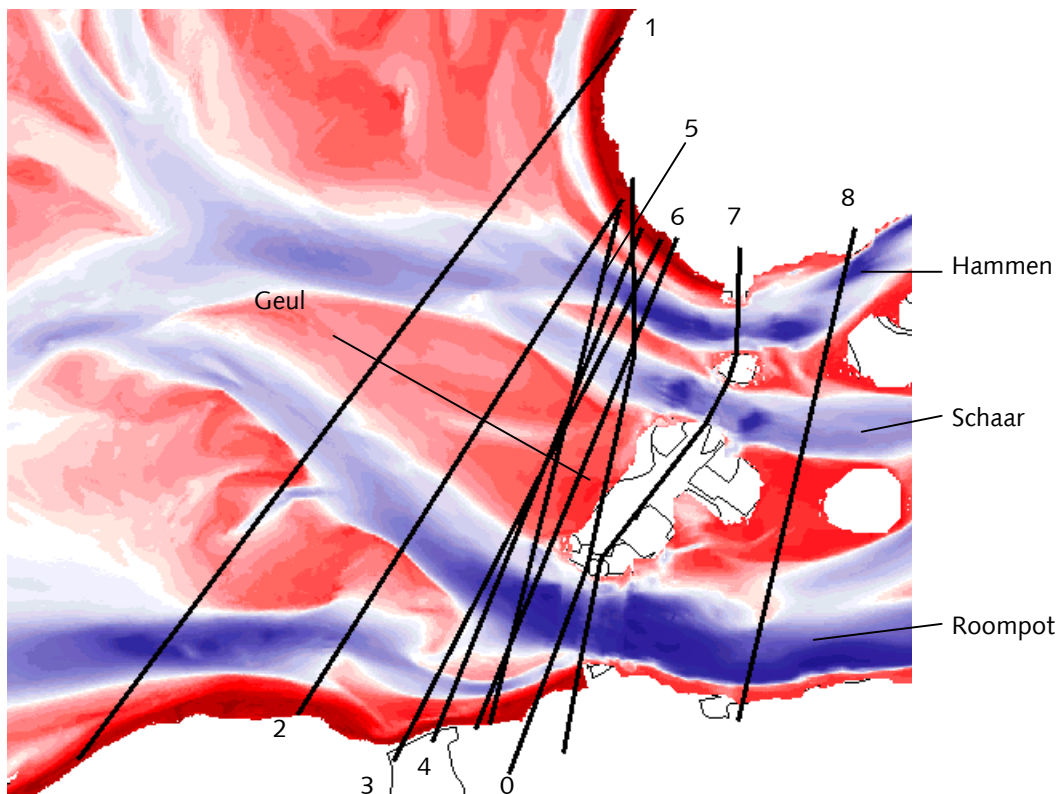


Figure 5.12: Locations of the profiles in the inlet

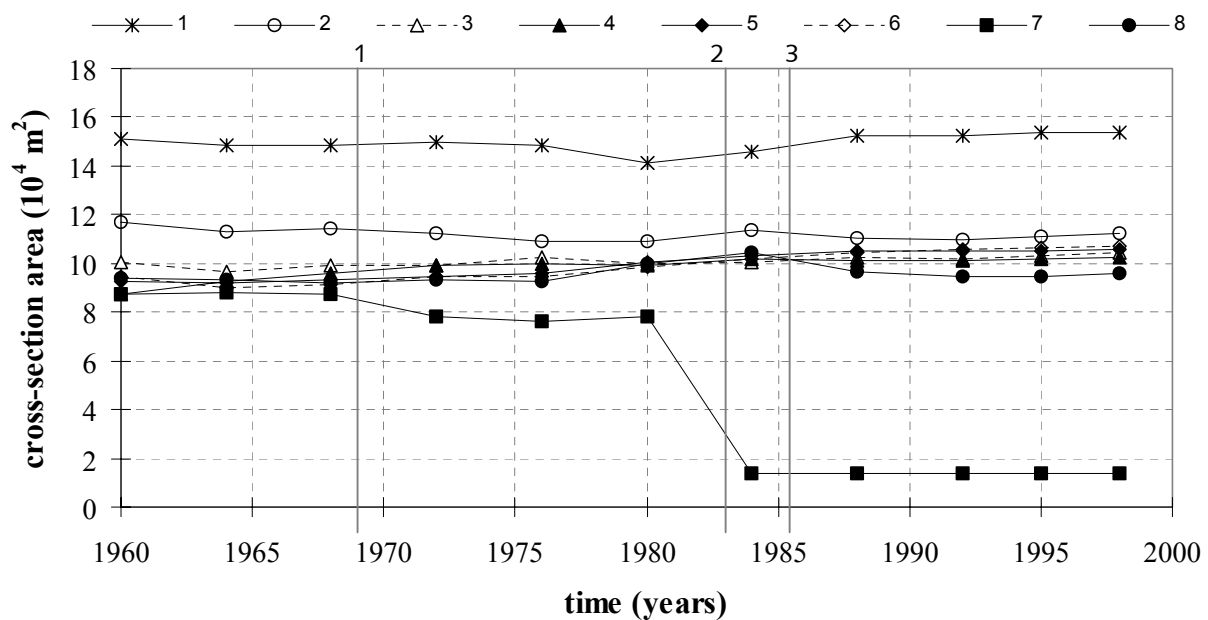


Figure 5.13: The development of the cross-sectional areas at different locations (1. Volkerak Dam (1969), larger basin area, 2. Start placing piers in inlet (1983), 3. Smaller basin area and cross-sectional area of the inlet (1986))

sectional area since 1988 is probably caused by the erosion resulting from turbulent currents in areas around the storm surge barrier.

5.4.2 Other Profiles

Figure 5.13 illustrates the cross-sectional areas of the locations 1 to 8 (located in Figure 5.12). The seabed profiles for these profiles are displayed in Appendix D1.

Profile 1 shows a decrease of the cross-sectional area until 1980 and an increase after 1980. This corresponds to the expected development of the outer tidal delta, namely an increase in sand volume until 1980 and a decrease of the sand volume after 1980.

Profile 2 also shows a net decrease until 1980 and a net increase from 1980 to 1998. It can be assumed that cross-section 1 and 2 are part of the outer tidal delta area and do not represent conditions within the inlet area.

Profile 3 and 4 both cross the old inlet area of the Veersegatmeer. These profiles illustrate the combined development of the Eastern Scheldt and the Veersegat inlets. Since our interest is restricted to the Eastern Scheldt inlet, profile 3 and 4 are ignored.

Profiles 5 and 6 show a similar development pattern. The cross-sectional areas increase after 1964. The rate of increase slows down after 1988. In reference to the discussion made in section 5.1, these profiles are located in areas affected by turbulent currents around the inlet.

Profile 8 shows a large increase in cross-sectional area from 1976 to 1984, after which the cross-sectional area decreased. This profile is located inside the basin behind the axis of the storm surge barrier. Thus it is not surprising that the pattern of cross-sectional development shown by profile 8 correspond to the expected development within the Eastern Scheldt basin.

From these evaluations, it can be concluded that only profiles 5 and 6 reflect conditions in the unprotected parts of the inlet area.

5.4.3 The Dam Location

The dam profile, profile 7, is the most important one. This profile has the smallest cross-sectional area. It therefore largely determines the maximum value of the tidal volumes. Profile 7 shows a decrease in cross-sectional area from 1968 to 1976. This decrease is partly caused by the closure of the "Geul" channel, that resulted in a reduction of the area of about 11646 m². According to the assessments given in section 5.1, erosion in the channels was expected during this period. In contrast a decrease in cross-sectional area of 11072 m² was observed between 1968 and 1976. Because this decrease in cross-sectional area is slightly less (about 574 m²) than should be caused by the closure of the "Geul" channel, it may be concluded that the expected erosion in the channels also occurred. After 1972, the cross-sectional area remains fairly constant until the period from 1983 to 1986. During this time, the piers and gates of the storm surge barrier were placed across the various channels forming the inlet. Accordingly, over this period the cross-sectional area is reduced to 14000 m² (Rijkswaterstaat, 1994). This is a decrease of 64000 m², a reduction of 82 % from its previous size.

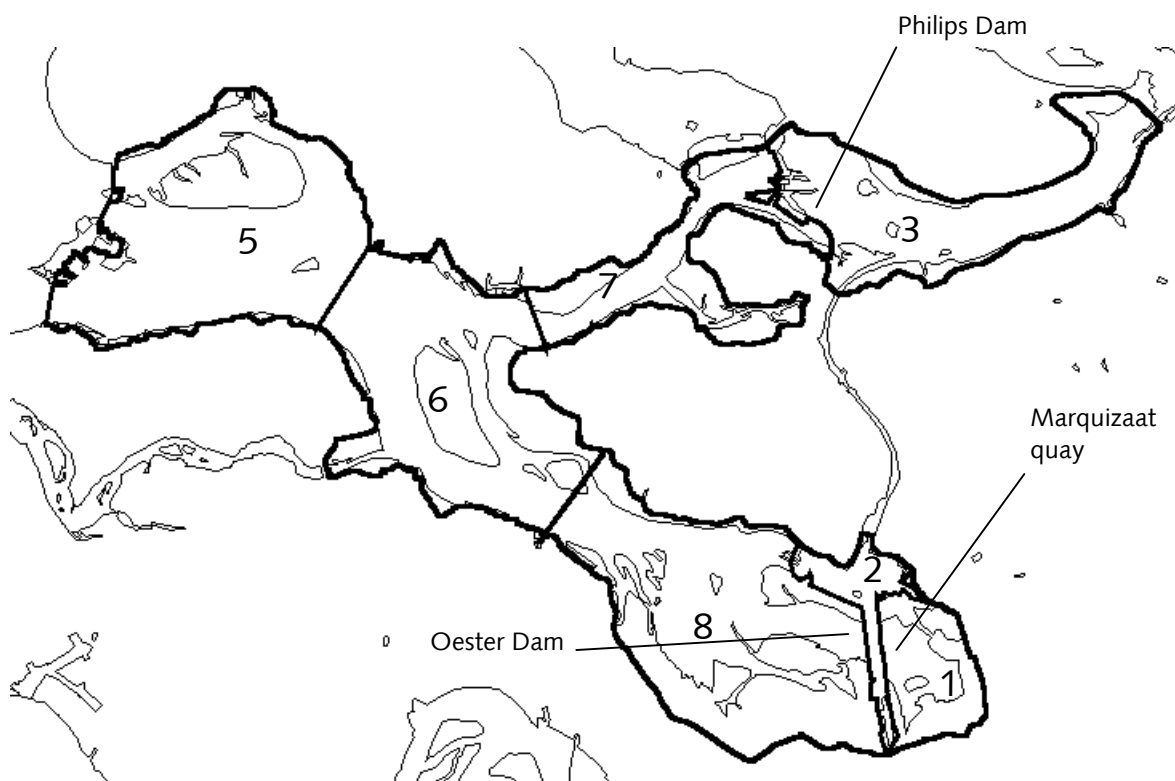


Figure 5.14: The different calculation sections of the basin.

Table 5.5: water surface area in m^2 at NAP.

Surface area at NAP ($10^7 m^2$)	1	2	3	5	6	7	8	total basin
1968	1.32	1.15	4.77	10.37	8.98	2.87	9.41	38.86
1983				9.49	8.71	2.82	9.16	30.17
1994				9.86	8.86	2.93	9.34	31.00

Table 5.6: The absolute error of the surface area.

absolute error ($10^7 m^3$)	1	2	3	5	6	7	8	total basin
1968	0.13	0.12	0.48	1.04	0.90	0.29	0.94	3.89
1983				0.95	0.87	0.28	0.92	3.02
1994				0.99	0.89	0.29	0.93	3.10

Table 5.7: The relative error of the volume of the basin.

relative error	1	2	3	5	6	7	8	total basin
1968	8.06%	3.93%	2.03%	0.94%	1.02%	1.25%	2.03%	1.32%
1983				0.82%	0.97%	1.19%	2.01%	1.10%
1994				0.85%	0.99%	1.22%	2.02%	1.12%

5.5 Calculation of the Volume of the Eastern Scheldt Basin

GIS methods were used to calculate the volume of the Eastern scheldt basin located below NAP. Calculations were made for each of the seven sections shown in Figure 5.14. Bathymetric data were available for sections 1, 2, and 3 for 1968. By the time of the 1983 and 1994 surveys, these sections were cut off from the Eastern Scheldt basin by the completed Philips Dam, Oester Dam, and Marquizaat quay.

Table 5.5 provides the calculated surface areas of the sections and the total basin at NAP. The surface area at NAP first decreases from 1968 to 1983 and then increases again.

The absolute error was computed by multiplying the estimated vertical error of 10 cm by the surface area of the basin at NAP. This process was applied to the calculations of the volumes for the individual sections and the total basin area. Table 5.6 provides the absolute error for the sections and for the total basin. The relative error, shown in Table 5.7, is calculated by dividing the absolute error by the calculated basin volume, shown in Table 5.8.

Table 5.8 provides the calculated volume of the basin below NAP. Table 5.9 summarises the change in basin volume. Table 5.9 shows that the water volume of the total basin increases from 1968 to 1994, the basin is eroding below NAP. The increase of water volume within the basin from 1968 to 1983 is $7.13 \times 10^7 \text{ m}^3$. This is significantly larger than the error margin and can therefore be attributed to erosion within the basin. This erosion was expected according to the assumptions presented in Section 5.1. The volume change from 1983 to 1994 of $1.92 \times 10^7 \text{ m}^3$ is within the error margin and therefore may not be significant. According to the theoretical evaluations given in Section 5.1, sedimentation was expected during this period.

Evaluation of the trends for the separate sections, it can be concluded that Sections 5, 6 and 7 are eroding from 1968 to 1983, with most erosion occurring in Section 5. The other changes are too small to be considered significant, and may be due to calculation or measurement errors.

Table 5.8: The volume of water in the basin under NAP.

volume below NAP (10^7 m^3)	1	2	3	5	6	7	8	total basin
1968	1.64	2.93	23.54	110.25	87.67	22.88	46.23	295.14
1983				115.02	89.83	23.70	45.61	274.16
1994				116.00	89.79	24.14	46.15	276.08

Table 5.9: The amount of erosion (negative) and sedimentation in the periods 1968-1983 and 1983-1994 with reference level NAP.

	5	6	7	8	total basin	sections 5, 6, 7 and 8
1968 - 1983	4.77	2.16	0.82	-0.61	-20.98	7.13
1983 - 1994	0.98	-0.04	0.43	0.54	1.92	1.92

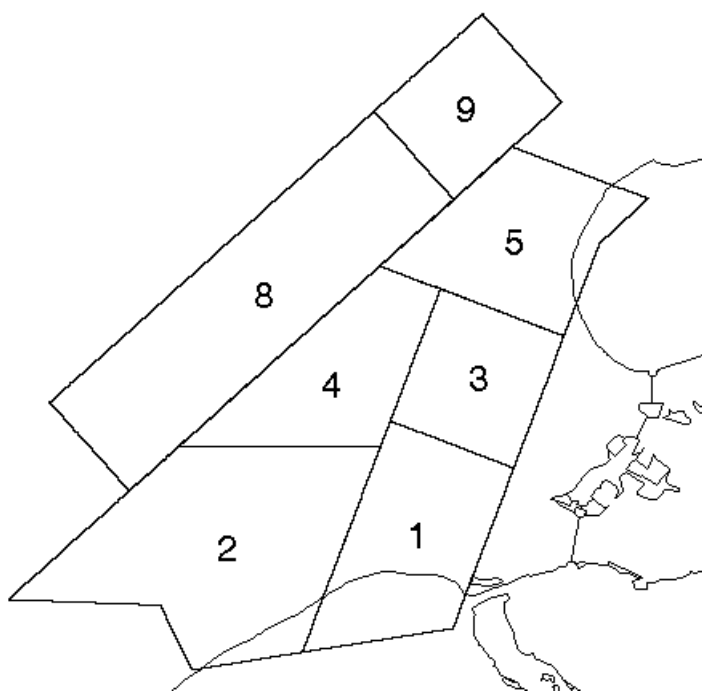


Figure 5.15: The standars compartments used by Haring (1948).

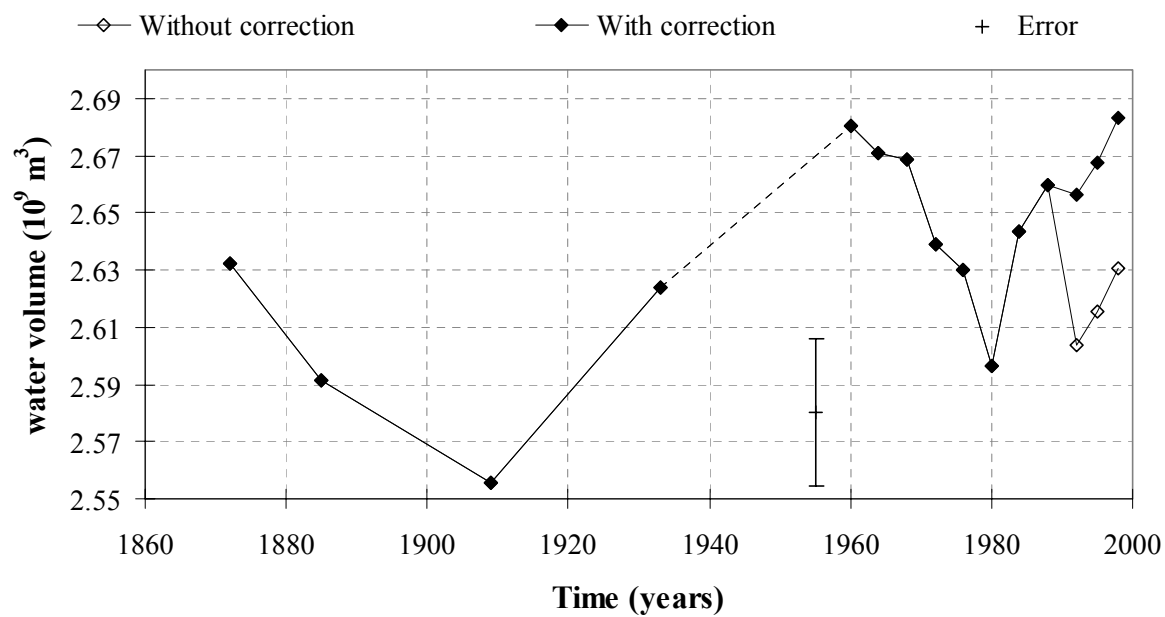


Figure 5.16: Water volume between the grid and reference level NAP.

5.6 Calculation of the Volume of the Outer Tidal Delta

The water volumes of the outer delta must be calculated within certain defined areas that defines the “limits”, or spatial extend, of the outer tidal delta. This extend can be defined in two ways.

Haring (1948) performed manual calculations of the outer tidal delta volumes by defining a series compartments having linear sides (Figure 5.15). By continuing Haring’s calculations with more recent observations, the development of the outer tidal delta can be seen over a time span of 125 years. Therefore some calculations were performed with more recent observations tabulated according to the compartments defined by Haring.

However, the use of arbitrary standard compartments does not completely allow the tracking of the true evolution of the outer tidal delta volumes. At different times, some of the compartments may extend beyond the limits of the delta, or the delta may extend beyond the compartments. These changes may vary from one time period to another as the delta position and shape changes. A more accurate tracking of the evolution of the outer tidal delta volume may be possible if the extend of the outer tidal delta is defined by a morphological boundary that is determined for each time period.

5.6.1 Haring’s (1948) Standard Compartments

Haring (1948) calculated the volume of the outer tidal delta of the Eastern Scheldt and Grevelingen for several years between 1873 and 1939. The calculations had to be done by hand, so the area was divided in standard compartments with linear boundaries (Figure 5.15). With the use of old sounding maps produced by the hydrographic service, within every compartment Haring constructed depth profiles perpendicular to the channels, and spaced 250 m apart. He calculated the volume by multiplying the cross-sectional area of every profile by the spacing (250 m). He then summed these values and made some adjustments for the compartment corners.

Figure 5.16 shows the calculated water volumes for the outer tidal delta, based on for the period 1873 to 1998. For the more recent time periods, an absolute error for this volume was estimated by multiplying the surface area of all compartments and the total surface area at NAP with the estimated vertical error of 10 cm. Appendix F3.1 contains these absolute error calculations. The overall error for the recent time period is about 1 % and is indicated in figure 5.16. The measurement error from 1872 to 1933 is probably larger, but is unknown.

Figure 5.16 shows a clear trend in the development of the water volume overlying the outer tidal delta. The volume of water overlying the outer tidal delta first decreased until 1910 (corresponding to delta growth) and then increased until 1960 (corresponding to delta erosion). This fluctuation in delta volume is probably related to an increase in tidal volume. The water volume decreases, or the outer tidal delta increases, from 1960 to 1980, while after 1980 the water volume increases, indicating an erosion of the outer tidal delta. These trends were predicted in the theoretical presentations made in Section 5.1.

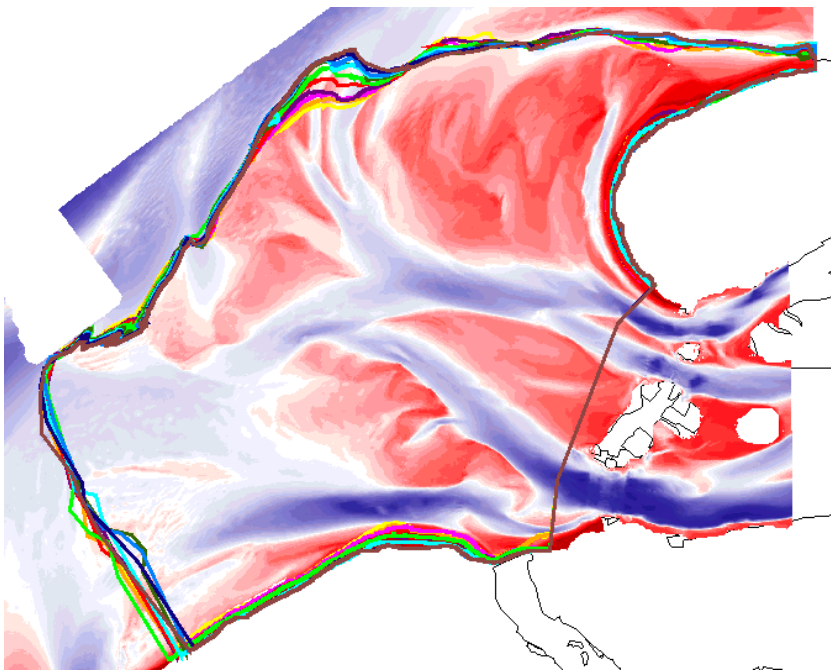
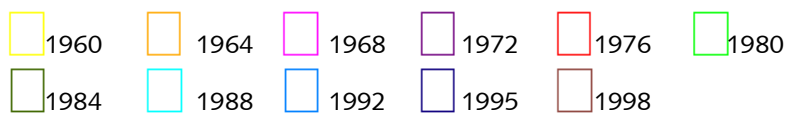
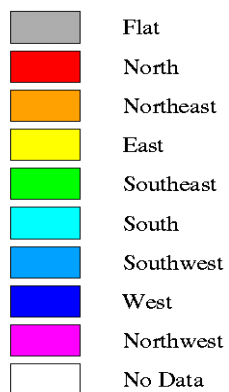


Figure 5.17: The morphological boundaries of the grids from 1960 to 1998.

Slope direction



Slope angle (degrees)

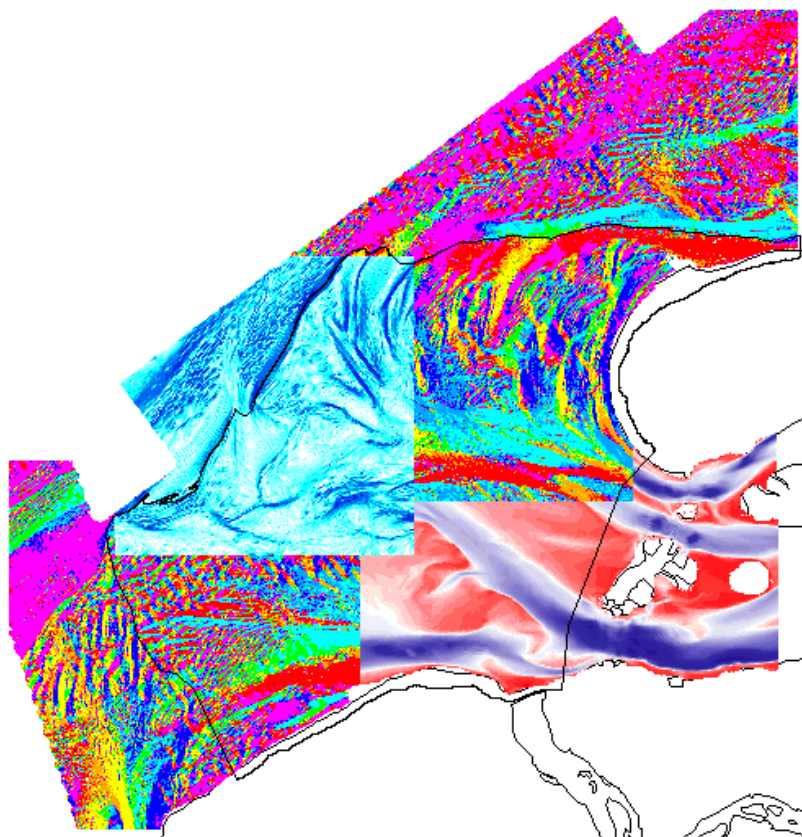
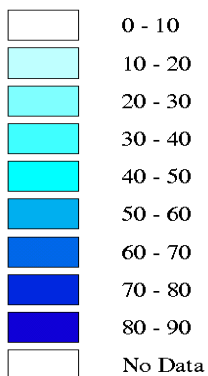


Figure 5.18: Slope direction and slope angle maps used to define the morphological boundaries

An initial analysis of the data produced a remarkable drop in overlying water volumes between 1988 and 1992. This drop is illustrated in Figure 5.16 by a dashed line labeled "without correction". Such a drop was not expected from the theory, and appeared suspicious. The raw data were requested and examined. Examination of the erosion-sedimentation patterns over the vertical profiles for the different compartments (collected in Appendix F4.1) revealed that compartment 8 has a sudden decrease in water volume between 1988 and 1992. This large decrease does not fit with the erosion-sedimentation patterns of the surrounding years. Further analysis revealed that this sudden drop in overlying water volume was caused by a sudden change in the bathymetric grids between the 1988 grid and those for the years 1992, 1995 and 1998. This volume difference was $5.9 \times 10^7 \text{ m}^3$, so this volume was used to correct the volumes of 1992, 1995, and 1998. This correction substantially corrected the long-term trend to a more likely pattern. The result of this correction can be seen in Figure 5.16 where the revised trend for 1992, 1995, and 1998 is continued as the solid line.

5.6.2 Morphological Boundaries

The morphological boundaries of the Eastern Scheldt outer tidal delta are not very distinct. The Eastern Scheldt outer tidal delta merges with other outer tidal deltas to both the north and the south. Its western limit lies within the North Sea. The Dutch Coast and the Eastern Scheldt storm surge barrier form its eastern boundary.

A channel defines the northern boundary of the Eastern Scheldt outer tidal delta. This channel controls the lateral deposition of sediment and thus the middle of the channel is taken as boundary between the two deltas. The middle of the channel was established by examining the directions of the slopes in the channel sides. The location of the channel centerline was traced and digitized by hand using ArcView (Figure 5.18).

The boundary between the seabed of the North Sea and the outer tidal delta was located where the steeper slopes of the rim of the delta merge into the gentler slope of the seabed. This condition is very difficult to establish, so the NAP -10 m contour was taken as this outer boundary. This contour appears to closely approximate the location of the slope change (Figure 5.18).

The southern boundary of the Eastern Scheldt outer tidal delta again falls along a contact between two deltas. Because deltas are shaped as a cone, the boundary between the two deltas has been taken at the location where the slopes of the two conic shapes converge. Because the slopes are very gentle, this boundary is not readily identified by looking at the dips of the slopes. The boundary is visible if you look at the direction of the smaller channels. This boundary was also traced and digitized manually using ArcView.

The boundary between the outer tidal delta and the inlet of the Eastern Scheldt is taken at the location where the behaviour of the cross-section discussed in Section 5.4 changes from inlet to outer tidal delta. This location is between profiles 2 and 3 in the south and profiles 2 and 5 in the north (see Figure 5.12). Figure 5.17 shows this chosen location.

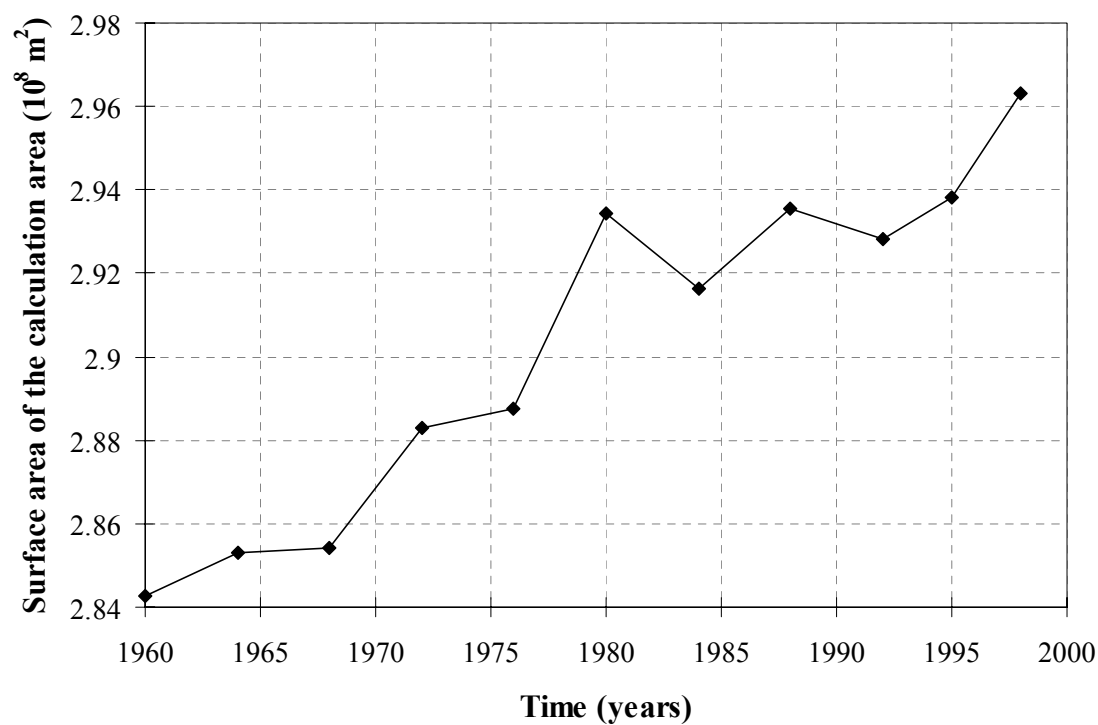


Figure 5.19: The surface area at NAP of the calculation area with the morphological boundaries changing over time.

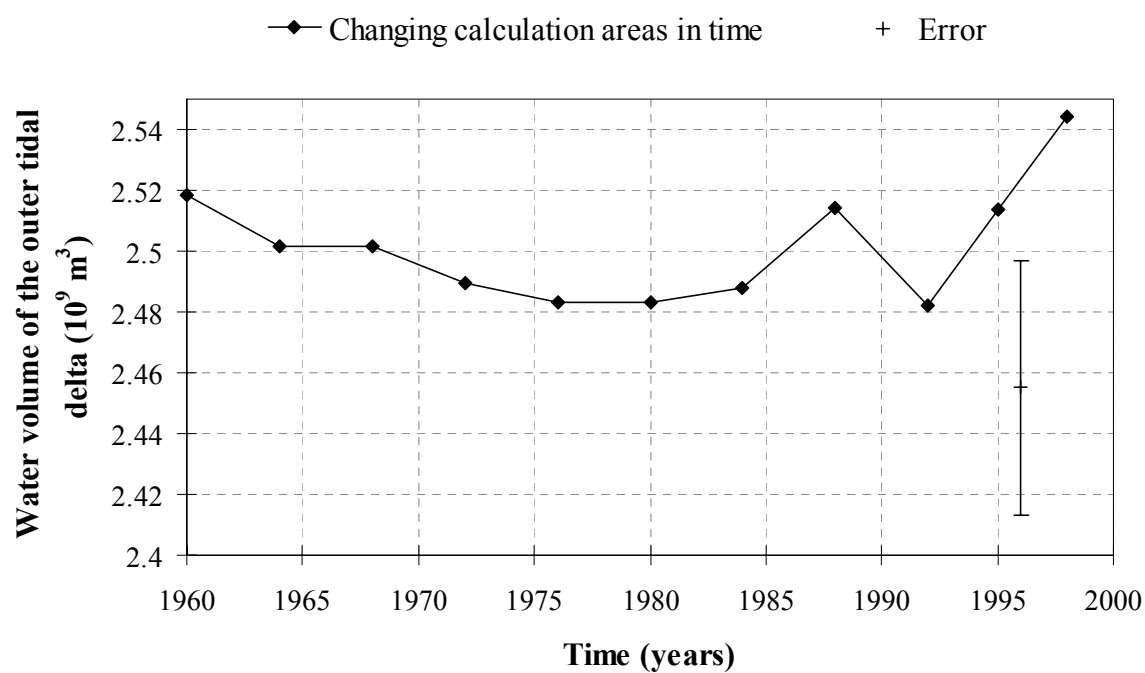


Figure 5.20: The water volume of the outer tidal delta below NAP calculated with the morphological boundaries changing over time.

The coastal boundary was defined slightly differently for different time periods because of the characteristics of the existing data sets. Table 5.10 shows the shallowest depth at which the coastal boundary is still continuous for each time period.

Table 5.10:

The shallowest depth at which the coastal boundary is continuous.

NAP - 3.5 m	NAP -1.5 m	NAP +1 m
1960	1964, 1968	1972, 1976, 1980, 1984, 1988, 1992, 1995, 1998

5.6.3 Discussion on the Calculation Boundaries

The main objective when calculating the volume of the outer tidal delta is to accurately account for the volume of all the morphological units belonging to the outer tidal delta. By using morphological boundaries that have consistent definitions, although they change over time, all the morphological units of the outer tidal delta are included in each analysis. This is useful when morphological units are moving and evolving. An example where this gives relevant results is the outer tidal delta of the Marsdiep (Mulder, 1999).

The volume change of the water overlying the outer tidal delta, shown in Figure 5.20, does not correspond to the changes in the surface area of the outer tidal delta, shown in figure 5.19. The surface area of the outer tidal delta shows a fairly constant and continual growth over time (Figure 5.19), but the water volume overlying the delta (Figure 5.20) shows a more irregular evolution with two minima occurring in about 1980 and 1992. It can be concluded that the changes in morphology have a greater effect on the delta volume than its growing surface area. In Figures 5.19 and 5.20 shows that the use of changing morphological boundaries provides a smoother, more averaged, picture of the evolving volume.

Despite this observation, it appeared advantageous to use a single fixed area covering all the morphological units of the outer tidal delta, because a fixed area can be compared from one time period to another. The analysis in the next chapter use the morphological boundary of 1998 as the common (fixed) boundary of the outer tidal delta.

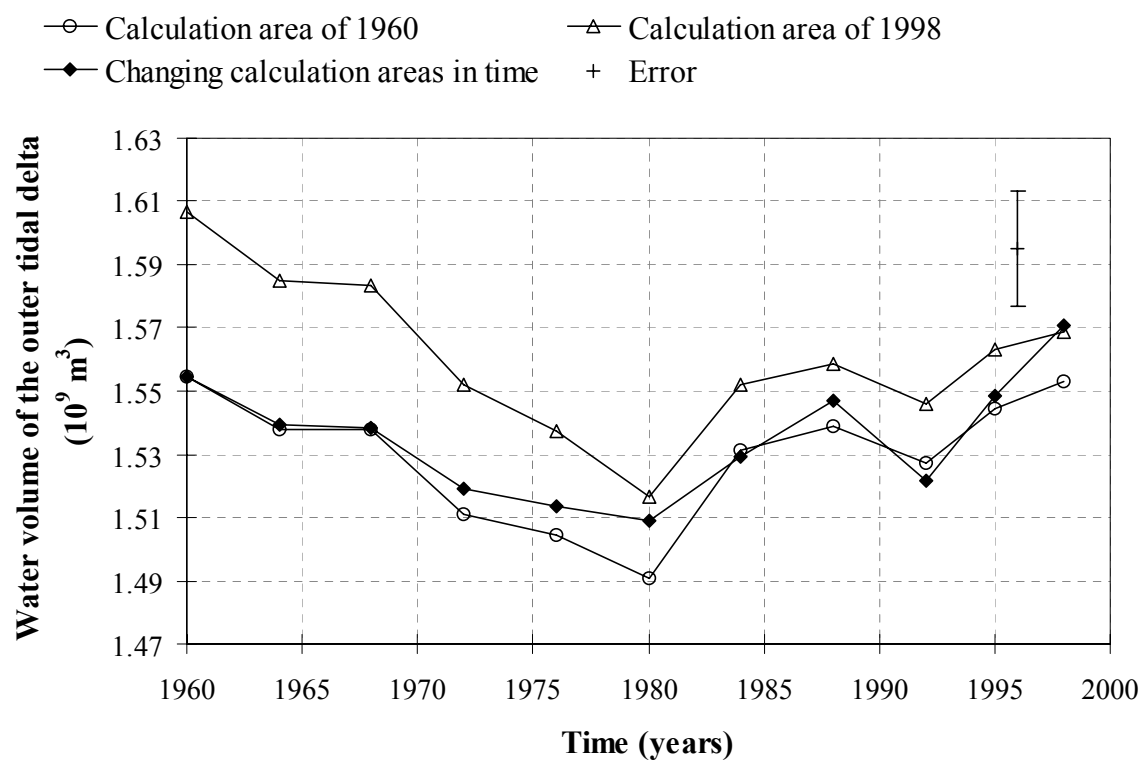


Figure 5.21: The water volumes of the outer tidal delta below NAP -3.5 m calculated with three different boundaries.

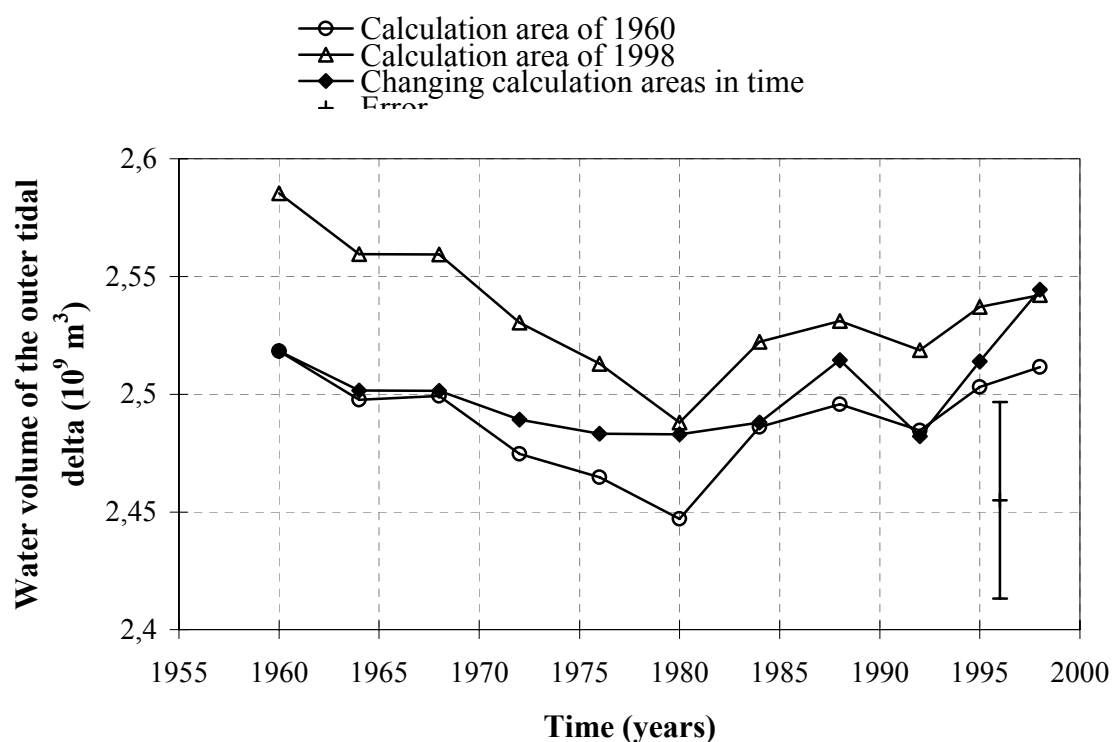


Figure 5.22: The water volumes of the outer tidal delta below NAP calculated with three different boundaries.

5.6.4 Resulting Volume Calculations

The water volume of the outer tidal delta was calculated using a morphological boundary that changed over time, and also using a morphological boundary that was fixed over time. Two such boundaries were used, the boundary enclosing the largest area (the boundary of 1998) and the boundary enclosing the smallest area (the boundary of 1960). Figure 5.21 shows the calculated volumes of the outer tidal delta below the elevation NAP -3.5 m with these three boundaries. Figure 5.22 shows the equivalent calculated volumes below elevation NAP. The volumes are also calculated below NAP -3.5 m, because the bathymetric data along the shoreline above NAP -3.5 m for the years 1960, 1964 and 1972 are absent. This absence of data may result in differences in water volume overlying the grids.

The absolute error was calculated by multiplying the surface area at NAP by the estimated vertical error of 10 cm. The relative error is calculated by dividing the absolute error by the calculated outer tidal delta water volumes overlying the grids. The errors of each year for the used boundaries are provided in Appendix F3.2. The maximum relative error for the calculated volumes below NAP -3.5 m is 1.7 %, while the error is 1.15 % for the calculated volumes below NAP.

Figures 5.21 and 5.22 show that the volume of water overlying the outer tidal delta decreases from 1960 to 1980 and increases from 1980 to 1998. This corresponds to a growth in the delta volume between 1960 and 1980, and a general erosion of the delta since 1980. This pattern corresponds to the theoretical projections made in Section 5.1. Table 5.11 summarizes the changes in volume of water overlying the outer tidal delta from 1968 to 1980 and from 1980 to 1998 can be seen

An odd decrease in water volume can be seen for 1992 in both Figures 5.21 and 5.22. The vertical sedimentation/erosion profiles provided in Appendix F4.2 show that this unexpected decrease can also be seen in the vertical sedimentation profile. The sedimentation from 1988 to 1992 shows a clear deviation from the surrounding vertical profiles. The cause of this deviation is not yet found, but it can be assumed that this anomaly is caused by an error. The error can be compensated for using the vertical sedimentation/erosion profiles. This can only be done for the calculations done with the morphological boundaries changing over time, because the deviations of the calculations done with the fixed boundaries are not distinct enough. The volume of 1992 calculated with the changing morphological boundaries over time should be increased with $3.6 \times 10^7 \text{ m}^3$.

Table 5.11: The change in water volume of the outer tidal delta in 10^7 m^3 .

	Calculation area of 1960 (smallest)		Calculation area of 1998 (largest)		Changing boundaries over time	
	NAP -3.5 m	NAP	NAP -3.5 m	NAP	NAP -3.5 m	NAP
1980 - 1968	-4.72	-5.23	-6.69	-7.12	-2.96	-1.84
1998 - 1980	6.20	6.46	5.21	5.40	6.20	6.14
1984 - 1968	-7.02	-1.32	-3.16	-3.71	-9.36	-1.34
1995 - 1984	1.32	1.70	1.11	1.48	1.91	2.59

6 Discussion of Results

Evaluation of the evolution of the coastal morphology of the Eastern Scheldt tidal basin allows the detection of trends and changes to morphologic parameters that may define the degree to which the overall system is approaching the state of large-scale (dynamic) equilibrium. Comparison of these parameter changes and trends to published empirical relationships may allow the prediction of the length of time required for the system to reach equilibrium.

6.1 Development of Eastern Scheldt; 1820 - Equilibrium Situation

The earliest quantitative records of conditions within the Eastern Scheldt estuary date from the 1820's. Since that time a series of bathymetric and hydrodynamic surveys have provided data that can be used to track and evaluate the coastal morphology in the region.

Although human influences began to affect the Eastern Scheldt estuary after about 1000 AD (see section 2.1.2), such influences were relatively modest because the population lacked the imperative or the capabilities to construct large enough dams or dikes to significantly influence the coastal morphology.

Human influences on the coastal morphology slowly grew during the 1800's. The tidal divide between the Eastern and Western Scheldt silted up and was closed in 1867 with the Kreekrakdam. The last hydraulic connection between the Eastern and Western Scheldt was closed in 1871 with the completion of the railway embankment along the Sloe Dam (Figure 2.4).

Truly important human influences followed the great storm of 1953 that left large parts of the southwestern Netherlands flooded. In response to this catastrophe, the Delta Project was initiated. This project undertook the construction of a series of dams that closed many inlets and shortened the exposed coastline from more than 700 km to just 25 km (see Section 2.1.3). The Delta Project construction works started to have direct impact on the Eastern Scheldt estuary in about 1969. Installation of the storm surge barrier across the inlet of the Eastern Scheldt began in 1983. The storm surge barrier and two other dams in the estuary, the Oester Dam and the Phillips Dam, were completed in 1986.

Table 6.1 summarises the trends and changes to critical morphological parameters and human influences within the Eastern Scheldt area from 1969 to 1995. The data summarized for the period during which the initial influences of the Delta Project could be expected (1969 – 1983) and for the period influenced by the installation and operation of the storm surge barrier (1983 – 1995).

Overall, the data suggest that the coastal morphology of the Eastern Scheldt tidal basin is slowly trending toward equilibrium. Construction of the various components of the Delta Project caused some perturbations in several parameters, but subsequently the trend of evolution has mostly reverted to the trend observed in earlier times.

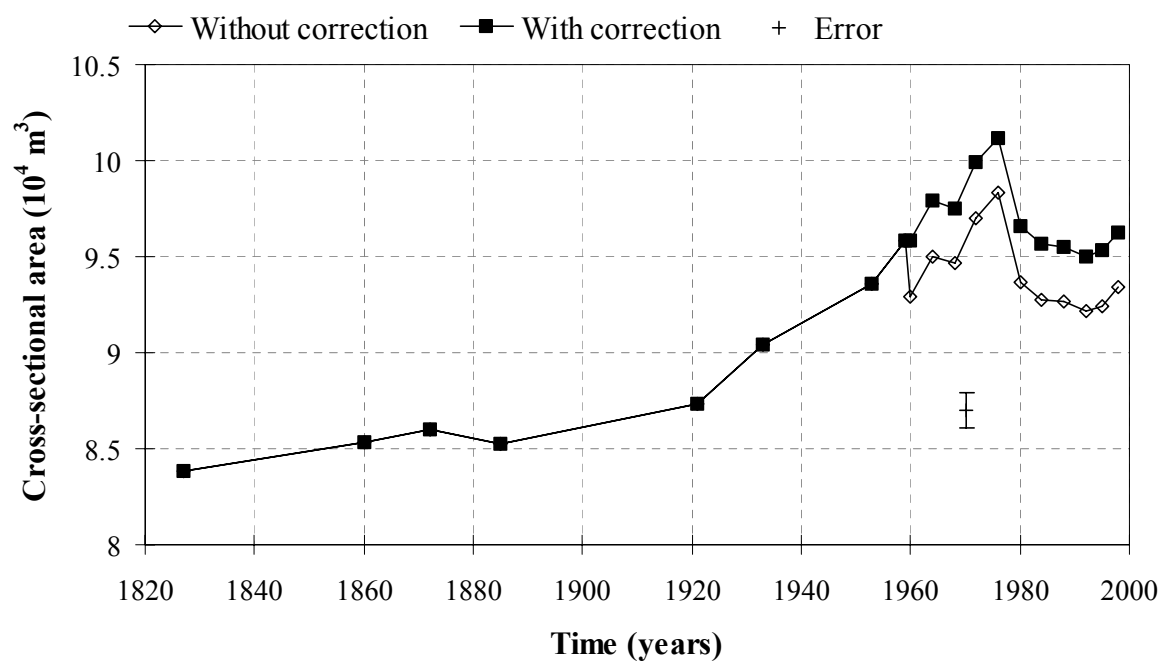


Figure 6.1: The cross-sectional area of the inlet at Harings location.

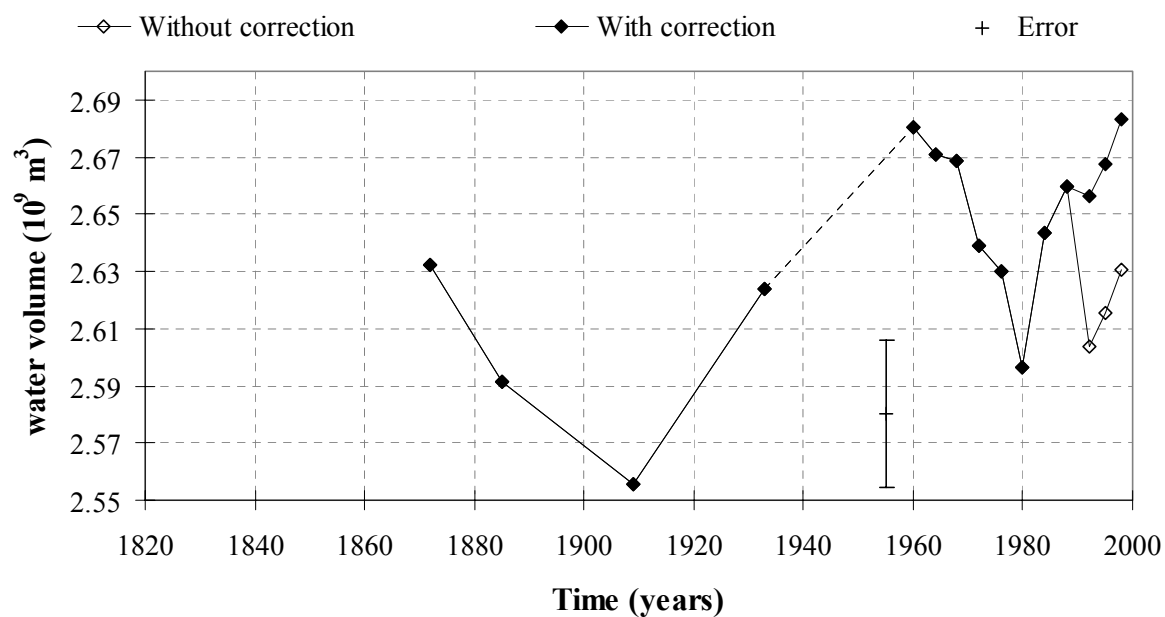


Figure 6.2: Volume of water between the grid and the NAP reference level

6.1.1 Natural Development of the Tidal Volume between 1820 and 1969

Haring (1967) evaluated historical data and quantified the coastal development of the Eastern Scheldt in the period prior to 1960.

Figure 6.1 shows the cross-sectional area of the Eastern Scheldt inlet from 1927 to the present. The increase in cross-sectional area from 1827 to 1960 indicates that over this period the tidal velocities through the inlet were larger than the equilibrium velocities. Erosion and enlargement of the inlet resulted. These larger velocities could have been caused by an increase in tidal prism. This, in turn, could have resulted from a gradually rising sea level or a change in tidal regime.

Figure 6.2 shows the trend in water volume that overlies the outer tidal delta from 1873 to 1998. These volumes increase when the tidal delta is eroded, and decrease when the tidal delta grows larger. A decrease in water volume from 1873 to 1910 thus suggests outer tidal delta growth, while an increase in water volume from 1910 to 1960 suggests erosion of the outer tidal delta. These trends suggest a gradual increase in tidal volume in the period 1910 to 1960.

The increase in the cross-sectional area of the Eastern Scheldt inlet (Figure 6.1) could be related to the observed sea level rise. However the trends do not coincide very well. Also the trends in the volume of water overlying the outer tidal delta do not suggest that sea level rise is the dominant factor, but do suggest that the increased tidal volumes are the major influence. Sea level rise may be the principle factor causing the increased tidal prisms and hence the increased tidal volumes through the inlet. More research is needed to confirm this concept. It is, however, of interest to note that human-induced changes, especially those of recent years during the Delta Project, are of similar orders of magnitude as the natural phenomena that caused changes to the system in the past.

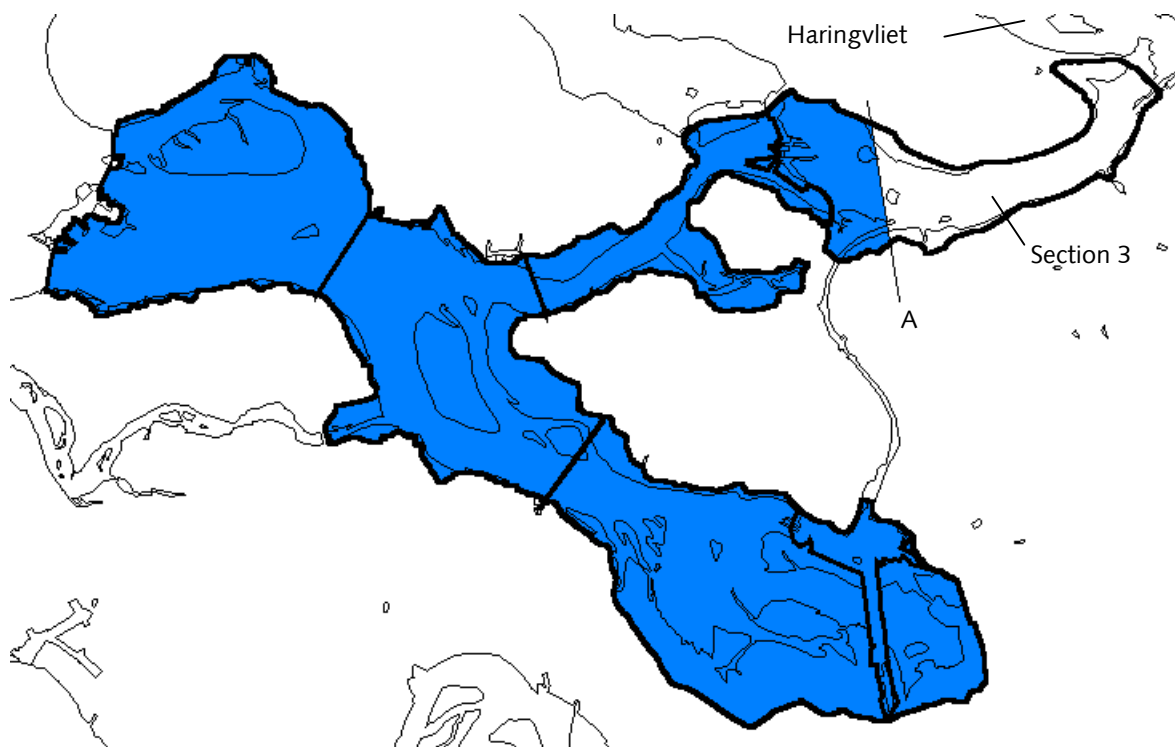


Figure 6.3: The total area of the Eastern Scheldt basin before the Delta Works. Location A is the natural tidal divide between the Haringvliet and the Eastern Scheldt.

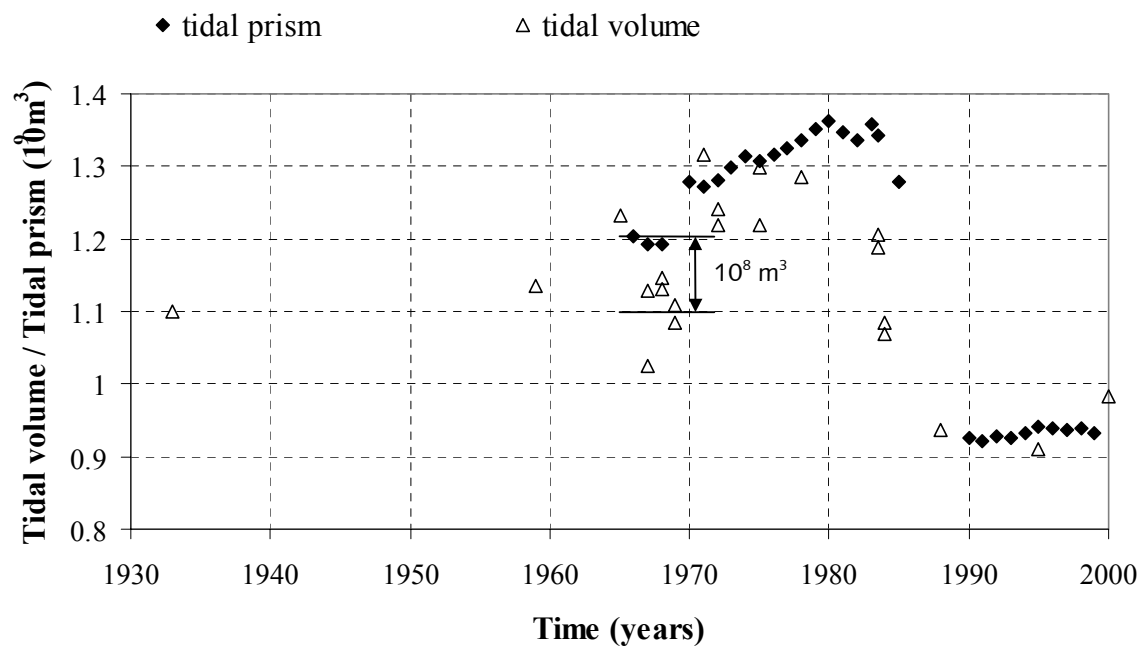


Figure 6.5: The tidal prism and tidal volume against time.

6.1.2 Effects of an Increasing Tidal Volume in the Period 1969 - 1977

During this period, changes in the coastal morphology in the Eastern Scheldt area appear to be largely influenced by an increase in the tidal prism. The various effects to the system components are discussed below.

Basin Area

Due to the construction of the Volkerak Dam, the basin area increased in 1969 as can be seen in Figure 5.1b and 5.1c.

The location of the natural tidal divide between the haringvliet and the Eastern Scheldt can be estimated using the tidal prism and tidal volume data. Knowing that the tidal prism should be equal to half of the tidal volume, Figure 6.4 shows that half of the tidal volume is 10^8 m^3 smaller than the tidal prism. The tidal prism is thus 10^8 m^3 too large, because the total area of section 3 is used to calculate the tidal prism, instead of only the part south of the tidal divide. The section 3 used for tidal prism calculations before 1969 should thus be $3.77 \times 10^7 \text{ m}^2$ smaller. This is 10^8 m^3 divided by a tidal range of 2.65 (section 3, 1968). Therefore, about the southern 20 % of the total area ($4.77 \times 10^7 \text{ m}^2$) of Section 3 was probably part of the Eastern Scheldt basin. The estimated location of the natural tidal divide is shown in Figure 6.3.

The total basin area prior to 1968 was $3.51 \times 10^8 \text{ m}^2$. Following closure of the Volkerak Dam in 1969, the basin area became $3.89 \times 10^8 \text{ m}^2$, an increase of 10.8 %.

Tidal Range

Not only did the construction of the Volkerak Dam cause an increase in basin area, it also changed the tidal range in the Sections 3 and 7. The tidal range increased by 0.4 m in section 7 and by 1 m in section 3 (Figure 5.8). This increase in tidal range is caused by a change in wave characteristics. The Volkerak Dam now reflects the tidal wave, whereas before the tidal wave used to collide gently with the tidal wave in the Haringvliet. This wave reflection causes a marked amplitude increase, especially in Section 3.

Tidal Prism

The increase in tidal range resulted in an increase in tidal prism of $8.6 \times 10^7 \text{ m}^3$. This can be seen in Figure 6.5. Because the smaller basin area due to the natural tidal divide before 1969 is not taken into account in the tidal prism calculations, this increase in tidal prisms shows the increase only caused by the increased tidal range.

The increase in tidal prism caused by the increase in basin area is the difference between tidal volume and tidal prism before 1969. This is 10^8 m^3 (figure 6.5). The total tidal prism thus increased by $1.86 \times 10^8 \text{ m}^3$. This is 16.5 % of the estimated tidal prism in 1968 ($1.13 \times 10^9 \text{ m}^3$).

Tidal Volume

The tidal volume should increase twice as much as the tidal prism, thus $3.72 \times 10^8 \text{ m}^3$. The tidal volume increase was about $3.4 \times 10^8 \text{ m}^3$ between 1969 and 1972 (Figure 6.5). This is an increase of 15 %. The increase differences between tidal volume and tidal prism are probably caused by measurement and calculation errors.

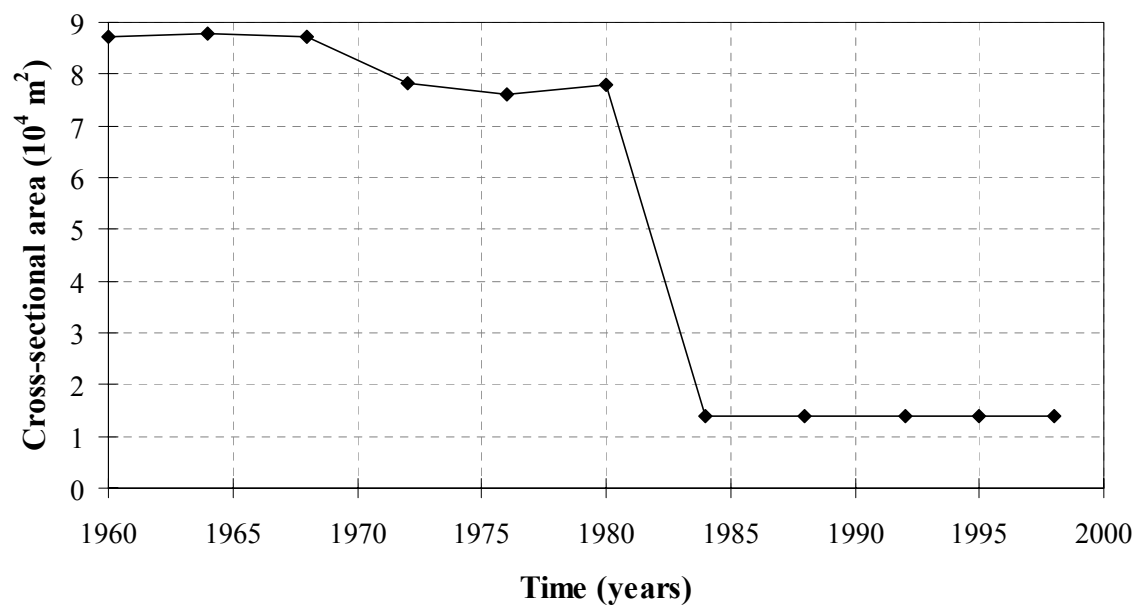


Figure 6.5: The cross-sectional area of the smallest cross-section of the inlet.

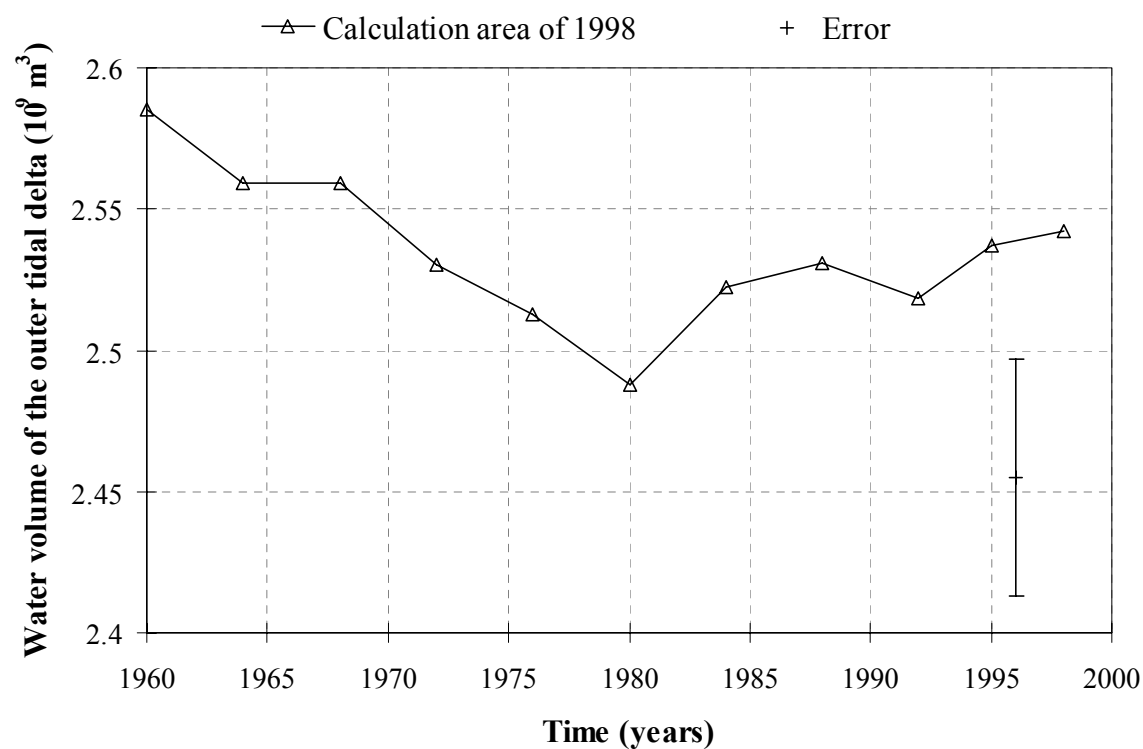


Figure 6.6: The water volume of the outer delta below NAP calculated with the morphological boundary of 1998.

Inlet Size

The smallest cross-sectional area of the inlet decreased by 11072 m² between 1968 and 1976. The closure of the "Geul" channel would in itself cause a decrease in cross-sectional area of 11646 m². Therefore the remaining channels must have increased their cross-sectional areas (due to erosion in the channels) by 574 m² in the period 1969 – 1974. This change is only 0.66 % of the total inlet cross-sectional area. The Eastern Scheldt storm surge barrier location has been protected from erosion since 1974.

Basin

The channels in the basin are eroding as expected. This erosion can be seen in the vertical erosion/sedimentation profile in appendix E4. The erosion between 1968 and 1983 for Sections 5, 6, 7 and 8 below NAP -2 m is about 10⁸ m³. In the inter-tidal area, sedimentation took place between 1968 and 1983 as can be seen in appendix E4. The amount of this sedimentation between NAP -2 and 2 m was 4.1x10⁷ m³ within Sections 5, 6, 7 and 8. This sedimentation can reduce the tidal prism by about 0.2 % per year. This decrease in tidal prism is too small to have any noticeable effect. The total amount of erosion below NAP +2 m between 1968 and 1983 is 5.9x10⁷ m³ in Sections 5, 6, 7 and 8. This corresponds to a basin volume increase of 1.76 %.

Outer Tidal Delta Conditions

Figure 6.6 shows the trends in the volume of water overlying the outer tidal delta. The decline in this water volume between 1968 and 1980 is due to a corresponding increase in the sand volume of the outer delta. This increased volume was predicted in the theoretical analyses described in Section 5.1. The volume change from 1968 to 1980 is about 7x10⁷ m³. This volume corresponds to about 2.7 % of the total delta volume.

Sand budget: basin - outer tidal delta

During the period 1969 – 1983 the amount of sedimentation on the outer tidal delta is estimated to be 4x10⁷ m³. During the same time, the amount of sedimentation in the inter-tidal regions of the basin is estimated to be 4.1x10⁷ m³. The estimated volume of erosion in the basin channels is 10⁸ m³. This volume is large enough to provide enough sediment to account for the sedimentation in both the inter-tidal areas of the basin and on the outer tidal delta. Some additional sediment may have even left the system.

6.1.3 Effect of a Decreasing of Tidal Volume in the Period 1977 - 1986

During this period, changes in the coastal morphology in the eastern Scheldt area appear to be largely influenced by a decrease in the tidal volume. The various effects to the system components are discussed below.

Basin area

During this period the construction of the Oester dam and the Philips Dam decreased the basin area from 3.89x10⁸ m² to 3.02x10⁸ m² at NAP. This is a decrease of 22 %. This decrease became permanent in 1986, when these dams went into service.

Tidal prism

The tidal prism decreased markedly from 1983 to 1986, as can be seen in Figure 6.4. This reduction is related to the installation of the storm surge barrier piers and gates. The reduction is

Table 6.1: An overview of the changes of the parameters.

	1969 - 1983			1983 – 1995		
	change + / -	Relative change	absolute change	change + / -	Relative change	absolute change
basin area	+	10.8 %	$3.8 \cdot 10^7 \text{ m}^2$	-	22.0 %	$8.7 \cdot 10^7 \text{ m}^3$
tidal prism	+	16.5 %	$18.6 \cdot 10^7 \text{ m}^3$	-	31.0 %	$42 \cdot 10^7 \text{ m}^3$
tidal volume	+	15.0 %	$34 \cdot 10^7 \text{ m}^3$	-	26.0 %	$68 \cdot 10^7 \text{ m}^3$
inlet human interference	-	13.4 %	11646 m^2	-	82 %	64000 m^2
inlet naturally	+	0.7 %	574 m^2			
water volume outer delta	-	1.5 %	$4 \cdot 10^7 \text{ m}^3$	+	0.6 %	$1.5 \cdot 10^7 \text{ m}^3$
basin volume	+	1.8 %	$5.9 \cdot 10^7 \text{ m}^3$			

$4.2 \times 10^8 \text{ m}^3$, or about 31 % of the original volume. After this large decrease the tidal prism remains fairly stable.

Tidal volume

Figures ** show a decrease of the tidal range in Sections 1, 2, and 3 after 1977. This implies that the construction of the Oester Dam and Philips Dam had a negative effect on the tidal volume. Figure 6.4 shows a rapid decrease in tidal volume through the inlet over 5 years that amounts to about $6.8 \times 10^8 \text{ m}^3$. This is a decrease of 26 %. This should be twice as much as the decrease in tidal prism ($8.4 \times 10^8 \text{ m}^3$). The difference is probably a result of the lack of tidal volume data between 1977 and 1983.

Tidal range

The decrease in tidal range after 1983 is 0.7 m in section 5, 0.8 m in section 6 and 1.1 m in section 8. After the tidal basin area decrease in 1986 the tidal range in the basin increased again, but not back to its former level. This implies that the inlet is not large enough and that the maximum velocities in the inlet have been reached.

Inlet Size

The cross-sectional area of the inlet cannot increase further due to seafloor protection. Due to the placing of the storm surge barrier piers and gates, the inlet cross-section actually decreases by 64000 m^2 between 1983 and 1986. This reduction is 82 % of the original inlet area.

Basin Conditions

The expected sedimentation in the channels can be seen in the vertical erosion/sedimentation profile in appendix E4. However the amount of sedimentation below NAP -2 m is only $7 \times 10^6 \text{ m}^3$, which is smaller than the computational error. Thus this sedimentation may not be occurring. In the inter-tidal area, erosion totaling $2 \times 10^7 \text{ m}^3$ occurs from 1983 to 1994. This is 0.19 % per year. These small yearly changes in tidal prism do not have a noticeable short-term effect.

Outer tidal delta

The outer tidal delta should erode, because the tidal volume is reduced. Figure 6.6 shows a gradual increase in the volume of water overlying the outer tidal delta, confirming a reduction in delta volume and delta erosion. The delta volume decreased by $5.4 \times 10^7 \text{ m}^3$ from 1980 to 1998, a decrease of 2.2 %.

Sediment budget: basin - outer tidal delta

The amount of erosion on the outer tidal delta between 1983 and 1995 is $1.5 \times 10^7 \text{ m}^3$. The change in basin volume is smaller than the error. The changes are a sedimentation volume of $7 \times 10^6 \text{ m}^3$ in the channels and an erosion volume of $2 \times 10^7 \text{ m}^3$ in the inter-tidal area. The erosion in the inter-tidal area is enough to supply for the sedimentation in the channels. Ignoring the error margins, it can be said that sand import into the basin is unlikely.

6.1.4 Changes after Completion of the Delta Works (1986 – present)

During this period, changes in the coastal morphology in the eastern Scheldt area appear to trend toward the establishment of large-scale equilibrium following the various disruptions caused by the Delta Works. The various effects to the system components are discussed below.

Inlet Size

In the inlet maximum current velocities occur. This will remain so or will even increase due to the sea level rise.

Outer Tidal Delta

The outer tidal delta will continue to erode due to the decreased tidal volume, until a new equilibrium is reached between the building and eroding forces on the outer tidal delta.

Figure 6.6 shows that the erosion rate of the outer tidal delta is decreasing. The sedimentation and erosion maps included in Appendix F2 show that the rate of bathymetric changes decrease following completion of the storm surge barrier. Between 1995 and 1998, the erosion at most locations did not exceed 3 m. The seabed defined along the various profiles also shows a decreased rate of changes between 1992 and 1998. The erosion and sedimentation profiles (Appendix F4) do not show a large decrease in erosion during the 1990's. Tonis (2000) found for the Haringvliet outer tidal delta an adaptation time of 11 years. The comparison of the development of the sand volume of both outer tidal deltas shows that the Eastern Scheldt outer tidal delta is even further away from its equilibrium than the Haringvliet outer tidal delta. It can be concluded that it will take more than 11 years, before an equilibrium is reached.

Basin Conditions

The volume of the basin below NAP +2 m will not change significantly, but a redistribution of the sediment will take place (see Appendix E3) and the coastal morphology within the basin is likely to continue to evolve. The inter-tidal area will erode while sedimentation will occur in the channels until the equilibrium velocities are reached. Existing data are insufficient to accurately estimate the time before the basin coastal morphology has reached equilibrium.

6.2 Equilibrium Relationships

Only the observations of the cross-sectional area of the inlet and the volume of the outer tidal delta provide enough data to be compared with the empirical relationships discussed in chapter 4. The empirical relationships may be used to estimate the final values for the cross-sectional area and the sand volume of the outer tidal delta.

6.2.1 Tidal Prism Versus Cross-sectional Area of the Inlet

Figure 6.7 shows the tidal prism versus cross-sectional area of the inlet for the Eastern Scheldt, as well as the empirical relationship between cross-sectional area and tidal prism proposed by O'Brien (1969) and Haring (1976). Haring developed his relationships based on the tidal volume rather than the tidal prism used by O'Brien. Because the tidal prism is half the tidal volume, Haring's equation can be changed to be suitable for tidal prisms by replacing the tidal volume by the tidal prism multiplied by 2.

▲ Cross-sectional area of dam location — Linear (O'Brien) — Linear (Haring)

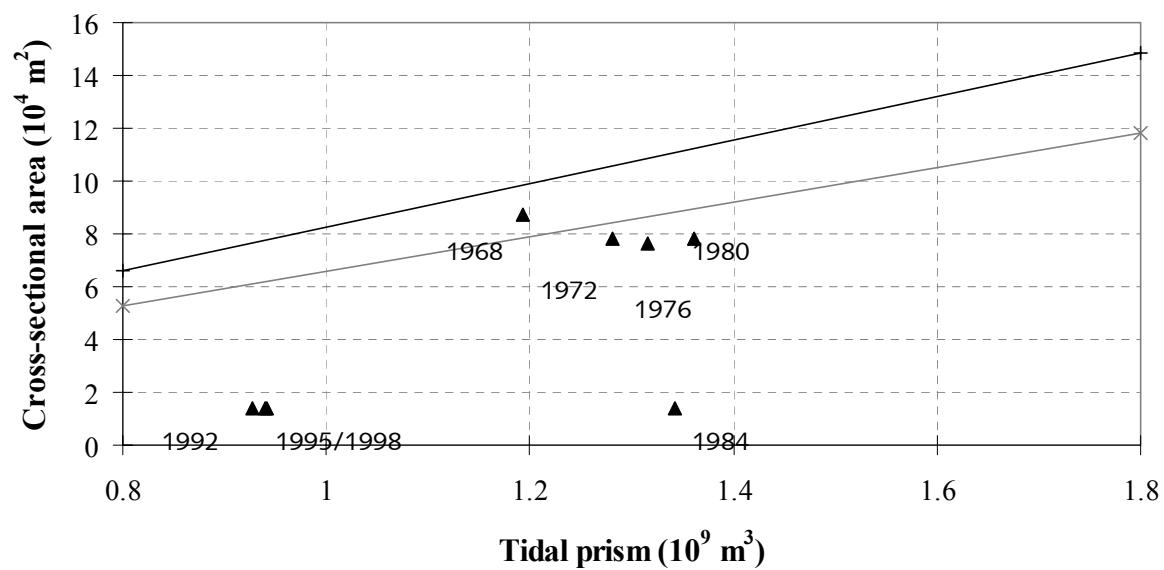


Figure 6.8: Cross-section area versus tidal prism

Table 6.2: The sand volume of the outer tidal delta

	Area of calculation area in 10^8 m^2	Total volume between NAP and NAP -15 m in 10^8 m^3	Water volume of the outer tidal delta in 10^8 m^3	Sand volume of the outer tidal delta in 10^8 m^3
1960	2.86	42.86	25.85	17.01
1964	2.86	42.91	25.59	17.31
1968	2.86	42.90	25.59	17.30
1972	2.86	42.83	25.30	17.53
1976	2.85	42.82	25.13	17.69
1980	2.85	42.82	24.88	17.94
1984	2.86	42.84	25.22	17.61
1988	2.85	42.79	25.31	17.48
1992	2.85	42.78	25.19	17.59
1995	2.85	42.74	25.37	17.37
1998	2.85	42.68	25.42	17.26

The development of the tidal prism and cross-section are clearly visible in Figure 6.7. From 1968 to 1972 the tidal prism increased while the inlet cross-sectional area decreased (see Section 6.1). After 1976, the system moves toward a state of equilibrium. The inlet cross-sectional area was drastically reduced between 1983 and 1986 as the storm surge barrier piers and gates were installed across the inlet channels. Since 1986, the inlet dimensions are controlled by the storm surge barrier and remain stable.

The empirical equilibrium relationships suggest that either the cross-section should increase or the tidal prism should decrease. Since the inlet cross-section cannot increase, the tidal prism should decrease.

According to the O'Brien empirical equilibrium relationship, the tidal prism for a cross-section of 14000 m^2 should be $2.13 \times 10^8 \text{ m}^3$. This means that the existing tidal prism should be reduced by $7.27 \times 10^8 \text{ m}^3$. With an average tidal range of 3 m, this would correspond to a basin with a surface area of $2.42 \times 10^8 \text{ m}^2$. This is 78 % of the present surface area of the Eastern Scheldt basin. According to the Haring empirical relationship, the tidal prism should be $1.69 \times 10^8 \text{ m}^3$. Using the same 3 m tidal range, this would correspond to a basin with a surface area about 83 % smaller than the current Eastern Scheldt basin.

The previous calculations show that the measures in the inlet have had a enormous effect on the Eastern Scheldt system. Although, the empirical relationship cannot be applied to the dam location, because the cross-sectional area cannot change due to the seabed protection and the storm surge barrier.

6.2.2 Tidal Prism versus Sand Volume of the Outer Tidal Delta

Walton and Adams (1976) calculated the sand volume of the outer tidal delta by determining the volumes enclosed by a coastal area without an outer tidal delta and one with an outer tidal delta. A coastal area without an outer tidal delta cannot be constructed easily for the Eastern Scheldt outer tidal delta, because it is bounded by adjacent outer tidal deltas of other tidal inlet. The sand volume of the outer tidal delta of the Eastern Scheldt was therefore determined by determining the extra sand volume due to the delta compared to a horizontal coastline at NAP -15 m.

The equilibrium sand volume for a tidal prism of $1.2 \times 10^9 \text{ m}^3$ is according to Walton and Adam's (1976) $9.6 \times 10^8 \text{ m}^3$. The sand volume of the Eastern Scheldt outer tidal delta is about $17 \times 10^8 \text{ m}^3$. The sand volumes calculated using Walton and Adam's (1976) empirical relationship results in a twice as small sand volume.

It can be concluded that with the current tidal prisms in the Eastern Scheldt the two calculation methods of the sand volume of the outer tidal delta can not be compared. This can be caused by differences in tidal environment, sediment supply, shape of coastline, etc.

The final equilibrium situation of the outer tidal delta cannot be determined with the available equilibrium relationships.

Table 7.1: An overview of the changes of the parameters.

	1969 - 1983			1983 - 1995		
	change + / -	Relative change	absolute change	change + / -	Relative change	absolute change
basin area	+	10.8 %	$3.8 \cdot 10^7 \text{ m}^2$	-	22.0 %	$8.7 \cdot 10^7 \text{ m}^3$
tidal prism	+	16.5 %	$18.6 \cdot 10^7 \text{ m}^3$	-	31.0 %	$42 \cdot 10^7 \text{ m}^3$
tidal volume	+	15.0 %	$34 \cdot 10^7 \text{ m}^3$	-	26.0 %	$68 \cdot 10^7 \text{ m}^3$
inlet human interference	-	13.4 %	11646 m^2	-	82 %	64000 m^2
inlet naturally	+	0.7 %	574 m^2			
water volume outer delta	-	1.5 %	$4 \cdot 10^7 \text{ m}^3$	+	0.6 %	$1.5 \cdot 10^7 \text{ m}^3$
basin volume	+	1.8 %	$5.9 \cdot 10^7 \text{ m}^3$			

7 Conclusions and Recommendations

7.1 Conclusions

This study has investigated the changes to the morphology of the Eastern Scheldt coastal system caused by the Delta Works. The results of this investigation form the basis for predicting long-term morphological development of the Eastern Scheldt coastal system. The study concludes:

- The inlet cross-sectional area was reduced when the Storm Surge Barrier piers and gates were installed. Thus inflow and outflow velocities are greater than for equilibrium conditions, defined by the empirical relationships. But the cross-sectional area of the inlet is unlikely to increase following installation of the seabed protection beginning in 1974. Therefore the tidal velocities through the Storm Surge Barrier are likely to remain larger than those defined by the equilibrium velocities for the inlet according to the empirical relationships.
- The outer tidal delta is currently eroding and is projected to reach an equilibrium situation after more than 11 years. The projected equilibrium volume for the outer tidal delta, as defined by the formula proposed by Walton and Adams (1976), results in a volume that is twice as small than at present. A new empirical relationship cannot be developed, nor the Walton and Adams formula adjusted, because no data defining an equilibrium situation for the outer tidal delta of the Eastern Scheldt is available.
- The basin volume below NAP +2 m is not expected to change, because the basin volume did not change between 1983 and 1994. The basin, however, is not in equilibrium. The vertical sedimentation and erosion profiles show a redistribution of the sediment, the inter-tidal area is eroding, while in the channels both sedimentation and erosion occurs. Estimation of the time until equilibrium is reached and the determination of the final equilibrium situation is not possible, due to a lack of detailed and frequent bathymetric data.
- Between 1969 and 1983 the eroded sediment of the basin was exported to the outer tidal delta. However the continued growth of the delta during this period was much greater than the measured volume lost from within the tidal basin. This remaining volume must have come from outside the system.
- In the period 1983 to 1994 the outer tidal delta was eroding, but the basin volume did not change. Thus there is no evidence to suggest that the basin is importing sediment. The sediment eroded from the outer tidal delta was apparently exported out of the study area during the period 1983 to 1994.
- The previous two observations and conclusions strongly suggest that the Eastern Scheldt coastal system is not a closed system, but imports sediments beyond the study area.
- The changes in cross-sectional area of the inlet and the volume of the outer tidal delta caused by human interventions are in the same order as the natural changes observed between 1827 and 1959, but they happened over a much shorter time period.

7.2 Recommendations

- Lack of sufficient quantitative measurements make it difficult to explain the natural processes affecting the coastal morphology of the Eastern Scheldt area before 1960. Natural phenomena, such as sea level rise or changes in the tidal regimes, are assumed to cause the changes during this period. More research might result in a better understanding of the time scales involved in the evolution of tidal inlets and outer tidal deltas.
- The current analysis of the Eastern Scheldt tidal basin is based on only three sets of bathymetric data collected over a period of 25 years. These data do not have enough temporal distribution to determine whether the basin is eroding or not. More frequent and complete bathymetric surveys of the basin, taken about every 4 years are necessary to determine this.
- Further research on the processes controlling the formation of sandy shoals in the Eastern Scheldt basin is needed. This would help to understand if sandy shoals fill up with sediment from channels or by importing sediment from the outer tidal delta. Volume calculations alone cannot give answers on this issue.
- A model defining the processes controlling the coastal morphology of the Eastern Scheldt could be used as an analogue for other inlets where major human interventions are being considered. One such case is the Haringvliet in the Netherlands, where the reopening of the sluices will come into effect in 2004. The Eastern Scheldt is the only known inlet where human interventions have caused an increase of the tidal prism during a certain period. This could help in considering the effects of an increase in tidal prism due to a reopening of the sluices of the Haringvliet.
- It is generally useful to continue the measurements of discharge and bathymetry after engineering works have been completed. This is the only way to monitor changes and understand the evolution of the system.

8 References

- Biegel, E.J., 1998.
"Geoprof, ARC/INFO-applicatie voor het maken van tijdreeksen van profiel-parameters, gebruikershandleiding, versie 2.0", Ingenieursbureau Sepra, Den Hoorn.
- Boogaard, L. uit den, unknown.
"Computer application 'Vakgis'", Rijkswaterstaat, RIKZ, The Hague, no manual available.
- Haring, J., 1948.
"Diepteveranderingen kustgebied Goeree-Walcheren", Rijkswaterstaat, Directie benedenrivieren, The Hague, report 5.
- Haring, J., 1967
"De verhouding van getijvolume en doorstroomprofiel in de zeegaten", Driemaandelijks bericht Deltawerken, No. 40, pp 518-524.
- Haring, J., 1978
"De geschiedenis van de ontwikkeling van de waterbeweging en van het profiel van de getijwateren en zeegaten van het zuidelijke deltabekken en van het hierbij aansluitende gebied voor de kust gedurende de perioden 1872-1933-1952-1968-1974", Rijkswaterstaat, Deltadienst, The Hague, report nr. K77M031E, pp. 11 and appendix 2a.
- Hayes, M.O., 1979
"Barrier island morphology as a function of tidal and wave regime", Academic press inc., pp1-27.
- Jarret, J.T., 1976
"Tidal prism - inlet area relationships", GITI Report 3, U.S. Army Coastal Engineering Research Center, Fort Belvoir, Virginia, 32 pp.
- Johnson, J.W., 1972
"Tidal inlets on the California, Oregon, and Washington coasts", Hydraulic Engineering Laboratory, University of California at Berkeley, Berkeley, California, Technical report HEL 24-12, pp. 1 – 37.
- Kleef, A.W. van, 1991.
"Empirical relationships for tidal inlets, basins and deltas", Institute of Geographical Research, University Utrecht, Utrecht, report GEOPRO 1991.19.
- Leconte, L.J., 1905.
"Discussion of 'Notes on the improvement of the river and harbour outlets in the United States', Paper No. 1009 by D.A. Watts", Transactions, American Society of Civil Engineers, Vol LV, Dec 1905, pp 306-308.
- Louters, T., Mulder, J.P.M., Postma, R., Hallie, F.P., 1991.
Changes in coastal morphological processes due to the closure of the tidal inlets in the SW Netherlands, Journal of Coastal Research vol. 7, no. 3, pp.635-652.
- Mulder, J.P.M., 1999.
"Zandverlies op dieper water", Rijkswaterstaat, RIKZ, The Hague, Work document RIKZ/OS 99.165x.

NITG-TNO, 1997.

"De ontstaansgeschiedenis van het Zeeuwse kustlandschap", CD-ROM, Versie 1.0.

O'Brien, M.P., 1931.

"Estuary tidal prisms related to entrance areas", Civil Engineering, Vol. 1, No. 8, pp. 738-739.

O'Brien, M.P., Feb. 1969.

"Equilibrium flow areas of inlets on sandy coasts", Journal of the Waterways and Harbors Division, Proceedings of the American Society of Civil Engineers, Vol. 95, No. WW1, pp. 43-52.

Rijks Geologische Dienst, 1980.

"Geologisch onderzoek pijlerdam Oosterschelde", Rijks Geologische Dienst, Haarlem, Report 10206B, appendix 3.

Rijkswaterstaat, 1958 to 1988.

"Driemaandelijks bericht Deltawerken", Rijkswaterstaat, Deltadienst, The Hague, Vol. 1 to 124, entire series.

Rijkswaterstaat, 1967.

"The North Sea from Blankenberghe to Zandvoort, current and tidal measurements 27 June 1967", Rijkswaterstaat, Deltadienst, The Hague, Report H620Z.

Rijkswaterstaat, 1994.

"Design plan Oosterschelde Storm Surge Barrier, overall design and design philosophy", Rijkswaterstaat, The Hague, pp. 15.

Rijkswaterstaat RIKZ, 1985.

"Tienjarig overzicht der waterhoogten, afvoeren en watertemperaturen 1961 – 1970", Rijkswaterstaat, RIKZ, The Hague, book.

Rijkswaterstaat RIKZ, 1989.

"Tienjarig overzicht der waterhoogten, afvoeren en watertemperaturen 1971 – 1980", Rijkswaterstaat, RIKZ, The Hague, book.

Rijkswaterstaat RIKZ, 1994.

"Tienjarig overzicht der waterhoogten, afvoeren en watertemperaturen 1981 – 1990", Rijkswaterstaat, RIKZ, The Hague, book.

Rijkswaterstaat RIKZ, 1994.

"Gemiddelde getijkromme 1991.0", Rijkswaterstaat, RIKZ, The Hague, book.

Schaap, H.Y., 1971.

"Noordzee kustgebied Blankenberghe-Haamstede stroom- en getijmeting 22 mei en 9 september 1969", Rijkswaterstaat, Deltadienst, The Hague.

Spek, A.J.F. van der, 1997.

"De geologische opbouw van de ondergrond van het mondingsgebied van de Westerschelde en de rol hiervan in de morfologische ontwikkeling", NITG-TNO, Haarlem, Report NITG 97-284-B.

Tönis, I, 2000.

"Haringvlietmonding: op zoek naar evenwicht, Morfologische ontwikkelingen van de Haringvlietmonding sinds 1970", Rijkswaterstaat, RIKZ, The Hague, report RIKZ/OS/2000.39x.

Vegt, G van der, 1998.

"De opvulling van de bodemdiepte schematisatie van de Oosterschelde",
Rijkswaterstaat, RIKZ, The Hague, working document RIKZ/OS-98.104x.

Vriend, H.J. de, J. Dronkers, M.J.F. Stive, A. van Dongeren & J.H. Wang, 1998.
"Coastal inlets and tidal basins", Lecture Note, Faculty of Civil Engineering and
Geosciences, Delft University of Technology, Delft.

Walton, T.L. and W.D. Adams, 1976.

"Capacity of inlet outer bars to store sand", Proc. 15th Coastal Engineering
Conference, ASCE, vol. 2, ch. 112, pp 1919 – 1937.

List of Appendices

Appendix A: Grids

- A1. Measurement methods of the bathymetric data.
- A2. Available bathymetric data.
- A3. Construction of the grids.
- A4. Errors.

Appendix B: Tidal volume

- B1. Measurement and calculation methods of the tidal volumes.
- B2. Tidal volumes.
- B3. Storage locations of the tidal volume data.
- B4. Errors.

Appendix C: Tidal prism

- C1. The mean high water and mean low water levels of the measurement locations.
- C2. The method used to calculate the MHW and MLW levels of the calculation sections.
- C3. The mean high water and mean low water levels of the calculation sections.
- C4. The calculated tidal prisms.
- C5. The errors.

Appendix D: Cross-sections

- D1. Cross-sections profiles.

Appendix E: Basin

- E1. Bathymetric maps of the basin.
- E2. Cross-section profiles of the basin.
- E3. Sedimentation and erosion maps of the basin.
- E4. Sedimentation and erosion profiles over the vertical.

Appendix F: Outer tidal delta

- F1. Bathymetric maps of the outer tidal delta.
- F2. Sedimentation and erosion maps of the outer tidal delta.
- F3. Calculated volumes of the outer tidal delta and the errors.
 - F3.1 Calculation with linear sections
 - F3.2 Calculations with morphological calculation areas
- F4. Sedimentation and erosion profile over the vertical.
 - F4.1 Vertical sedimentation and erosion profiles of the calculations with linear sections
 - F4.2 Vertical sedimentation and erosion profiles of the calculations with morphological calculation areas

Appendix A: Grids**Appendix A1: Measurement methods of the bathymetric data****Appendix A2: Available bathymetric data****Appendix A3: Construction of the grids****Appendix A4: Errors**

Appendix A1: Measurement methods of the bathymetric data

In the Netherlands location of the coast and the seabed are periodically determined within the framework of the Monitoring of the Water Situation of the Country (MWTL). A distinction in monitoring is made between coastal measurements and field soundings.

The coastal measurements are carried out once a year and consist of depth measurements and height measurements. The measurements are carried out along imaginary lines perpendicular to the coast. These so-called direction lines are at a distance from one another of 200 to 250 m and stretch out about one km into the sea.

The depth measurements are carried out from ships using an automatic sounding system combined with a computerised positioning system.

The height measurements for the beach and dunes are collected with laser altimetry. The surface of the earth is scanned from an aircraft using a laser beam. The underlying terrain is recorded in three dimensions using this method. The height along the direction lines is determined from this digital height model. Before this method photogrammetry was used to determine the height. The surface of the earth was photographed from three different directions. With the use of 3D photo interpretation the height along the direction lines were determined.

Field measurements begin where coastal measurements leave off and continue to the toe of the underwater bank, what lies at the level of NAP -20 m. The measurements are carried out at multiple sections (figure A2.1). The frequency of recording of the separate sections depend on the dynamics of the area and is once a year to once in six years. The complicated seabed topography with banks and channel systems, the outer delta's and estuaries are sailed almost everywhere with a distance between direction lines of 200 m. The direction lines are aimed perpendicular to the channels axes. The shallow areas of the flats are measured by a shallow draught vessel during high tide.

The direction line measurements are converted to a grid using interpolation techniques over a defined area.

Appendix A2: Available bathymetric data

Figure A2.1: The field sounding sections

Table A2.1: Available bathymetric data.

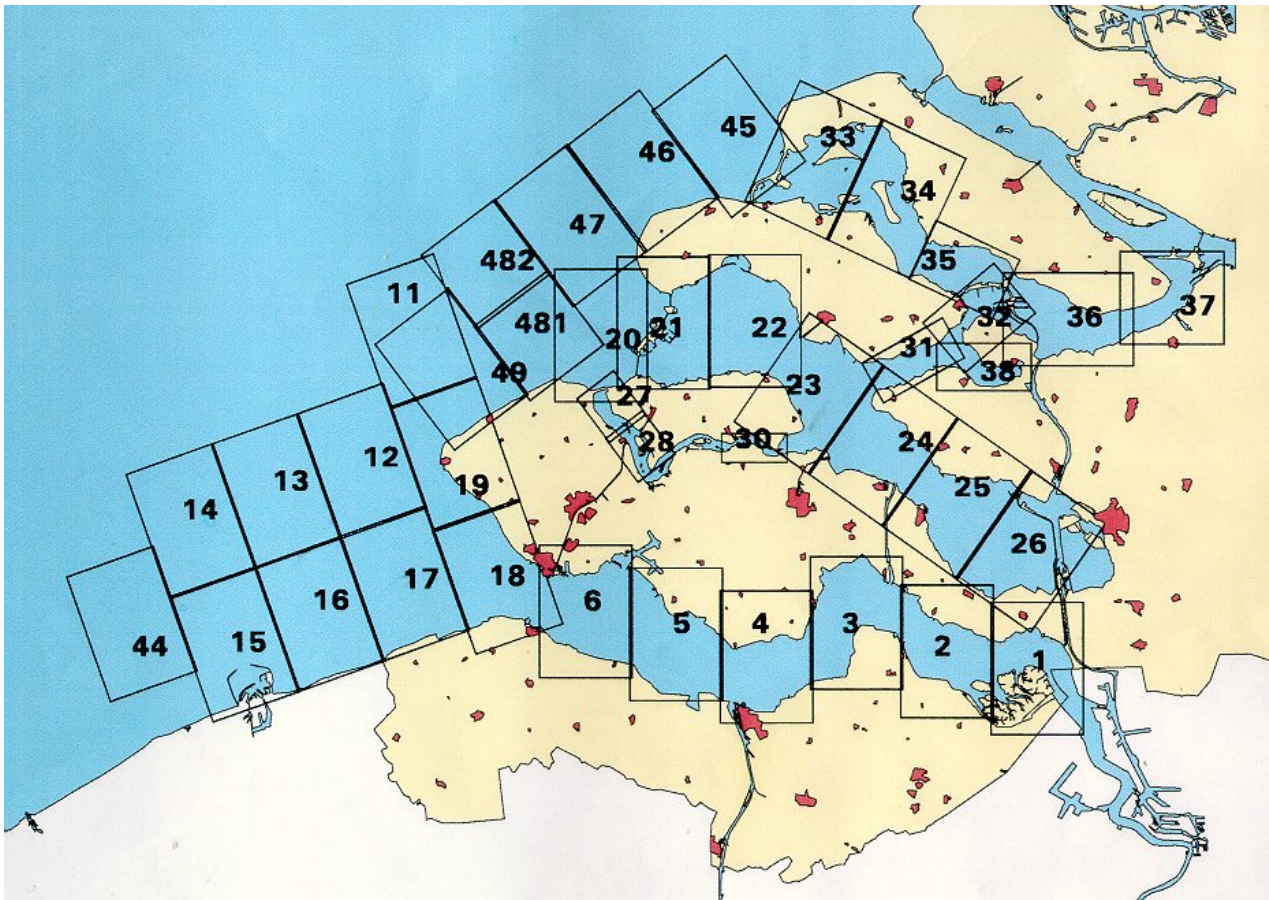


Figure A2.1: The field sounding sections

Table A2.1: Available bathymetric data with the column numbers corresponding to the section numbers indicated in figure A.2.1.

								basin							
	outer delta														
	46	47	481	482	49	20	21	22	23	24	25	26	31	32	
1956															
1957															
1958															
1959															
1960															
1961															
1962															
1963															
1964															
1965															
1966															
1967															
1968															
1969															
1970															
1971															
1972															
1973															
1974															
1975															
1976															
1977															
1978															
1979															
1980															
1981															
1982															
1983															
1984															
1985															
1986															
1987															
1988															
1989															
1990															
1991															
1992															
1993															
1994															
1995															
1996															
1997															
1998															
1999															
2000															
2001															

	= not measured
	= available as map
	= available as digital grid

Appendix A3: Construction of the grids

Table A3.1: Table A3.1: Available field sounding data of the outer tidal delta of the Eastern Scheldt and the year of the section fill up.

Table A3.2: The fill of the remaining gaps in the grids.

Sections	20	21	46	47	481	482	49
1960	x	x	x	x	x	ND, digitised later	x
1964	x	x	x	x	x	x	x
1968	x	x	x	x	x	x	x
1972	x	x	x	x	x	ND, 1973	x
1976	x	x	x	x	x	x	x
1980	x	x	x	x	x	x	x
1984	x	x	x	x	x	x	NM, 1983
1988	x	x	x	NM, average of 1987 and 1989	x	x	x
1992	x	x	x	x	x	x	x
1995	x	NM, 1994	x	x	x	x	x
1998	x	NM, 1997	NM, 1995	x	x	x	x

Table A3.1: Available field sounding data of the outer tidal delta of the Eastern Scheldt (with x = available as digital grid, ND = not digitally available, NM = not measured) and the year of the section fill up.

	large gaps filled up with	edge mismatch filled up with	interpolation, search radius in m
1960	-	-	5
1964	-	-	5
1968	-	-	5
1972	section 20, average of 1968 and 1976		10
1976	-	-	5
1980	section 481, average of 1976 and 1984	-	10
1984	section 20, 1986	section 49, average of 1980 and 1988	20
1988	section 20, average of 1987 and 1989	section 47, average of 1984 and 1992	20
1992	-	-	10
1995	section 20, average of 1992 and 1998	-	5
1998	-	-	5

Table A3.2: The fill of the remaining gaps in the grids.

Construction of the grids of the outer delta and inlet

To derive grids covering the area of the outer delta, different field sounding sections and coastal measurements have to be combined. The yearly coastal measurements are carried out at the coast of Schouwen since 1966, at the coast of Walcheren since 1967 and at the coast of Noord-Beveland since 1965.

At first the field soundings and the coastal measurements for every year of interest are merged. Since the coastal measurement data of 1960 and 1964 is missing, it is substituted by the coastal measurement data of 1966 (Schouwen), 1967 (Walcheren) and 1965 (Noord-Beveland).

After merging the field soundings with the coastal measurements large gaps appear, due to missing grids of field sounding sections. The missing sections are filled up with sections of other available years (Table A3.1). Especially for this study section 482 of 1960 and 1973 has been digitised. Section 482 of 1973 was digitised to replace this section of the year 1972, because only half of this section was measured in 1972.

After filling up the section gaps, large gaps are still present. These gaps are also filled up with sections of other years. After filling up gaps with sections from other years, the small gaps remaining are filled up using interpolation techniques. (Table A3.2)

Construction of the grids of the basin

As can be seen in table A2.1 no grids are available covering the Eastern Scheldt basin before 1986. After 1986 digital data is available, it is possible to make a covering grid for the years 1986, 1987 and 1989 and also for 1993-1995. These grids do not cover the entire basin, because no measurements are done above NAP +0 m. These grids are usable to calculate the volume of the basin below NAP +0 m.

Another source of bathymetry data is the input of sea bottoms in computer assimilations. The influence of the Delta Works to the hydrodynamics of the Eastern Scheldt was determined with the use of computer assimilations. Bathymetric profiles of 1968 and 1983 were used in these computer models and are still available at RIKZ in Middelburg. The bathymetry of 1968 is available as a text file with x-y-z-values. This can be interpolated and transformed into a usable grid. The remaining gaps are also filled up by interpolation. The bathymetry of 1983 is available as grid usable in GIS.

A grid of the Eastern Scheldt is also used in a computer model to predict the wave run up. This grid is available as ASCII-file and can be easily transformed into a grid. This grid contains the soundings of the years 1993, 1994 and 1995 (table A2.1). The gaps at the locations of the shallow areas were filled up with data from 1991 and 1992. The remaining gaps are filled up with data of 1983. The process of constructing this grid is described by van der Vegt (1998).

Grids with bathymetric data covering the whole basin area is thus only available for the years 1968, 1983 and 1994. Grids with data below NAP +0 m is available for the years 1986, 1987 and 1989.

Appendix A4: Error

Measurement error

Several factors can cause errors. The measurement process is affected by: the squat of the ship, the determination of the co-ordinates of the ship location and the correction of measurements with reference to tide and NAP. These are all systematic errors. Random errors can be caused by human mistakes such as reading and writing errors. The standard deviation caused by all these factors can vary between 17 and 23 cm (Louters et al, 1996).

The digitising and interpolation procedure also introduces errors.

Maps however are composed of many measurements. In this way errors are averaged. In this study the error is estimated at 10 cm. This error was used in previous studies (Tönis et al, 2001)

Appendix B: Tidal volume

Appendix B1: Measurement and calculation methods of the tidal volumes

Appendix B2: Tidal volumes

Appendix B3: Storage locations of the tidal volume data

Appendix B4: Errors

Appendix B1: Measurement and calculation methods of the tidal volume

The tidal volume is calculated by multiplying the velocity of a channel with the cross-sectional area of the channel. To get a more accurate result the velocities should be measured simultaneously at several different locations and depths in the channel and multiplied by a representative part of the cross-sectional area.

The current velocities in a channel are measured with an “Ott-molen” and the current direction with an Elmar-flowdirection meter. The gathered data was entered into a computer and saved on a tape on the ship. The Ott-molen was already used in 1960 and is still used for velocity measurements.

Since 1996 the tidal volume is measured by sailing direction lines and meanwhile measuring the velocities using an Acoustic Doppler Current Profiler (ADCP). The location of the ship is determined using the DGPS-location system.

Appendix B2: Tidal volumes

Table B2.1: The ebb and flood volumes of the separate channels and the total inlet in 10^8 m³.

Table B2.2: The tidal volumes of the separate channels and the total inlet in 10^8 m³.

Table B2.1: The ebb and flood volumes of the separate channels and the total inlet in 10^8 m^3 .

date	Schaar		Hammen		Roompot		Geul		Total inlet	
	ebb	flood	ebb	flood	ebb	flood	ebb	flood	ebb	flood
01-01-33										
01-01-59										
01-06-65	4.68	5.16 (Schaar & Hammen)			6.91	6.44	0.94	1.57	12.56	13.20
02-06-65	4.93	5.35 (Schaar & Hammen)			6.94	6.48	1.08	1.57	12.87	13.26
27-06-67									11.85	10.73
28-06-67									10.97	9.52
27-08-68	2.14	1.80	2.38	2.60	6.32	6.07	0.55	0.78	11.38	11.25
28-08-68	2.15	1.85	2.42	2.77	6.43	5.80	0.55	0.94	11.55	11.36
10-09-69	1.98	1.91	2.44	2.66	5.80	5.99	0.54	0.86	10.57	11.39
11-09-69	1.95	1.84	2.26	2.61	5.80	5.83	0.54	0.87	10.49	11.11
06-10-71		2.39		3.11		6.98		0.69		13.14
07-10-71	2.54	2.55	2.84	3.10	6.98	7.17	0.35	0.89	12.56	13.67
08-10-71	2.59	2.36	2.77	2.88						
09-08-72	2.75	2.35	2.89	2.80	6.93	6.66			12.52	11.82
10-09-72	2.86	2.36	2.93	2.86	6.98	6.85			12.72	12.12
04-09-75	2.78	2.37	2.59	2.48	7.11	7.03			12.48	11.88
05-09-75	2.87	2.52	2.70	2.71	7.50	7.67			13.07	12.90
19-07-78			2.81	2.94						
25-07-78	2.90	2.58								
26-07-78					7.68	7.63			12.85	12.83
28-07-78			2.27	2.62						
01-08-78	2.81	2.38								
02-08-78					7.70	7.81				
19-07-83	2.61	2.57	2.22	2.53	6.70	7.14			11.52	12.24
26-07-83	2.82	2.57	2.37	2.38	6.99	6.98			12.19	11.92
01-08-83	2.44	2.13	2.26	2.22	6.20	6.15			10.90	10.50
29-12-83	2.58	2.53	1.88	1.76	6.29	6.65			10.76	10.94
31-03-84			2.25	2.62						
31-03-84			2.45	2.42						
11-04-84	2.17	2.26								
27-09-84					7.95	7.61				
07-02-85					8.09	8.15				
20-06-85	2.53									
24-06-85		1.76								
23-07-85	2.99	2.31								
26-07-85			1.97	2.19						
14-09-85			1.44							
27-09-85		1.53								
10-10-85	1.58									
21-11-85	1.35	1.71								
27-11-85					7.58					
10-12-85			1.81							
26-04-86					5.69					
22-05-86			2.30							
22-05-86			2.45							
26-05-86		1.97								
21-09-86					5.74	6.61				
22-09-87				1.71						
23-09-87					6.22	5.56				
17-02-88			2.05						9.88	8.86
18-02-88	1.85									
22-02-88				1.98						
23-02-88					5.98					
14-04-88		2.06								
04-07-88						4.83				
24-04-90			1.68							
25-04-90				2.20						
26-04-90		1.68								
24-08-95					5.53	4.85			9.40	8.80
07-09-95			1.90	1.85						
08-09-95	1.97	2.10								
13-12-96	2.00									
19-12-96		1.60							10.07	9.61
21-12-99			1.88							
22-12-99					6.20	5.19				
20-03-00				2.24						
22-03-00		2.18								
23-03-00	2.00									

Table B2.2: The tidal volumes of the separate channels and the total inlet in 10^8 m^3 .

date	Schaar	Hammen	Roompot	Geul	Total inlet
01-01-33					22.00
01-01-59					22.70
01-06-65	9.84		13.35	2.51	25.76
02-06-65	10.27		13.42	2.65	26.13
27-06-67					22.58
28-06-67					20.49
27-08-68	3.94	4.97	12.38	1.33	22.63
28-08-68	3.99	5.19	12.23	1.49	22.91
10-09-69	3.89	5.10	11.79	1.40	21.96
11-09-69	3.79	4.87	11.63	1.41	21.60
06-10-71					
07-10-71	5.08	5.94	14.16	1.23	26.22
08-10-71	4.95	5.65			
09-08-72	5.10	5.69	13.59		24.34
10-09-72	5.22	5.79	13.83		24.84
04-09-75	5.15	5.08	14.14		24.36
05-09-75	5.39	5.42	15.17		25.97
19-07-78		5.75			
25-07-78	5.48				
26-07-78			15.31		25.69
28-07-78		4.90			
01-08-78	5.18				
02-08-78			15.51		
19-07-83	5.18	4.75	13.83		23.76
26-07-83	5.39	4.75	13.97		24.10
01-08-83	4.57	4.47	12.35		21.39
29-12-83	5.11	3.65	12.94		21.70
31-03-84		4.88			
31-03-84		4.87			
11-04-84	4.42				
27-09-84			15.56		
07-02-85			16.24		
20-06-85					
24-06-85					
23-07-85	5.30				
26-07-85		4.15			
14-09-85					
27-09-85					
10-10-85					
21-11-85	3.06				
27-11-85					
10-12-85					
26-04-86					
22-05-86					
22-05-86					
26-05-86					
21-09-86			12.35		
22-09-87					
23-09-87			11.79		
17-02-88					
18-02-88					
22-02-88	3.90	4.03	10.81		18.74
23-02-88					
14-04-88					
04-07-88					
24-04-90					
25-04-90					
26-04-90					
24-08-95			10.38		
07-09-95		3.75			18.19
08-09-95	4.07				
13-12-96					
19-12-96					
21-12-99					
22-12-99					
20-03-00	4.18	4.12	11.38		19.68
22-03-00					
23-03-00					

Appendix B3: Storage locations of the tidal volume data

Addresses of the storage locations

Table B3.1: The report and archive numbers, titles and storage locations of the tidal volume data.

M:

Zeeuws archief
Hofplein 16
Postbus 70
4330 AB Middelburg
The Netherlands
+31-118678800
info@zeeuwsarchief.nl
www.zeeuwsarchief.nl

V:

Meetdienst Zeeland
Prins Hendrikweg 3
4382 NR Vlissingen
The Netherlands
+31-118422000

Table B3.1: The report and archive numbers, titles and storage locations (M = Middelburg and V = Vlissingen, see left page) of the tidal volume data.

	Report nr.	Archife nr.	Measurement location	Only ebb or flood	Location
1933	K77M031E	De geschiedenis van de ontwikkeling van de waterbeweging en van het profiel van de getijwateren en zeegaten....., J. Haring, 1978			B
1959					
1-06-65	H584Z		total inlet		M
2-06-65	H584Z		total inlet		M
27-06-67	H620Z		total inlet		M
28-06-67	H624Z - H626Z		total inlet		M
27-08-68	H647Z		total inlet		M
28-08-68	H647Z		total inlet		M
10-09-69	H665Z		total inlet		M
11-09-69	H665Z		total inlet		M
6-10-71	H680Z		total inlet	flood	M
7-10-71	H680Z		total inlet		M
8-10-71	H680Z		schaar/hammen		M
9-08-72	H690Z		total inlet		M
10-08-72	H690Z		total inlet		M
4-09-75	H719Z		total inlet		M
5-09-75	H719Z		total inlet		M
19-07-78	H733Z		hammen		M
25-07-78	H733Z		schaar		M
26-07-78	H733Z		roompot		M
28-07-78	H733Z		hammen		M
1-08-78	H733Z		schaar		M
2-08-78	H733Z		roompot		M
19-07-83			total inlet		V
26-07-83			total inlet		V
1-08-83			total inlet		V
29-12-83			total inlet		V
31-03-84			hammen		V
11-04-84			schaar		V
27-09-84			roompot		V
7-02-85	M85.3.019	85.03	roompot		V
20-06-85	M85.3.143	85.04	schaar	ebb	V
24-06-85	M85.3.143	85.04	schaar	flood	V
23-07-85	M85.3.162	85.06	schaar		V
26-07-85	M85.3.163	85.06	hammen		V
14-09-85	M85.3.188	85.10	hammen		V
27-09-85	M85.3.210	85.09	schaar		V
10-10-85	M85.3.212	85.08	schaar	ebb	V
21-11-85	M85.3.226	85.15	schaar		V
27-11-85	M85.3.227	85.15	roompot		V
10-12-85	M85.3.261	85.14	hammen	ebb	V
26-04-86	M86.3.049	86.09	roompot		V
22-05-86	M86.3.051	86.15	hammen	ebb	V
26-05-86	M86.3.062	86.15	schaar		V
21-09-86	M86.3.106	86.22	roompot		V
22-09-87	ZLMD-87.N.056	87.12	hammen	flood	V
23-09-87	ZLMD-87.N.057	87.12	roompot		V
17-02-88	ZLMD-88.N.027	88.03	hammen	ebb	V
18-02-88	ZLMD-88.N.031	88.04	schaar	ebb	V
22-02-88	ZLMD-88.N.026	88.03	hammen	flood	V
23-02-88	ZLMD-88.N.030	88.05	roompot	ebb	V
14-04-88	ZLMD-88.N.038	88.04	schaar	flood	V
4-07-88	ZLMD-88.N.045	88.05	roompot	flood	V
24-04-90	ZLMD-90.N.069	90.05	hammen	ebb	V
25-04-90	ZLMD-90.N.067	90.05	hammen	flood	V
26-04-90	ZLMD-90.N.070	90.06	schaar	flood	V
24-08-95	ZLMD-95.N.036	95.14	roompot		V
7-09-95	ZLMD-95.N.038	95.14	hammen		V
8-09-95	ZLMD-95.N.037	95.14	schaar		V
13-12-96	ZLMD-96.N.046		schaar	ebb	V
19-12-96	ZLMD-96.N.046		schaar	flood	V
21-12-99	ZLMD-00.N.007		hammen	ebb	V
22-12-99	ZLMD-00.N.014		roompot	ebb	V
22-12-99	ZLMD-00.N.019		roompot	flood	V
20-03-00	ZLMD-00.N.023		hammen	flood	V
22-03-00	ZLMD-00.N.027		schaar	flood	V
23-03-00	ZLMD-00.N.025		schaar	ebb	V

Appendix B4: Errors

Table B4.1: The used ebb and flood volumes in 10^8 m^3 to calculate the errors.

	Schaar		Hammen		Roompot		Geul		Total inlet	
date	ebb	flood	ebb	flood	ebb	flood	ebb	flood	ebb	flood
01-06-65					6.91	6.44	0.94	1.57	12.56	13.20
02-06-65					6.94	6.48	1.08	1.57	12.87	13.26
27-06-67									11.85	10.73
28-06-67									10.97	9.52
27-08-68	2.14	1.80	2.38	2.60	6.32	6.07	0.55	0.78	11.38	11.25
28-08-68	2.15	1.85	2.42	2.77	6.43	5.80	0.55	0.94	11.55	11.36
10-09-69	1.98	1.91	2.44	2.66	5.80	5.99	0.54	0.86	10.57	11.39
11-09-69	1.95	1.84	2.26	2.61	5.80	5.83	0.54	0.87	10.49	11.11
6-10-71		2.39		3.11		6.98		0.69		13.14
7-10-71	2.54	2.55	2.84	3.10	6.89	7.17	0.35	0.89	12.56	13.67
8-10-71	2.59	2.36	2.77	2.88						
4-09-75	2.78	2.37	2.59	2.48	7.11	7.03			12.48	11.88
5-09-75	2.87	2.52	2.70	2.71	7.50	7.67			13.07	12.90

Table B4.2: The errors of the ebb and flood volumes.

	Schaar		Hammen		Roompot		Geul		Total inlet	
date	ebb	flood	ebb	flood	ebb	flood	ebb	flood	ebb	flood
01-06-65					0%	1%	13%	0%	2%	0%
27-06-67									7%	11%
27-08-68	0%	2%	2%	6%	2%	4%	1%	17%	1%	1%
10-09-69	2%	4%	7%	2%	0%	3%	0%	1%	1%	2%
6-10-71		6%		1%		3%		22%		4%
7-10-71		7%		7%						
4-09-75	3%	6%	4%	8%	5%	8%			5%	8%

Table B4.3: The used tidal volumes in 10^8 m^3 to calculate the errors.

date	Schaar	Hammen	Roompot	Geul	Total inlet
01-06-65			13.35	2.51	25.76
02-06-65			13.42	2.65	26.13
27-06-67					22.58
28-06-67					20.49
27-08-68	3.94	4.97	12.38	1.33	22.63
28-08-68	3.99	5.19	12.23	1.49	22.91
10-09-69	3.89	5.10	11.79	1.40	21.96
11-09-69	3.79	4.87	11.63	1.41	21.60
07-10-71	5.08	5.94	14.07	1.23	26.22
08-10-71	4.95	5.65			
04-09-75	5.15	5.08	14.14		24.36
05-09-75	5.39	5.42	15.17		25.97

Table B4.4: The errors of the tidal volumes.

year	Schaar	Hammen	Roompot	Geul	Total inlet
1965			0%	5%	1%
1967					9%
1968	1%	4%	1%	11%	1%
1969	3%	5%	1%	1%	2%
1971	3%	5%			
1971	4%	10%			
1975	4%	6%	7%		6%

Appendix C: Tidal amplitude and tidal prism

- C1: The mean high and mean low water levels of the measurement locations**
- C2: The mean high and mean low water levels of the calculation sections**
- C3: The method used to calculate the mean high and mean low water levels of the calculation sections**
- C4: The calculated tidal prisms**
- C5: The errors**

Description

With the tidal amplitudes (MHW and MLW levels) of the measurement locations shown in appendix A1 the MHW and MLW levels of the calculation sections (figure **) are calculated. The combination of the measurement data to calculate the MHW and MLW levels of the calculation sections are shown in appendix A2. The calculated MHW and MLW levels of the calculation sections are shown in appendix A3. With these water levels the volume of the grid of 1968 between MHW and MLW is calculated using GIS. By adding up the calculated volumes of the sections the tidal prism is calculated. The results can be seen in appendix A4. The maximum error of the tidal prism is estimated with the estimated error of the grids. The maximum absolute error is calculated by multiplying the surface area at NAP +2 m with the error of the grids of 10 cm. The relative error is calculated by dividing the absolute error by the calculated grid volumes between MHW and MLW. The calculated errors can be seen in appendix A5.

Appendix C1: The mean high and mean low water levels of the measurement locations

- Figure C1.1: The water level measurement locations in the basin area.
- Figure C1.2: The MHW and MLW level of Roompot binnen, Burgsluis and Colijnsplaat.
- Figure C1.3: The tidal range of Roompot binnen, Burgsluis and Colijnsplaat.
- Table C1.1: The MHW and MLW levels and the tidal range of Roompot binnen, Burgsluis and Colijnsplaat.
- Figure C1.4: The MHW and MLW level of Kreekrak, Bergen op Zoom, Razernijpolder and Bergse Diepsluis.
- Figure C1.5: The tidal range of Kreekrak, Bergen op Zoom, Razernijpolder and Bergse Diepsluis.
- Table C1.2: The MHW and MLW levels and the tidal range of Kreekrak, Bergen op Zoom, Razernijpolder and Bergse Diepsluis.
- Figure C1.6: The MHW and MLW level of Zierikzee, Krammer, Bruinisse and Krammersluizen.
- Figure C1.7: The tidal range of Zierikzee, Krammer, Bruinisse and Krammersluizen.
- Table C1.3: The MHW and MLW levels and the tidal range of Zierikzee, Krammer, Bruinisse and Krammersluizen.
- Figure C1.8: The MHW and MLW level of Wemeldinge, Steenbergse Sas, Dintelsas and Rak Zuid.
- Figure C1.9: The tidal range of Wemeldinge, Steenbergse Sas, Dintelsas and Rak Zuid.
- Table C1.4: The MHW and MLW levels and the tidal range of Wemeldinge, Steenbergse Sas, Dintelsas and Rak Zuid.
- Figure C1.10: The MHW and MLW level of Stavenisse.
- Figure C1.11: The tidal range of Stavenisse.
- Table C1.5: The MHW and MLW levels and the tidal range of Stavenisse.
-

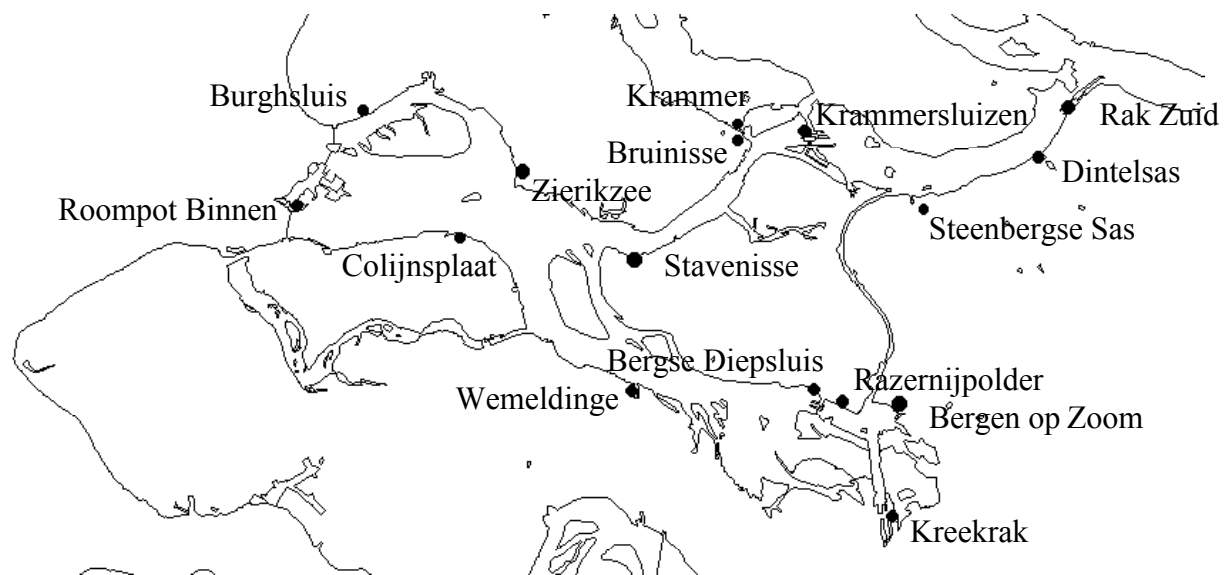


Figure C1.1: The water level measurement locations in the basin area.

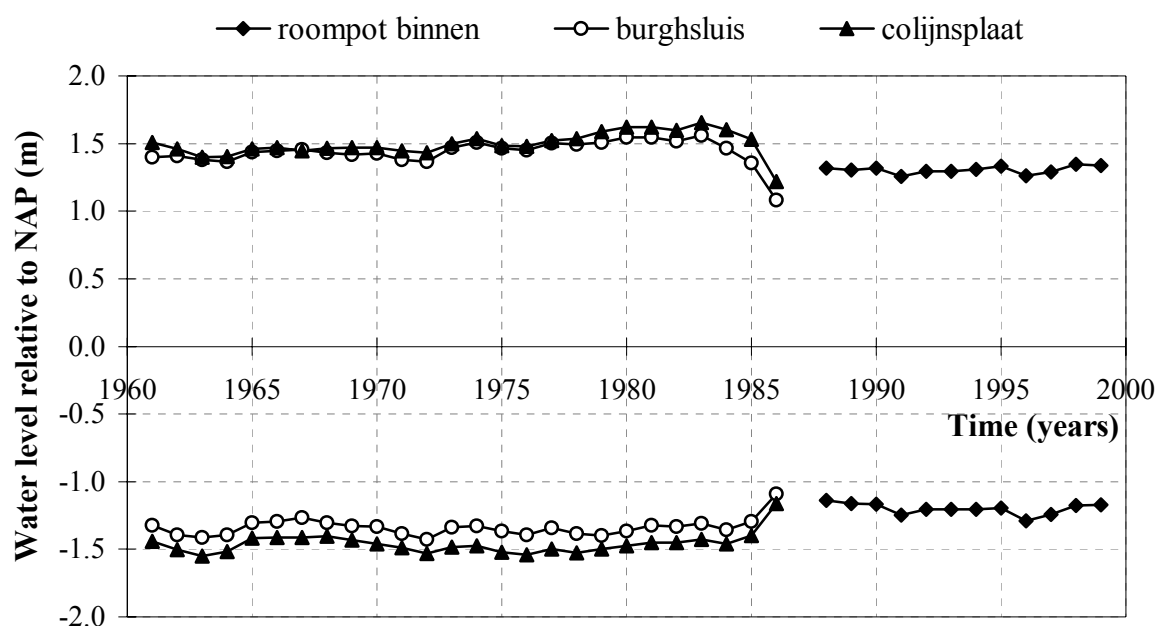


Figure C1.2: The MHW and MLW level of Roompot binnen, Burghsluis and Colijnsplaat.

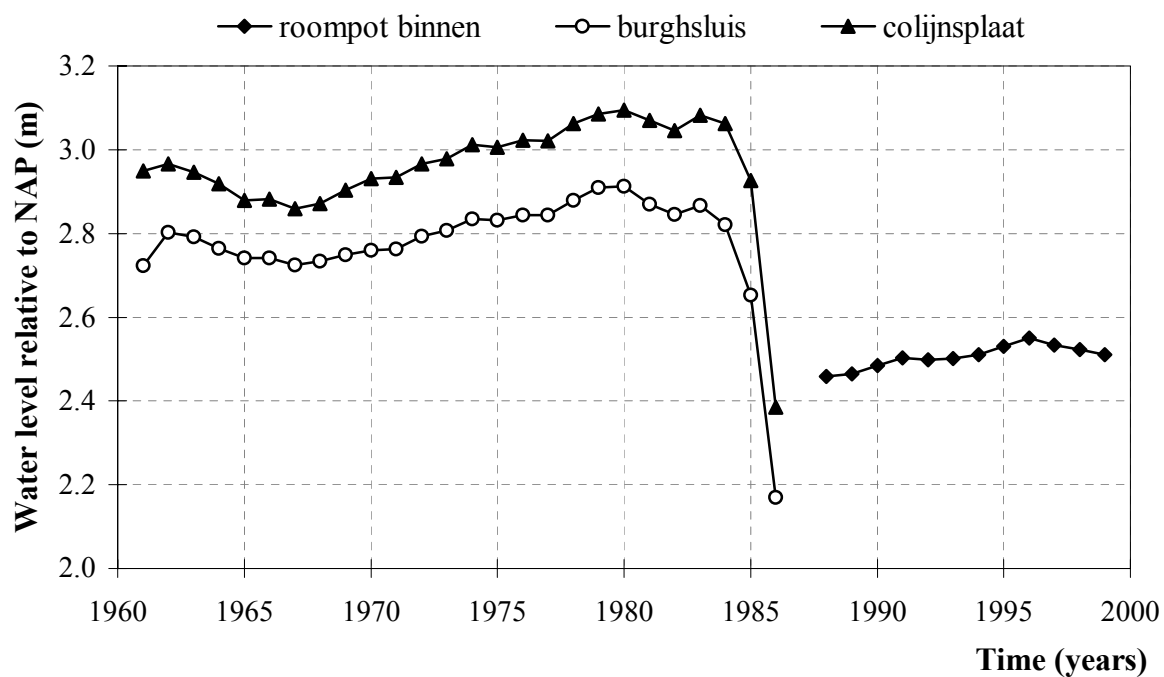


Figure C1.3: The tidal range of Roompot binnen, Burghsluis and Colijnsplaat.

Table C1.1: The MHW and MLW levels and the tidal range of Roompot binnen, Burgsluis and Colijnsplaat in meters relative to NAP.

	roompot binnen			burghsluis			colijnsplaat		
	MHW	MLW	tidal range	MHW	MLW	tidal range	MHW	MLW	tidal range
1961				1.40	-1.32	2.72	1.51	-1.44	2.95
1962				1.41	-1.39	2.80	1.46	-1.50	2.97
1963				1.38	-1.41	2.79	1.40	-1.55	2.95
1964				1.37	-1.40	2.76	1.40	-1.52	2.92
1965				1.44	-1.30	2.74	1.46	-1.42	2.88
1966				1.45	-1.30	2.74	1.47	-1.41	2.88
1967				1.46	-1.27	2.72	1.45	-1.41	2.86
1968				1.43	-1.30	2.73	1.47	-1.41	2.87
1969				1.42	-1.33	2.75	1.47	-1.43	2.90
1970				1.43	-1.33	2.76	1.47	-1.46	2.93
1971				1.38	-1.38	2.76	1.45	-1.49	2.93
1972				1.37	-1.43	2.79	1.43	-1.53	2.97
1973				1.47	-1.34	2.81	1.50	-1.48	2.98
1974				1.51	-1.33	2.84	1.54	-1.48	3.01
1975				1.46	-1.37	2.83	1.49	-1.52	3.01
1976				1.45	-1.39	2.84	1.48	-1.54	3.02
1977				1.50	-1.34	2.84	1.52	-1.50	3.02
1978				1.49	-1.39	2.88	1.54	-1.53	3.06
1979				1.51	-1.40	2.91	1.59	-1.50	3.09
1980				1.55	-1.37	2.91	1.62	-1.48	3.10
1981				1.55	-1.32	2.87	1.62	-1.45	3.07
1982				1.52	-1.33	2.85	1.60	-1.45	3.05
1983				1.56	-1.31	2.87	1.65	-1.43	3.08
1984				1.47	-1.35	2.82	1.60	-1.46	3.06
1985				1.36	-1.30	2.65	1.53	-1.40	2.93
1986				1.08	-1.09	2.17	1.22	-1.16	2.39
1987				measurement location removed			measurement location removed		
1988	1.32	-1.14	2.46						
1989	1.30	-1.16	2.46						
1990	1.32	-1.17	2.48						
1991	1.26	-1.25	2.50						
1992	1.29	-1.20	2.50						
1993	1.30	-1.21	2.50						
1994	1.31	-1.20	2.51						
1995	1.33	-1.20	2.53						
1996	1.26	-1.29	2.55						
1997	1.29	-1.24	2.53						
1998	1.35	-1.18	2.52						
1999	1.34	-1.17	2.51						

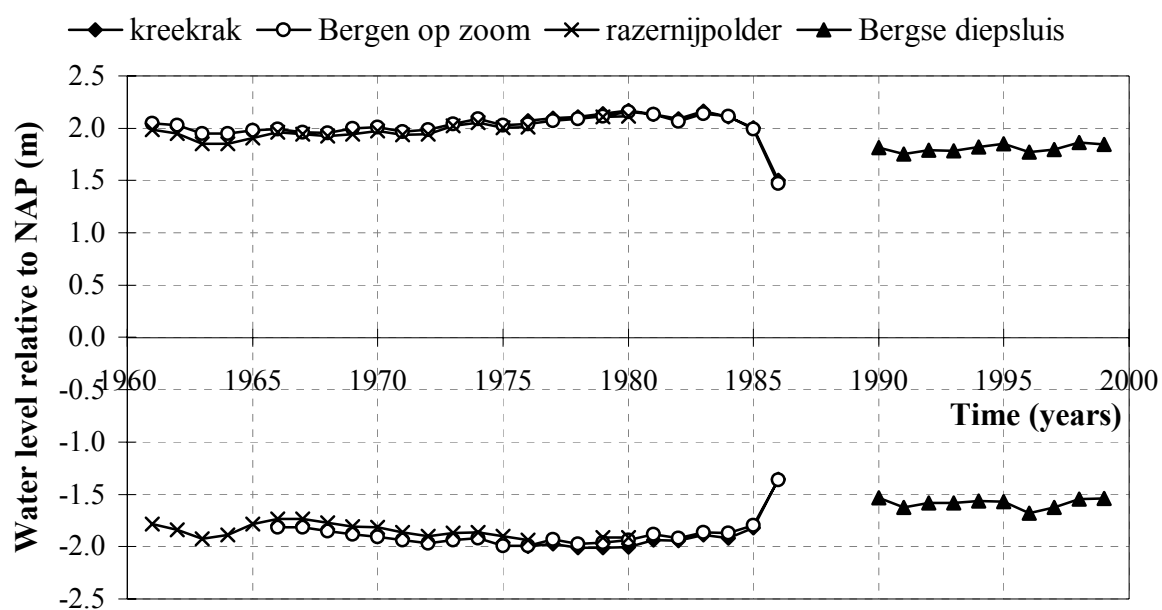


Figure C1.4: The MHW and MLW level of Kreekrak, Bergen op Zoom, Razernijpolder and Bergse Diepsluis.

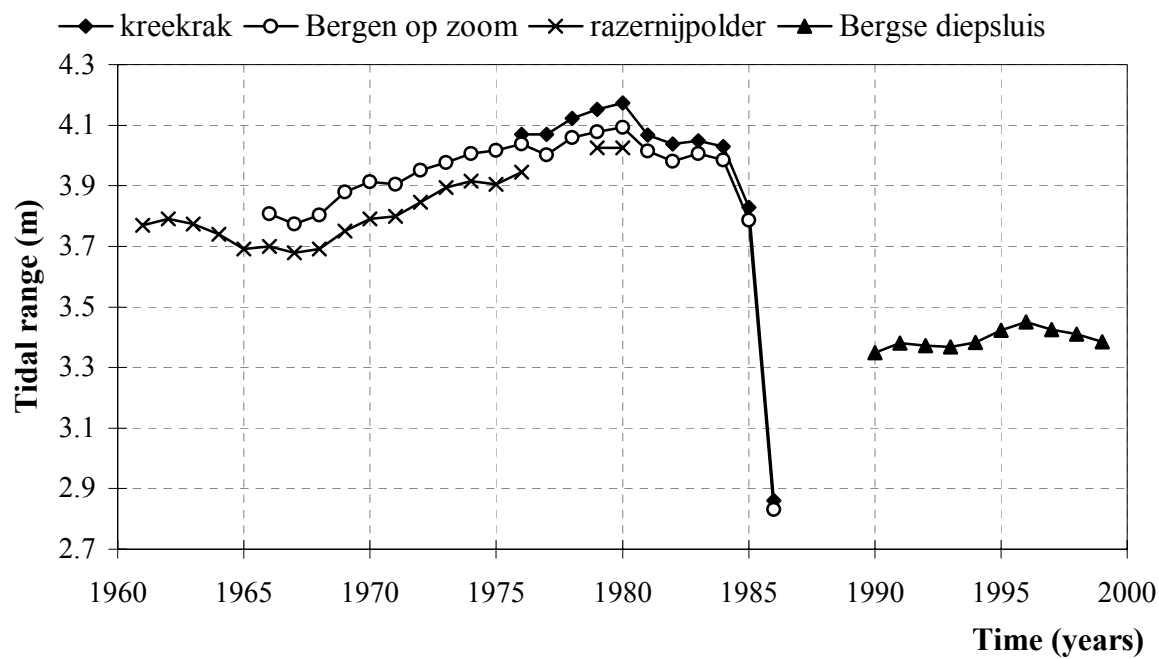


Figure C1.5: The tidal range of Kreekrak, Bergen op Zoom, Razernijpolder and Bergse Diepsluis.

Table C1.2: The MHW and MLW levels and the tidal range of Kreekrak, Bergen op Zoom, Razernijpolder and Bergse Diepsluis in meters relative to NAP.

	Kreekrak			Bergen op zoom			Razernijpolder			Bergse diepsluis		
	MHW	MLW	tidal range	MHW	MLW	tidal range	MHW	MLW	tidal range	MHW	MLW	tidal range
1961				2.05			1.99	-1.78	3.77			
1962				2.03			1.95	-1.84	3.79			
1963				1.95			1.85	-1.92	3.77			
1964				1.95			1.85	-1.89	3.74			
1965				1.98			1.91	-1.78	3.69			
1966				1.99	-1.81	3.81	1.96	-1.74	3.70			
1967				1.96	-1.81	3.77	1.94	-1.73	3.68			
1968				1.95	-1.85	3.80	1.92	-1.77	3.69			
1969				2.00	-1.88	3.88	1.94	-1.81	3.75			
1970				2.01	-1.90	3.91	1.98	-1.82	3.79			
1971				1.97	-1.94	3.91	1.94	-1.86	3.80			
1972				1.98	-1.97	3.95	1.94	-1.90	3.85			
1973				2.04	-1.94	3.98	2.02	-1.87	3.89			
1974				2.09	-1.92	4.01	2.05	-1.86	3.92			
1975				2.03	-1.99	4.02	2.00	-1.90	3.91			
1976	2.07	-2.00	4.07	2.04	-2.00	4.04	2.01	-1.93	3.94			
1977	2.10	-1.97	4.07	2.07	-1.93	4.00						
1978	2.11	-2.01	4.12	2.09	-1.97	4.06						
1979	2.14	-2.01	4.15	2.12	-1.96	4.08	2.11	-1.92	4.03			
1980	2.17	-2.00	4.17	2.16	-1.93	4.09	2.12	-1.91	4.03			
1981	2.13	-1.94	4.07	2.13	-1.88	4.02	measurement location removed					
1982	2.09	-1.94	4.04	2.06	-1.92	3.98						
1983	2.16	-1.89	4.05	2.14	-1.87	4.01						
1984	2.11	-1.92	4.03	2.12	-1.87	3.99						
1985	2.01	-1.82	3.83	1.99	-1.80	3.79						
1986	1.50	-1.36	2.86	1.47	-1.36	2.83						
1987	DNM placed			Oesterdam finished								
1988												
1989												
1990										1.82	-1.53	3.35
1991										1.75	-1.63	3.38
1992										1.79	-1.58	3.37
1993										1.79	-1.58	3.37
1994										1.82	-1.56	3.38
1995										1.85	-1.57	3.42
1996										1.77	-1.68	3.45
1997										1.80	-1.63	3.42
1998										1.87	-1.55	3.41
1999										1.85	-1.54	3.39

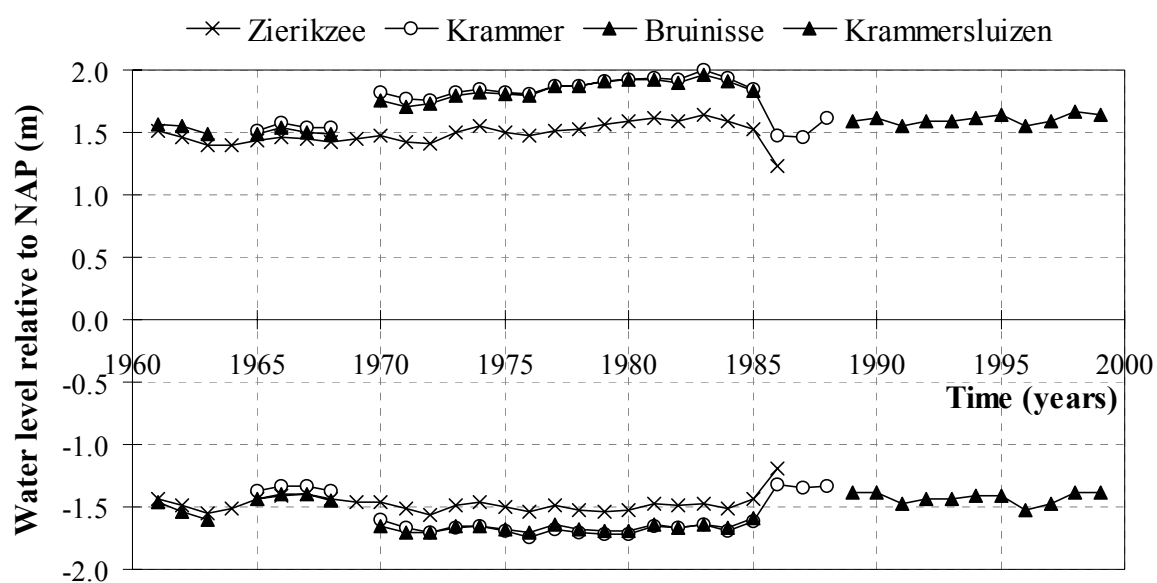


Figure C1.6: The MHW and MLW level of Zierikzee, Krammer, Bruinisse and Krammersluizen.

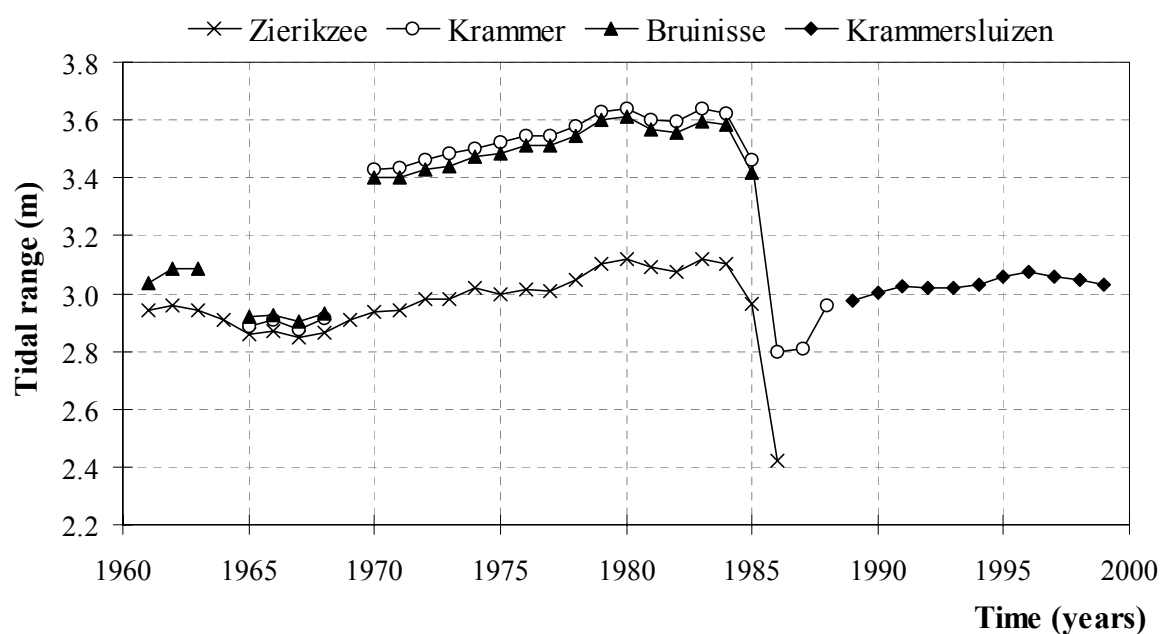


Figure C1.7: The tidal range of Zierikzee, Krammer, Bruinisse and Krammersluizen.

Table C1.3: The MHW and MLW levels and the tidal range of Zierikzee, Krammer, Bruinisse and Krammersluizen in meters relative to NAP.

	Zierikzee			Krammer			Bruinisse			Krammersluizen		
	MHW	MLW	tidal range	MHW	MLW	tidal range	MHW	MLW	tidal range	MHW	MLW	tidal range
1961	1.51	-1.43	2.94				1.57	-1.47	3.03			
1962	1.47	-1.49	2.96				1.55	-1.54	3.09			
1963	1.40	-1.55	2.94				1.48	-1.60	3.09			
1964	1.39	-1.51	2.91									
1965	1.43	-1.43	2.86	1.51	-1.37	2.89	1.49	-1.43	2.92			
1966	1.46	-1.41	2.87	1.57	-1.34	2.91	1.53	-1.39	2.93			
1967	1.45	-1.40	2.85	1.54	-1.33	2.87	1.50	-1.40	2.90			
1968	1.43	-1.44	2.86	1.54	-1.37	2.91	1.49	-1.45	2.93			
1969	1.45	-1.46	2.91									
1970	1.47	-1.47	2.94	1.83	-1.60	3.43	1.75	-1.65	3.40			
1971	1.42	-1.52	2.94	1.77	-1.66	3.43	1.70	-1.70	3.40			
1972	1.41	-1.57	2.98	1.76	-1.71	3.46	1.73	-1.70	3.43			
1973	1.50	-1.48	2.98	1.82	-1.66	3.48	1.79	-1.65	3.44			
1974	1.55	-1.47	3.02	1.85	-1.65	3.50	1.82	-1.65	3.47			
1975	1.50	-1.50	3.00	1.83	-1.70	3.52	1.81	-1.68	3.49			
1976	1.47	-1.54	3.01	1.80	-1.74	3.55	1.80	-1.71	3.51			
1977	1.52	-1.49	3.01	1.87	-1.67	3.55	1.87	-1.64	3.51			
1978	1.52	-1.53	3.05	1.87	-1.71	3.58	1.87	-1.68	3.55			
1979	1.57	-1.54	3.10	1.91	-1.72	3.63	1.90	-1.70	3.60			
1980	1.60	-1.53	3.12	1.93	-1.71	3.64	1.92	-1.69	3.61			
1981	1.62	-1.47	3.09	1.94	-1.66	3.60	1.93	-1.64	3.57			
1982	1.59	-1.49	3.08	1.93	-1.67	3.59	1.89	-1.66	3.56			
1983	1.65	-1.47	3.12	2.00	-1.64	3.64	1.96	-1.64	3.59			
1984	1.60	-1.51	3.10	1.93	-1.69	3.62	1.92	-1.67	3.58			
1985	1.52	-1.44	2.96	1.84	-1.62	3.46	1.84	-1.59	3.42			
1986	1.23	-1.19	2.42	1.48	-1.32	2.80	measurement location removed					
1987	measurement location removed			1.47	-1.34	2.81						
1988				1.62	-1.34	2.96						
1989				measurement location removed						1.59	-1.38	2.98
1990										1.62	-1.39	3.00
1991										1.55	-1.48	3.02
1992										1.59	-1.43	3.02
1993										1.59	-1.43	3.02
1994										1.62	-1.41	3.03
1995										1.65	-1.41	3.06
1996										1.56	-1.52	3.08
1997										1.59	-1.47	3.06
1998										1.66	-1.39	3.05
1999										1.65	-1.38	3.03

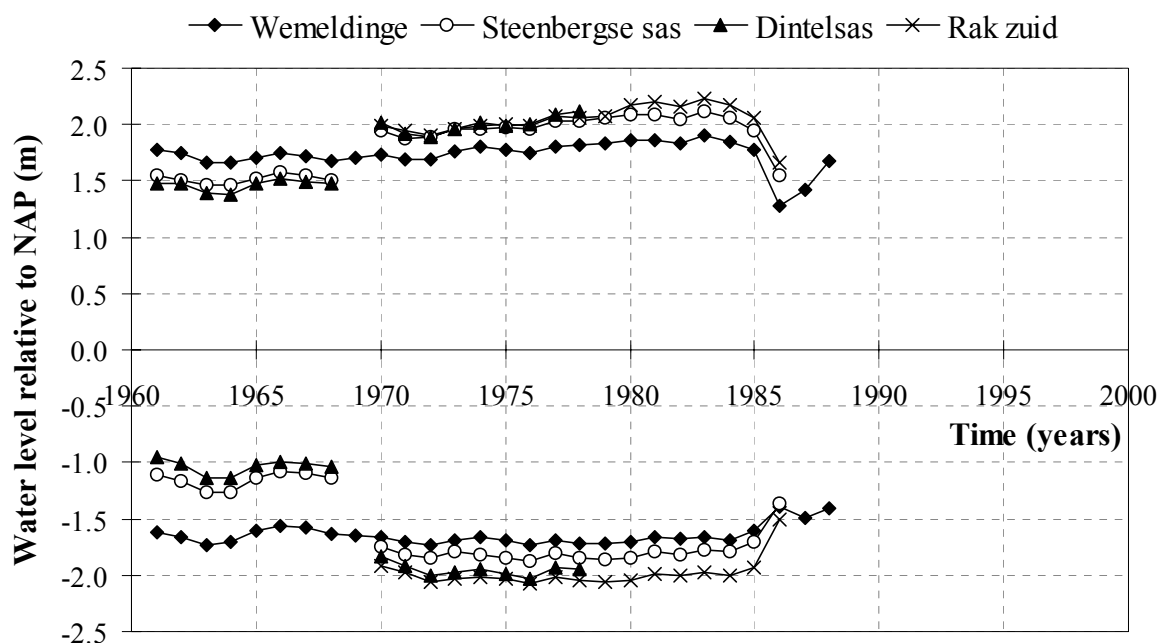


Figure C1.8: The MHW and MLW level of Wemeldinge, Steenbergse Sas, Dintelsas and Rak Zuid.

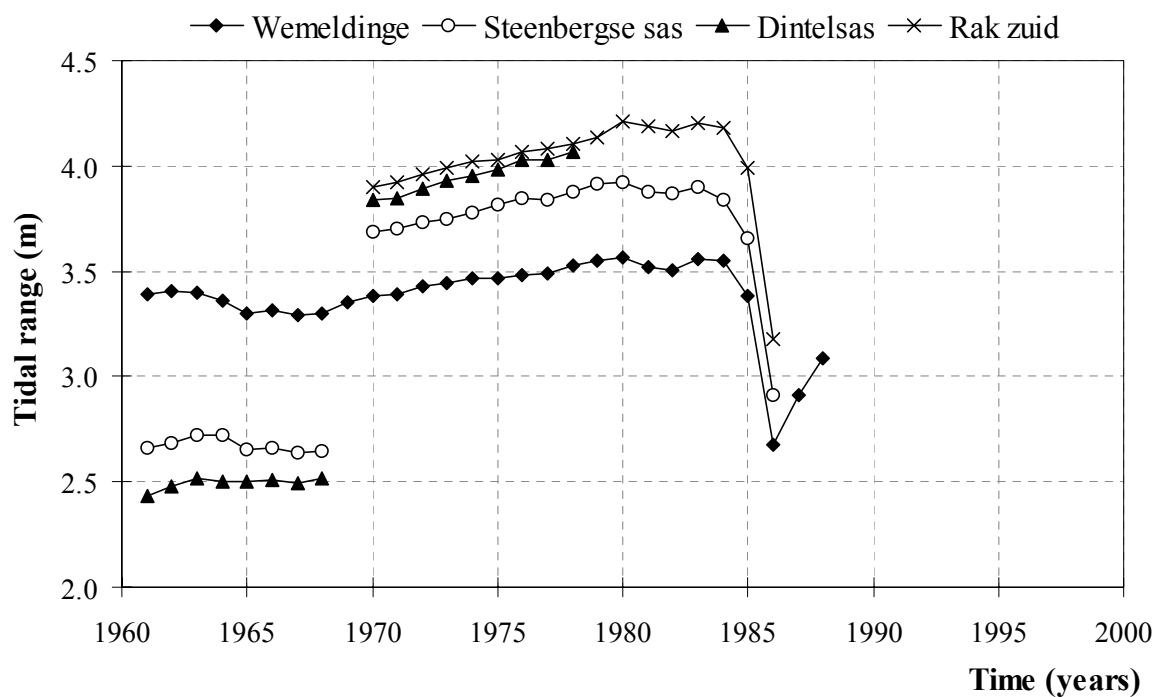


Figure C1.9: The tidal range of Wemeldinge, Steenbergse Sas, Dintelsas and Rak Zuid.

Table C1.4: The MHW and MLW levels and the tidal range of Wemeldinge, Steenbergse Sas, Dintelsas and Rak Zuid in meters relative to NAP.

[illegible]

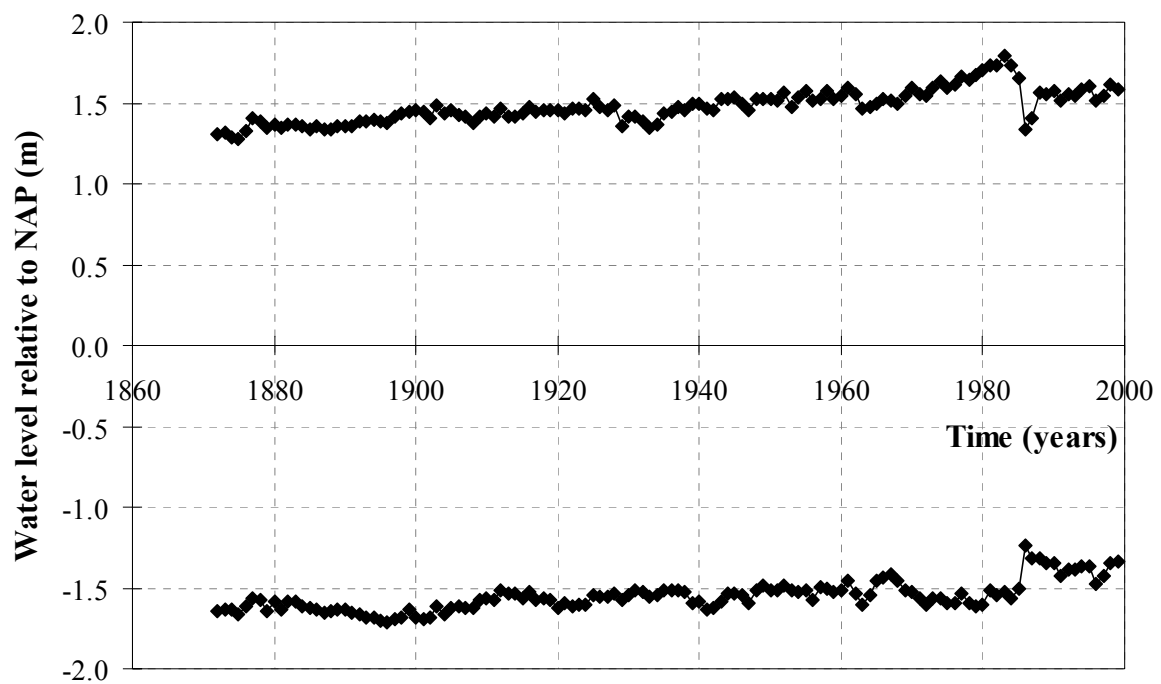


Figure C1.10: The MHW and MLW level of Stavenisse.

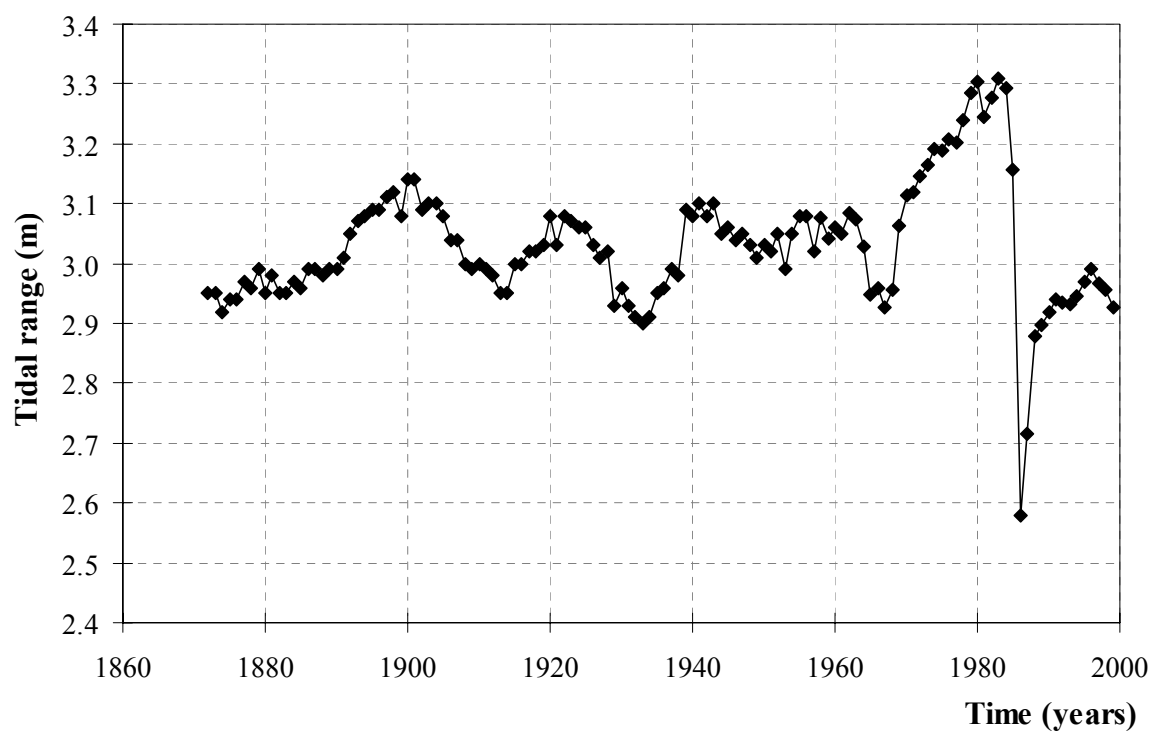


Figure C1.11: The tidal range of Stavenisse.

Table C1.5: The MHW and MLW levels and the tidal range of Stavenisse in meters relative to NAP.

	Stavenisse				Stavenisse				Stavenisse		
	MHW	MLW	tidal range		MHW	MLW	tidal range		MHW	MLW	tidal range
1872	1.31	-1.64	2.95	1915	1.44	-1.56	3.00	1958	1.57	-1.51	3.08
1873	1.32	-1.63	2.95	1916	1.48	-1.52	3.00	1959	1.52	-1.52	3.04
1874	1.29	-1.63	2.92	1917	1.45	-1.57	3.02	1960	1.54	-1.52	3.06
1875	1.28	-1.66	2.94	1918	1.46	-1.56	3.02	1961	1.59	-1.46	3.05
1876	1.33	-1.61	2.94	1919	1.46	-1.57	3.03	1962	1.55	-1.53	3.08
1877	1.41	-1.56	2.97	1920	1.46	-1.62	3.08	1963	1.47	-1.61	3.08
1878	1.39	-1.57	2.96	1921	1.44	-1.59	3.03	1964	1.48	-1.55	3.03
1879	1.35	-1.64	2.99	1922	1.47	-1.61	3.08	1965	1.49	-1.46	2.95
1880	1.37	-1.58	2.95	1923	1.47	-1.60	3.07	1966	1.53	-1.43	2.96
1881	1.35	-1.63	2.98	1924	1.46	-1.60	3.06	1967	1.52	-1.41	2.93
1882	1.37	-1.58	2.95	1925	1.52	-1.54	3.06	1968	1.50	-1.46	2.96
1883	1.37	-1.58	2.95	1926	1.48	-1.55	3.03	1969	1.55	-1.52	3.06
1884	1.36	-1.61	2.97	1927	1.46	-1.55	3.01	1970	1.59	-1.52	3.12
1885	1.34	-1.62	2.96	1928	1.49	-1.53	3.02	1971	1.55	-1.57	3.12
1886	1.36	-1.63	2.99	1929	1.36	-1.57	2.93	1972	1.54	-1.61	3.15
1887	1.34	-1.65	2.99	1930	1.42	-1.54	2.96	1973	1.60	-1.57	3.17
1888	1.34	-1.64	2.98	1931	1.42	-1.51	2.93	1974	1.63	-1.56	3.19
1889	1.36	-1.63	2.99	1932	1.39	-1.52	2.91	1975	1.60	-1.59	3.19
1890	1.36	-1.63	2.99	1933	1.35	-1.55	2.90	1976	1.61	-1.60	3.21
1891	1.36	-1.65	3.01	1934	1.37	-1.54	2.91	1977	1.66	-1.54	3.20
1892	1.39	-1.66	3.05	1935	1.44	-1.51	2.95	1978	1.64	-1.60	3.24
1893	1.39	-1.68	3.07	1936	1.45	-1.51	2.96	1979	1.67	-1.61	3.29
1894	1.40	-1.68	3.08	1937	1.48	-1.51	2.99	1980	1.70	-1.60	3.30
1895	1.39	-1.70	3.09	1938	1.46	-1.52	2.98	1981	1.74	-1.51	3.25
1896	1.38	-1.71	3.09	1939	1.50	-1.59	3.09	1982	1.73	-1.55	3.28
1897	1.42	-1.69	3.11	1940	1.50	-1.58	3.08	1983	1.79	-1.52	3.31
1898	1.44	-1.68	3.12	1941	1.47	-1.63	3.10	1984	1.73	-1.56	3.29
1899	1.45	-1.63	3.08	1942	1.46	-1.62	3.08	1985	1.66	-1.50	3.16
1900	1.46	-1.68	3.14	1943	1.52	-1.58	3.10	1986	1.34	-1.24	2.58
1901	1.45	-1.69	3.14	1944	1.52	-1.53	3.05	1987	1.40	-1.31	2.72
1902	1.41	-1.68	3.09	1945	1.53	-1.53	3.06	1988	1.57	-1.31	2.88
1903	1.49	-1.61	3.10	1946	1.50	-1.54	3.04	1989	1.55	-1.34	2.90
1904	1.44	-1.66	3.10	1947	1.46	-1.59	3.05	1990	1.58	-1.34	2.92
1905	1.46	-1.62	3.08	1948	1.52	-1.51	3.03	1991	1.51	-1.43	2.94
1906	1.43	-1.61	3.04	1949	1.52	-1.49	3.01	1992	1.55	-1.38	2.93
1907	1.42	-1.62	3.04	1950	1.52	-1.51	3.03	1993	1.55	-1.39	2.93
1908	1.38	-1.62	3.00	1951	1.51	-1.51	3.02	1994	1.58	-1.36	2.95
1909	1.42	-1.57	2.99	1952	1.56	-1.49	3.05	1995	1.61	-1.36	2.97
1910	1.44	-1.56	3.00	1953	1.48	-1.51	2.99	1996	1.52	-1.47	2.99
1911	1.42	-1.57	2.99	1954	1.53	-1.52	3.05	1997	1.55	-1.42	2.97
1912	1.47	-1.51	2.98	1955	1.57	-1.51	3.08	1998	1.61	-1.34	2.96
1913	1.42	-1.53	2.95	1956	1.51	-1.57	3.08	1999	1.59	-1.34	2.93
1914	1.42	-1.53	2.95	1957	1.53	-1.49	3.02				

Appendix C2: The calculation methods of the MHW and MLW levels of the calculation section.

Figure C2.1: The water level measurement locations in the basin area and the calculation sections.

The calculation methods of the MHW and MLW levels of the calculation sections.

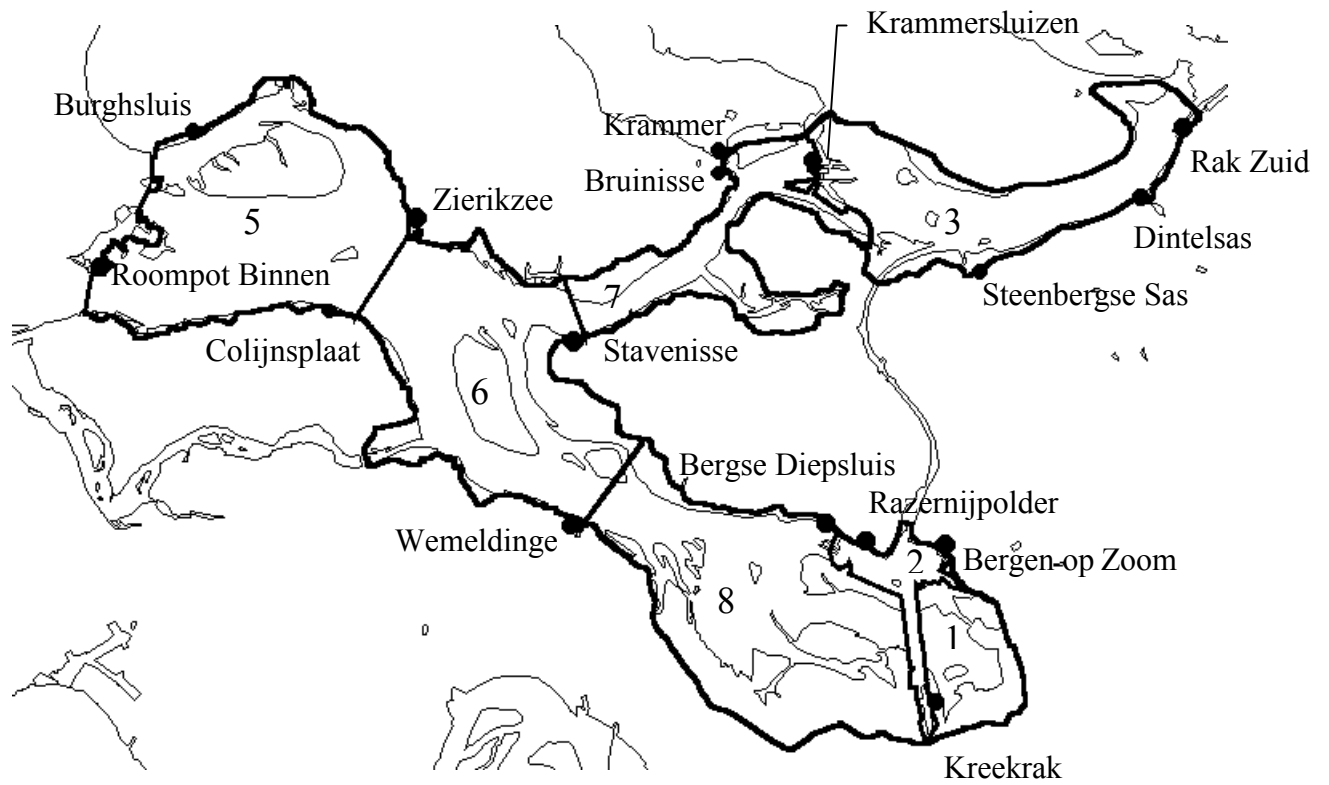


Figure C2.1: The water level measurement locations and the calculation sections.

Calculation methods of the water levels of the calculation sections with WL = water level and MHWL = mean high water level and MLWL = mean low water level.

Section 1:

1961 - 1986 MHWL = MHWL of Bergen op Zoom
 1966 - 1986 MLWL = MLWL of Bergen op Zoom

Section 2:

1961 - 1976 MHWL = (MHWL of Razernijpolder + MHWL of Bergen op Zoom)/2
 1966 - 1976 MLWL = (MLWL of Razernijpolder + MLWL of Bergen op Zoom)/2
 1977 - 1986 WL = WL of Bergen op Zoom

Section 3:

1961 - 1963 WL = ((WL of Bruinisse + WL of Steenbergse Sas)/2 + WL of Dintelsas)/2
 1964 WL = (WL of Steenbergse Sas + WL of Dintelsas)/2
 1965 - 1968 WL = (((WL of Krammer + WL of Bruinisse)/2 + WL of Steenbergse Sas)/2 + WL of Dintelsas)/2
 1970 - 1985 WL = (((WL of Krammer + WL of Bruinisse)/2 + WL of Steenbergse Sas)/2 + WL of Rak zuid)/2

Section 5:

1961 - 1986 WL = (WL of Burghsluis + (WL of Zierikzee + WL of Colijnsplaat)/2)/2
 1988 - 1999 WL = (WL of Roompot binnen + (WL of Roompot binnen + WL of Stavenisse)/2)/2

Section 6:

1961 - 1986 WL = ((WL of Zierikzee + WL of Colijnsplaat)/2 + WL of Wemeldinge)/2
 1988 WL = ((WL of Roompot binnen + WL of Stavenisse)/2 + WL of Wemeldinge)/2
 1990 - 1999 WL = ((WL of Roompot binnen + WL of Stavenisse)/2 + (WL of Stavenisse + Bergse diepsluis)/2)/2

Section 7:

1965 - 1985 WL = ((WL of Stavenisse + ((WL of Krammer + WL of Bruinisse)/2 + WL of Steenbergse Sas)/2)/2
 1989 - 1999 WL = (WL of Stavenisse + WL of Krammersluis)/2

Section 8:

1961 - 1975 WL = WL of Wemeldinge * 1/4 + WL of Razernijpolder * 3/4
 1976 - 1986 WL = WL of Wemeldinge * 1/3 + WL of Kreekrak * 2/3

Appendix C3: The MHW and MLW levels of the calculation section.

Figure C2.1: The MHW levels of the calculation sections.

Table C2.1: The MHW levels of the calculation sections.

Figure C2.2: The MLW levels of the calculation sections.

Table C2.2: The MLW levels of the calculation sections.

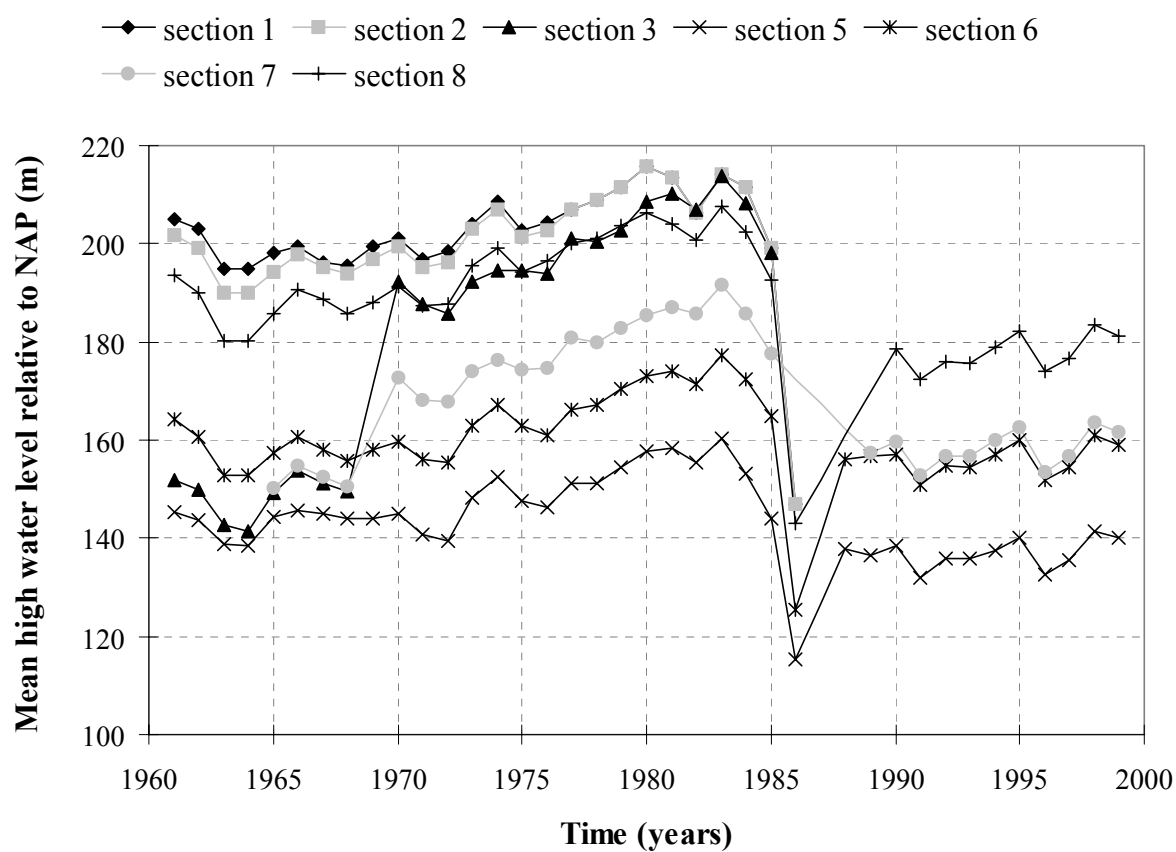


Figure C2.1: The MHW levels of the calculation sections.

Table C2.1: The MHW levels of the calculation sections in meters relative to NAP.

	Section 1	Section 2	Section 3	Section 5	Section 6	Section 7	Section 8
1961	2.05	2.02	1.52	1.45	1.64		1.94
1962	2.03	1.99	1.50	1.44	1.61		1.90
1963	1.95	1.90	1.43	1.39	1.53		1.80
1964	1.95	1.90	1.41	1.38	1.53		1.80
1965	1.98	1.94	1.49	1.44	1.57	1.50	1.86
1966	1.99	1.98	1.54	1.46	1.61	1.55	1.91
1967	1.96	1.95	1.51	1.45	1.58	1.53	1.89
1968	1.95	1.94	1.50	1.44	1.56	1.51	1.86
1969	2.00	1.97		1.44	1.58		1.88
1970	2.01	1.99	1.92	1.45	1.60	1.73	1.91
1971	1.97	1.95	1.88	1.41	1.56	1.68	1.88
1972	1.98	1.96	1.86	1.39	1.55	1.68	1.88
1973	2.04	2.03	1.92	1.48	1.63	1.74	1.96
1974	2.09	2.07	1.95	1.53	1.67	1.76	1.99
1975	2.03	2.01	1.94	1.48	1.63	1.75	1.94
1976	2.04	2.03	1.94	1.46	1.61	1.75	1.96
1977	2.07	2.07	2.01	1.51	1.66	1.81	2.00
1978	2.09	2.09	2.00	1.51	1.67	1.80	2.01
1979	2.12	2.12	2.03	1.54	1.70	1.83	2.04
1980	2.16	2.16	2.09	1.58	1.73	1.85	2.06
1981	2.13	2.13	2.10	1.58	1.74	1.87	2.04
1982	2.06	2.06	2.07	1.55	1.71	1.86	2.01
1983	2.14	2.14	2.14	1.60	1.77	1.92	2.08
1984	2.12	2.12	2.08	1.53	1.73	1.86	2.02
1985	1.99	1.99	1.98	1.44	1.65	1.78	1.93
1986	1.47	1.47		1.15	1.25		1.43
1987							
1988				1.38	1.56		
1989				1.36		1.57	
1990				1.38	1.57	1.60	1.79
1991				1.32	1.51	1.53	1.72
1992				1.36	1.55	1.57	1.76
1993				1.36	1.54	1.57	1.76
1994				1.38	1.57	1.60	1.79
1995				1.40	1.60	1.63	1.82
1996				1.33	1.52	1.54	1.74
1997				1.35	1.55	1.57	1.77
1998				1.41	1.61	1.64	1.83
1999				1.40	1.59	1.62	1.81

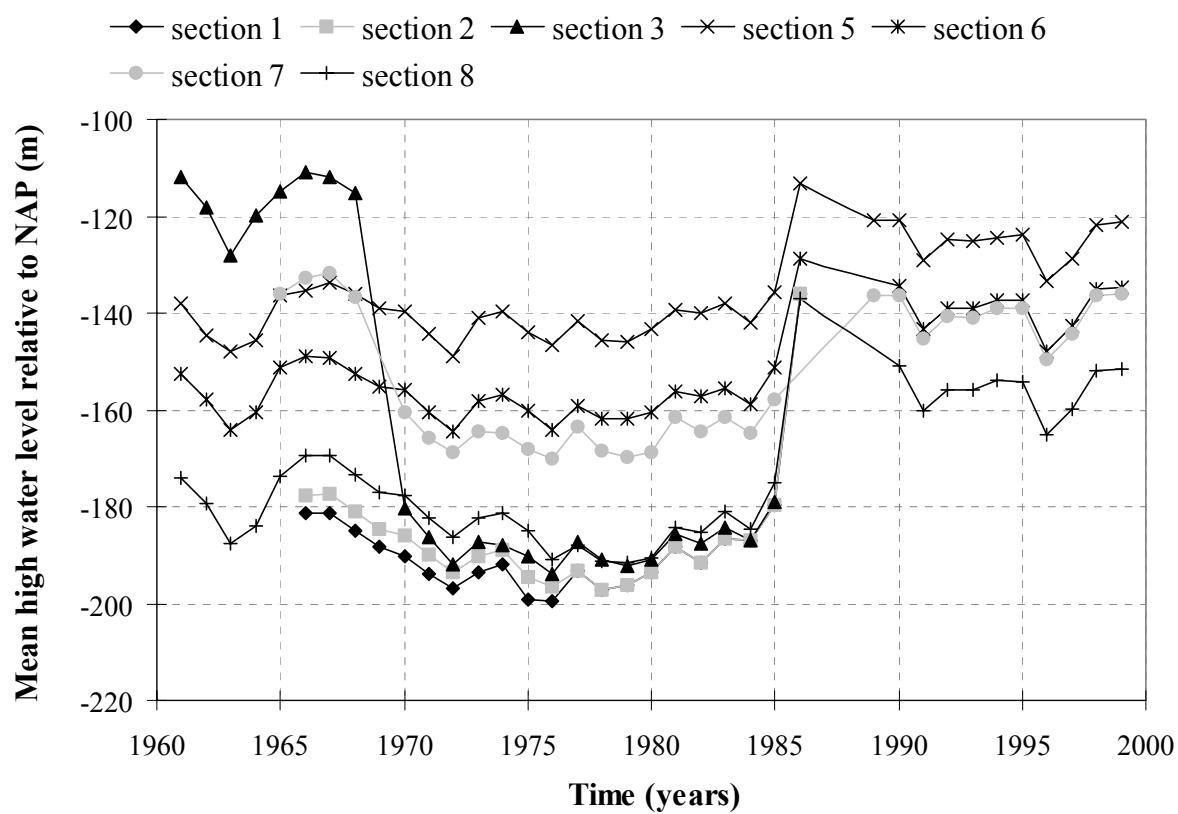


Figure C2.2: The MLW levels of the calculation sections.

Table C2.2: The MLW levels of the calculation sections in meters relative to NAP.

	Section 1	Section 2	Section 3	Section 5	Section 6	Section 7	Section 8
1961			-1.12	-1.38	-1.52		-1.74
1962			-1.18	-1.45	-1.58		-1.79
1963			-1.28	-1.48	-1.64		-1.88
1964			-1.20	-1.46	-1.61		-1.84
1965			-1.15	-1.36	-1.51	-1.36	-1.74
1966	-1.81	-1.78	-1.11	-1.35	-1.49	-1.33	-1.70
1967	-1.81	-1.77	-1.12	-1.34	-1.49	-1.32	-1.69
1968	-1.85	-1.81	-1.15	-1.36	-1.52	-1.37	-1.73
1969	-1.88	-1.85		-1.39	-1.55		-1.77
1970	-1.90	-1.86	-1.80	-1.40	-1.56	-1.61	-1.78
1971	-1.94	-1.90	-1.86	-1.44	-1.60	-1.66	-1.82
1972	-1.97	-1.94	-1.92	-1.49	-1.64	-1.69	-1.86
1973	-1.94	-1.90	-1.87	-1.41	-1.58	-1.64	-1.82
1974	-1.92	-1.89	-1.88	-1.40	-1.57	-1.65	-1.81
1975	-1.99	-1.95	-1.90	-1.44	-1.60	-1.68	-1.85
1976	-2.00	-1.96	-1.94	-1.47	-1.64	-1.70	-1.91
1977	-1.93	-1.93	-1.87	-1.42	-1.59	-1.63	-1.88
1978	-1.97	-1.97	-1.91	-1.46	-1.62	-1.68	-1.91
1979	-1.96	-1.96	-1.92	-1.46	-1.62	-1.70	-1.91
1980	-1.93	-1.93	-1.91	-1.43	-1.60	-1.69	-1.91
1981	-1.88	-1.88	-1.86	-1.39	-1.56	-1.62	-1.84
1982	-1.92	-1.92	-1.88	-1.40	-1.57	-1.64	-1.85
1983	-1.87	-1.87	-1.84	-1.38	-1.56	-1.61	-1.81
1984	-1.87	-1.87	-1.87	-1.42	-1.59	-1.65	-1.85
1985	-1.80	-1.80	-1.79	-1.36	-1.51	-1.58	-1.75
1986	-1.36	-1.36		-1.13	-1.29		-1.37
1987							
1988				-1.18	-1.32		
1989				-1.21		-1.36	
1990				-1.21	-1.35	-1.36	-1.51
1991				-1.29	-1.43	-1.45	-1.60
1992				-1.25	-1.39	-1.41	-1.56
1993				-1.25	-1.39	-1.41	-1.56
1994				-1.24	-1.37	-1.39	-1.54
1995				-1.24	-1.37	-1.39	-1.54
1996				-1.33	-1.48	-1.50	-1.65
1997				-1.29	-1.43	-1.44	-1.60
1998				-1.22	-1.35	-1.36	-1.52
1999				-1.21	-1.35	-1.36	-1.51

Appendix C4: The volumes between MHW and MLW of the calculation section and the tidal prism.

Figure C4.1: The volume between MHW and MLW of the calculation sections.

Figure C4.2: The tidal prism.

Table C4.1: The volume between MHW and MLW of the calculation sections and the tidal prism.

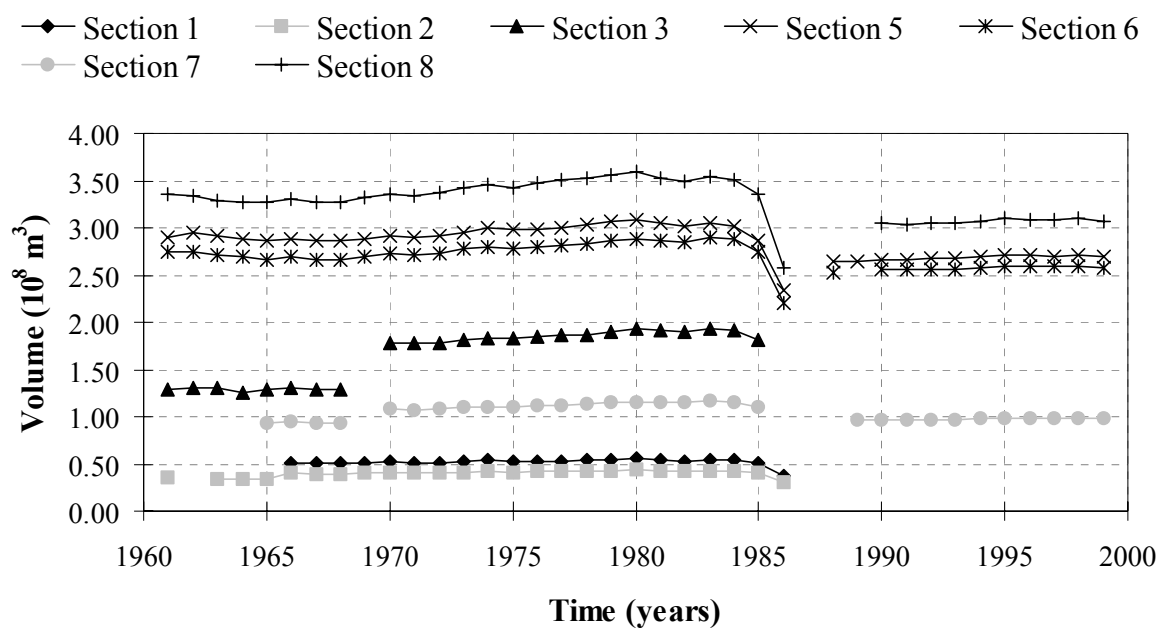


Figure C4.1: The volume between MHW and MLW of the calculation sections.

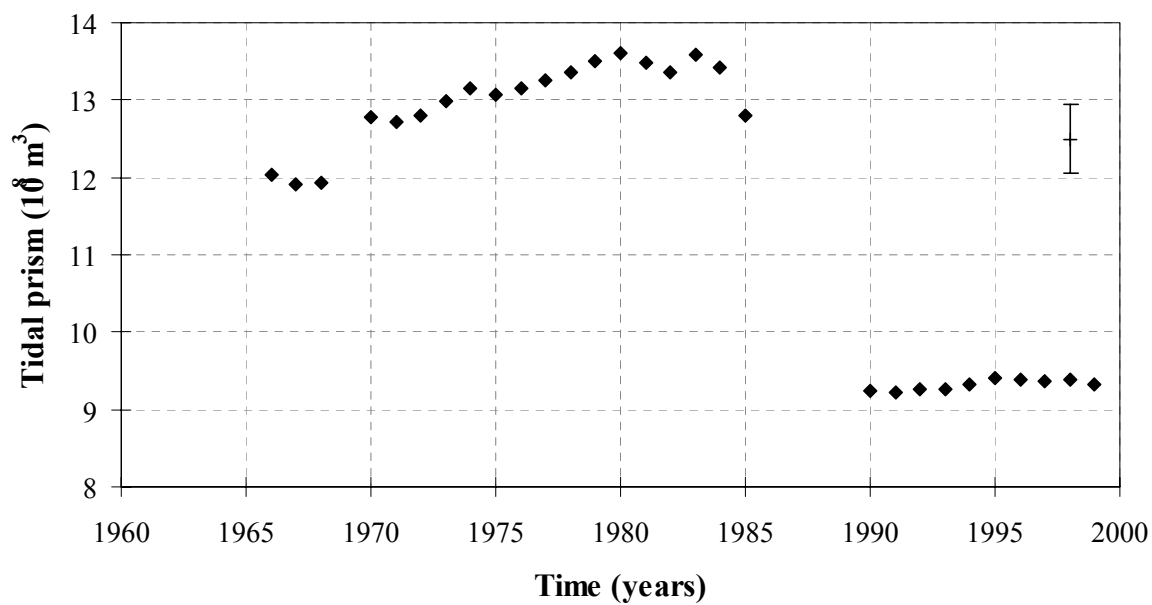


Figure C4.2: The tidal prism.

Table C4.1: The grid volumes between MHW and MLW of the calculation sections in 10^8 m^3 and the tidal prism in 10^8 m^3 .

	Section 1	Section 2	Section 3	Section 5	Section 6	Section 7	Section 8	Tidal prism
1961		0.35	1.30	2.89	2.74		3.36	
1962			1.31	2.94	2.75		3.35	
1963		0.34	1.30	2.91	2.71		3.29	
1964		0.34	1.26	2.88	2.69		3.27	
1965		0.34	1.29	2.86	2.67	0.93	3.27	
1966	0.51	0.40	1.30	2.88	2.69	0.94	3.30	12.03
1967	0.50	0.40	1.29	2.86	2.66	0.93	3.27	11.92
1968	0.50	0.40	1.29	2.86	2.66	0.93	3.27	11.92
1969	0.52	0.40		2.89	2.70		3.31	
1970	0.52	0.41	1.78	2.91	2.73	1.08	3.35	12.78
1971	0.51	0.40	1.78	2.90	2.72	1.07	3.34	12.72
1972	0.51	0.41	1.79	2.92	2.73	1.08	3.37	12.81
1973	0.53	0.41	1.81	2.95	2.77	1.09	3.43	12.99
1974	0.54	0.42	1.83	3.00	2.80	1.11	3.45	13.15
1975	0.52	0.41	1.83	2.98	2.78	1.11	3.42	13.06
1976	0.53	0.42	1.84	2.98	2.79	1.11	3.48	13.15
1977	0.53	0.42	1.86	2.99	2.81	1.12	3.51	13.25
1978	0.54	0.43	1.87	3.03	2.84	1.13	3.53	13.36
1979	0.54	0.43	1.89	3.06	2.87	1.15	3.57	13.51
1980	0.55	0.43	1.93	3.08	2.88	1.15	3.59	13.62
1981	0.54	0.43	1.92	3.04	2.87	1.15	3.52	13.47
1982	0.53	0.42	1.91	3.02	2.84	1.15	3.50	13.36
1983	0.55	0.43	1.94	3.06	2.89	1.17	3.55	13.58
1984	0.54	0.43	1.91	3.02	2.88	1.15	3.51	13.43
1985	0.51	0.40	1.82	2.86	2.74	1.10	3.35	12.79
1986	0.38	0.31		2.34	2.21		2.58	
1987								
1988				2.64	2.53			
1989				2.64	8.77	0.96		
1990				2.67	2.56	0.97	3.05	9.25
1991				2.67	2.55	0.96	3.04	9.22
1992				2.68	2.57	0.97	3.05	9.27
1993				2.68	2.56	0.97	3.05	9.26
1994				2.69	2.57	0.98	3.07	9.32
1995				2.71	2.60	0.99	3.10	9.41
1996				2.72	2.60	0.98	3.09	9.38
1997				2.70	2.59	0.98	3.09	9.36
1998				2.71	2.60	0.99	3.10	9.40
1999				2.69	2.58	0.98	3.07	9.32

Appendix C5: Errors

Table C5.1: The surface areas of the calculation sections and the total basin at NAP +2 m.

Table C5.2: The absolute error of the calculation sections and the tidal prism.

Table C5.3: The relative errors of the calculation sections and the tidal prism.

Table C5.1: The surface areas of the calculation sections and the total basin at NAP +2 m in 10⁶ m².

	Section 1	Section 2	Section 3	Section 5	Section 6	Section 7	Section 8	Total basin	Sections 5, 6, 7, and 8
1968	22.8	13.7	62.9	111.2	97.7	40.3	104.5	453.0	353.6

Table C5.2: The absolute error of the calculation sections and the tidal prisms in 10⁶ m³.

	Section 1	Section 2	Section 3	Section 5	Section 6	Section 7	Section 8	Tidal prism	Sections 5, 6, 7, and 8
Absolute error	2.3	1.4	6.3	11.1	9.8	4.0	10.4	45.3	35.4

Table C5.3: The relative errors of the calculation sections and the tidal prism.

	Section 1	Section 2	Section 3	Section 5	Section 6	Section 7	Section 8	Tidal prism
1961		3.92%	4.85%	3.84%	3.56%		3.11%	
1962		3.94%	4.82%	3.78%	3.55%		3.12%	
1963		4.05%	4.84%	3.82%	3.60%		3.17%	
1964		4.06%	4.99%	3.86%	3.62%		3.19%	
1965		4.04%	4.88%	3.88%	3.66%	4.34%	3.19%	
1966	4.46%	3.42%	4.82%	3.86%	3.63%	4.27%	3.16%	3.77%
1967	4.52%	3.46%	4.88%	3.89%	3.67%	4.32%	3.19%	3.80%
1968	4.53%	3.46%	4.86%	3.88%	3.67%	4.31%	3.20%	3.80%
1969	4.42%	3.41%		3.85%	3.61%		3.15%	
1970	4.40%	3.38%	3.52%	3.82%	3.58%	3.72%	3.12%	3.54%
1971	4.47%	3.41%	3.53%	3.83%	3.59%	3.76%	3.12%	3.56%
1972	4.44%	3.38%	3.52%	3.81%	3.57%	3.73%	3.10%	3.54%
1973	4.33%	3.32%	3.48%	3.77%	3.52%	3.68%	3.05%	3.49%
1974	4.25%	3.28%	3.44%	3.71%	3.48%	3.64%	3.02%	3.45%
1975	4.34%	3.32%	3.44%	3.73%	3.51%	3.64%	3.05%	3.47%
1976	4.32%	3.30%	3.41%	3.73%	3.50%	3.62%	3.00%	3.44%
1977	4.28%	3.26%	3.37%	3.71%	3.48%	3.58%	2.98%	3.42%
1978	4.24%	3.23%	3.36%	3.67%	3.44%	3.56%	2.96%	3.39%
1979	4.18%	3.20%	3.32%	3.63%	3.41%	3.51%	2.93%	
1980	4.12%	3.17%	3.26%	3.61%	3.39%	3.49%	2.91%	3.33%
1981	4.18%	3.22%	3.28%	3.65%	3.41%	3.51%	2.96%	3.36%
1982	4.30%	3.28%	3.30%	3.68%	3.44%	3.51%	2.99%	3.39%
1983	4.17%	3.21%	3.25%	3.63%	3.37%	3.45%	2.94%	3.34%
1984	4.20%	3.23%	3.30%	3.69%	3.40%	3.50%	2.98%	3.37%
1985	4.46%	3.40%	3.46%	3.88%	3.56%	3.66%	3.11%	3.54%
1986	6.02%	4.45%		4.75%	4.43%		4.05%	
1987								
1988				4.21%	3.86%			
1989				4.21%	1.11%	4.20%		
1990				4.17%	3.82%	4.14%	3.42%	3.82%
1991				4.17%	3.82%	4.19%	3.44%	3.83%
1992				4.15%	3.81%	4.15%	3.42%	3.81%
1993				4.15%	3.82%	4.15%	3.42%	3.82%
1994				4.13%	3.80%	4.12%	3.40%	3.80%
1995				4.10%	3.75%	4.06%	3.36%	3.76%
1996				4.09%	3.76%	4.13%	3.38%	3.77%
1997				4.11%	3.77%	4.13%	3.38%	3.78%
1998				4.11%	3.76%	4.07%	3.37%	3.76%
1999				4.14%	3.79%	4.11%	3.40%	3.79%

Appendix F: Outer tidal delta

F1: Bathymetric maps of the outer tidal delta

F2: Sedimentation and erosion maps of the outer tidal delta

F3: Calculated volumes of the outer tidal delta and the errors

F4: Sedimentation and erosion profiles over the vertical

Appendix F1: Bathymetric maps of the outer tidal delta

Bathymetric map of 1960

Bathymetric map of 1964

Bathymetric map of 1968

Bathymetric map of 1972

Bathymetric map of 1976

Bathymetric map of 1980

Bathymetric map of 1984

Bathymetric map of 1988

Bathymetric map of 1992

Bathymetric map of 1995

Bathymetric map of 1998

Appendix F2: Sedimentation and erosion maps of the outer tidal delta

Sedimentation and erosion map between 1960 and 1964.
Sedimentation and erosion map between 1964 and 1968.
Sedimentation and erosion map between 1968 and 1972.
Sedimentation and erosion map between 1972 and 1976.
Sedimentation and erosion map between 1976 and 1980.
Sedimentation and erosion map between 1980 and 1984.
Sedimentation and erosion map between 1984 and 1988.
Sedimentation and erosion map between 1988 and 1992.
Sedimentation and erosion map between 1992 and 1995.
Sedimentation and erosion map between 1995 and 1998.

Appendix F3: Calculated volumes of the outer tidal delta and the errors

Appendix F3.1: Calculations with linear sections

Appendix F3.2: Calculations with morphological calculation areas

Appendix F3.1: Calculations with linear sections

Figure F3.1.1: The linear calculation sections.

Table F3.1.1: The surface area of the calculation sections at NAP.

Table F3.1.2: The absolute error.

Table F3.1.3: The volumes of the calculation sections below NAP.

Table F3.1.4: The relative errors.

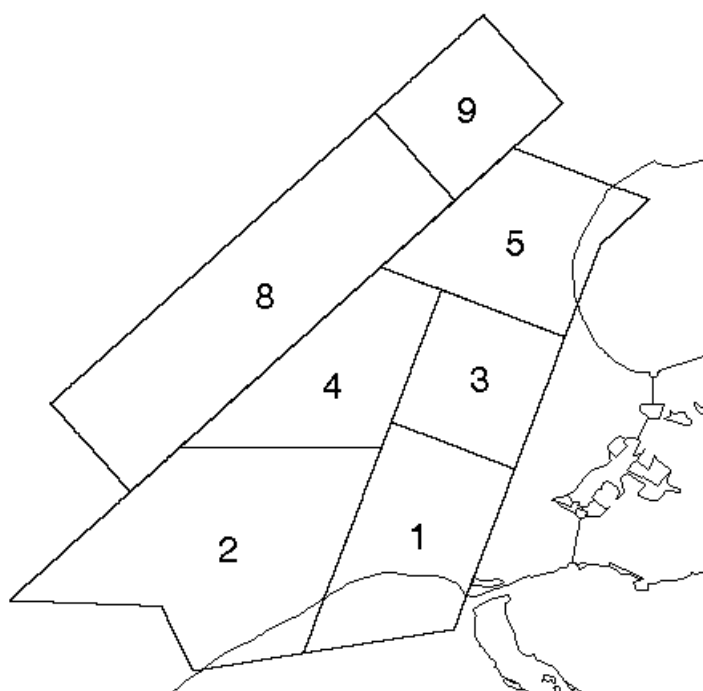


Figure F3.1.1: The linear calculation sections.

Table F3.1.1: The surface area of the calculation sections at NAP in 10^7 m^2 .

	Section 1	Section 2	Section 3	Section 4	Section 5	Section 8	Section 9	Total area
1964	2.76	6.59	2.68	3.41	3.30	7.39	2.48	28.61
1968	2.77	6.55	2.68	3.41	3.30	7.39	2.48	28.58
1976	2.76	6.58	2.68	3.41	3.30	7.42	2.48	28.63
1980	2.76	6.58	2.68	3.41	3.31	7.39	2.48	28.60
1984	2.75	6.58	2.68	3.41	3.32	7.40	2.48	28.62
1988	2.75	6.58	2.68	3.41	3.31	7.42	2.48	28.63
1992	2.75	6.57	2.68	3.41	3.31	7.17	2.48	28.37
1995	2.75	6.50	2.68	3.41	3.31	7.15	2.48	28.28
1998	2.73	6.57	2.68	3.41	3.30	7.15	2.48	28.32

Table F3.1.2: The absolute error in 10^7 m^3 .

	Section 1	Section 2	Section 3	Section 4	Section 5	Section 8	Section 9	Total area
1964	0.28	0.66	0.27	0.34	0.33	0.74	0.25	2.86
1968	0.28	0.66	0.27	0.34	0.33	0.74	0.25	2.86
1976	0.28	0.66	0.27	0.34	0.33	0.74	0.25	2.86
1980	0.28	0.66	0.27	0.34	0.33	0.74	0.25	2.86
1984	0.28	0.66	0.27	0.34	0.33	0.74	0.25	2.86
1988	0.27	0.66	0.27	0.34	0.33	0.74	0.25	2.86
1992	0.27	0.66	0.27	0.34	0.33	0.72	0.25	2.84
1995	0.27	0.65	0.27	0.34	0.33	0.71	0.25	2.83
1998	0.27	0.66	0.27	0.34	0.33	0.71	0.25	2.83

Table F3.1.3: The volumes of the calculation sections below NAP in 10^7 m^3 .

	Section 1	Section 2	Section 3	Section 4	Section 5	Section 8	Section 9	Total area
1964	31.30	68.15	25.18	35.03	13.75	70.83	22.85	267.09
1968	30.57	67.68	25.47	35.24	13.79	71.38	22.72	266.85
1976	29.78	66.74	26.07	34.90	13.42	69.59	22.48	262.98
1980	29.85	66.67	25.59	34.95	13.30	67.19	22.13	259.66
1984	29.95	67.64	25.98	35.66	13.69	68.73	22.69	264.35
1988	29.88	68.05	25.85	35.68	14.16	69.54	22.79	265.95
1992	29.61	67.99	25.52	35.44	14.56	64.54	22.71	260.36
1995	29.67	67.70	25.60	35.54	15.15	65.13	22.74	261.53
1998	29.76	68.50	25.72	35.53	15.15	65.62	22.78	263.06

Table F3.1.4: The relative errors.

	Section 1	Section 2	Section 3	Section 4	Section 5	Section 8	Section 9	Total area
1964	0.88%	0.97%	1.06%	0.97%	2.40%	1.04%	1.08%	1.07%
1968	0.91%	0.97%	1.05%	0.97%	2.40%	1.04%	1.09%	1.07%
1976	0.93%	0.99%	1.03%	0.98%	2.46%	1.07%	1.10%	1.09%
1980	0.92%	0.99%	1.05%	0.98%	2.49%	1.10%	1.12%	1.10%
1984	0.92%	0.97%	1.03%	0.96%	2.42%	1.08%	1.09%	1.08%
1988	0.92%	0.97%	1.03%	0.96%	2.34%	1.07%	1.09%	1.08%
1992	0.93%	0.97%	1.05%	0.96%	2.27%	1.11%	1.09%	1.09%
1995	0.93%	0.96%	1.05%	0.96%	2.19%	1.10%	1.09%	1.08%
1998	0.92%	0.96%	1.04%	0.96%	2.18%	1.09%	1.09%	1.08%

Appendix F3.2: Calculations with morphological calculation areas

Figure F3.2.1: The morphological calculation areas.

Table F3.2.1: The surface area of the calculation areas at NAP -3 m and NAP.

Table F3.2.2: The absolute error.

Table F3.2.3: The volumes of the calculation sections below NAP -3 m and NAP.

Table F3.2.4: The relative errors.

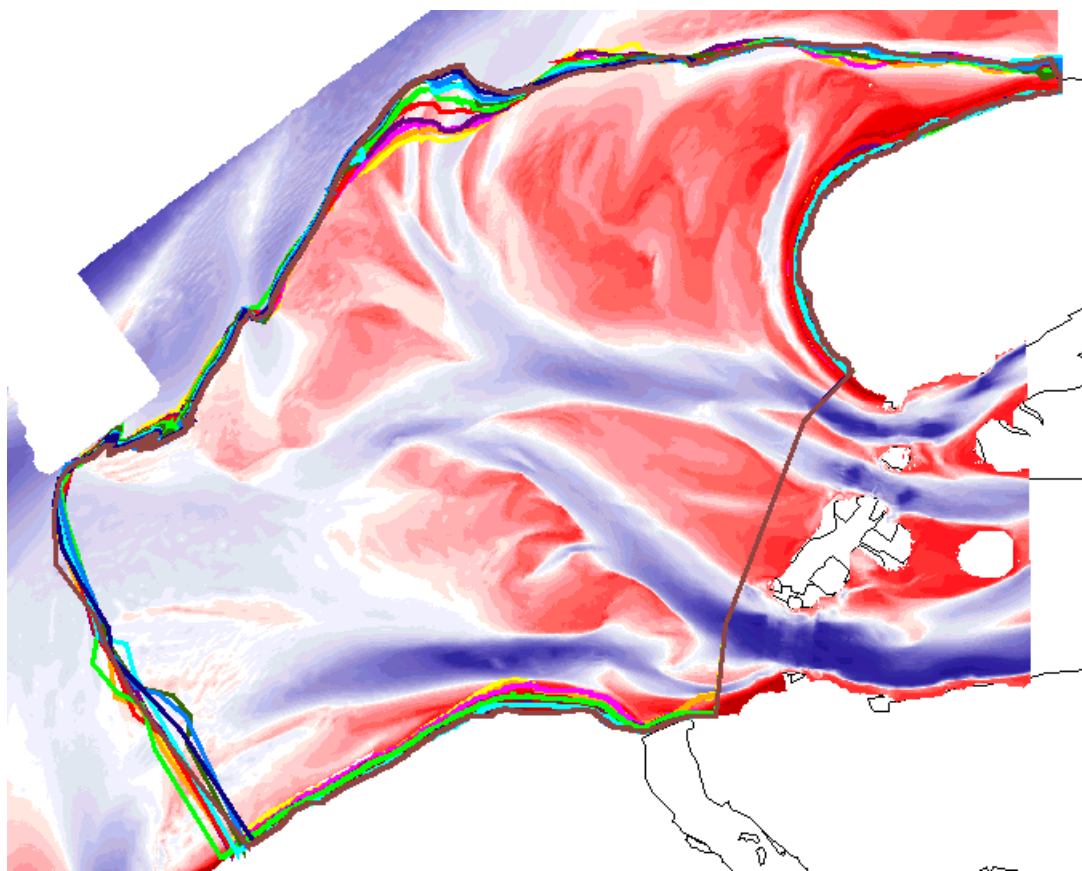
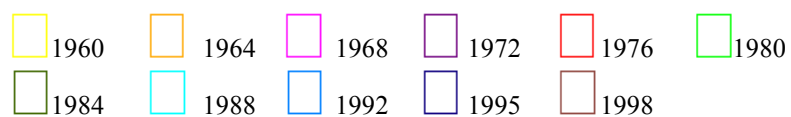


Figure F3.2.1: The morphological calculation areas.

Table F3.2.1: The surface area of the calculation areas at NAP -3 m and NAP in 10^8 m^2 .

	calculation area of 1960		calculation area of 1998		changing calculation areas in time	
	NAP -3.5 m	NAP +0 m	NAP -3.5 m	NAP +0 m	NAP -3.5 m	NAP +0 m
1960	2.57	2.81	2.61	2.86	2.57	2.81
1964	2.55	2.81	2.58	2.86	2.55	2.82
1968	2.57	2.81	2.60	2.86	2.57	2.82
1972	2.57	2.81	2.61	2.86	2.59	2.83
1976	2.54	2.81	2.58	2.85	2.57	2.84
1980	2.51	2.81	2.55	2.85	2.56	2.86
1984	2.52	2.81	2.56	2.86	2.53	2.82
1988	2.54	2.80	2.58	2.85	2.57	2.84
1992	2.55	2.80	2.59	2.85	2.56	2.82
1995	2.57	2.80	2.61	2.85	2.59	2.83
1998	2.58	2.80	2.62	2.85	2.62	2.85

Table F3.2.2: The absolute error in 10^8 m^3 .

	calculation area of 1960		calculation area of 1998		changing calculation areas in time	
	NAP -3.5 m	NAP +0 m	NAP -3.5 m	NAP +0 m	NAP -3.5 m	NAP +0 m
1960	0.26	0.28	0.26	0.29	0.26	0.28
1964	0.25	0.28	0.26	0.29	0.25	0.28
1968	0.26	0.28	0.26	0.29	0.26	0.28
1972	0.26	0.28	0.26	0.29	0.26	0.28
1976	0.25	0.28	0.26	0.29	0.26	0.28
1980	0.25	0.28	0.26	0.29	0.26	0.29
1984	0.25	0.28	0.26	0.29	0.25	0.28
1988	0.25	0.28	0.26	0.29	0.26	0.28
1992	0.26	0.28	0.26	0.29	0.26	0.28
1995	0.26	0.28	0.26	0.28	0.26	0.28
1998	0.26	0.28	0.26	0.28	0.26	0.28

Table F3.2.3: The volumes of the calculation sections below NAP -3 m and NAP in 10^8 m^3 .

	calculation area of 1960		calculation area of 1998		changing calculation areas in time	
	NAP -3.5 m	NAP +0 m	NAP -3.5 m	NAP +0 m	NAP -3.5 m	NAP +0 m
1960	15.54	25.18	16.06	25.85	15.54	25.18
1964	15.38	24.98	15.85	25.59	15.40	25.02
1968	15.38	24.99	15.84	25.59	15.39	25.01
1972	15.11	24.75	15.52	25.30	15.19	24.89
1976	15.04	24.65	15.37	25.13	15.13	24.83
1980	14.91	24.47	15.17	24.88	15.09	24.83
1984	15.31	24.86	15.52	25.22	15.29	24.88
1988	15.39	24.96	15.59	25.31	15.47	25.14
1992	15.27	24.85	15.46	25.19	15.22	24.82
1995	15.44	25.03	15.63	25.37	15.48	25.14
1998	15.53	25.12	15.69	25.42	15.71	25.44

Table F3.2.4: The relative errors.

	calculation area of 1960		calculation area of 1998		changing calculation areas in time	
	NAP -3.5 m	NAP +0 m	NAP -3.5 m	NAP +0 m	NAP -3.5 m	NAP +0 m
1960	1.65%	1.12%	1.63%	1.11%	1.65%	1.12%
1964	1.66%	1.13%	1.63%	1.12%	1.66%	1.13%
1968	1.67%	1.12%	1.64%	1.12%	1.67%	1.13%
1972	1.70%	1.13%	1.68%	1.13%	1.70%	1.14%
1976	1.69%	1.14%	1.68%	1.14%	1.70%	1.14%
1980	1.68%	1.15%	1.68%	1.15%	1.70%	1.15%
1984	1.65%	1.13%	1.65%	1.13%	1.65%	1.13%
1988	1.65%	1.12%	1.65%	1.13%	1.66%	1.13%
1992	1.67%	1.13%	1.68%	1.13%	1.68%	1.13%
1995	1.67%	1.12%	1.67%	1.12%	1.67%	1.12%
1998	1.66%	1.11%	1.67%	1.12%	1.67%	1.12%

Appendix F4: Vertical sedimentation and erosion profiles

Appendix F4.1: Vertical sedimentation and erosion profiles of the calculations with linear sections

Appendix F4.2: Vertical sedimentation and erosion profiles of the calculations with morphological calculation areas

Appendix F4.1: Vertical sedimentation and erosion profiles of the calculations with linear sections

Vertical sedimentation and erosion profile of section 1

Vertical sedimentation and erosion profile of section 2

Vertical sedimentation and erosion profile of section 3

Vertical sedimentation and erosion profile of section 4

Vertical sedimentation and erosion profile of section 5

Vertical sedimentation and erosion profile of section 8

Vertical sedimentation and erosion profile of section 9

Appendix F4.2: Vertical sedimentation and erosion profiles of the calculations with morphological calculation areas

Vertical sedimentation and erosion profile of the calculation area of 1960

Vertical sedimentation and erosion profile of the calculation area of 1998

Vertical sedimentation and erosion profile of the changing calculation areas in time

Appendix E: Basin

E1: Bathymetric maps of the basin

E2: Cross-section profiles of the basin

E3: Sedimentation and erosion maps of the basin

E4: Sedimentation and erosion profiles over the vertical

Appendix E1: Bathymetric maps of the basin

Bathymetric map of 1968

Bathymetric map of 1983

Bathymetric map of 1994

Appendix E2: Cross-section profiles of the basin

Figure E2.1: The locations of the cross-section.

Table E2.1: The coordinates of the cross-section locations.

Cross-section profile 0

Cross-section profile 1

Cross-section profile 2

Cross-section profile 3

Cross-section profile 4

Cross-section profile 5

Cross-section profile 6

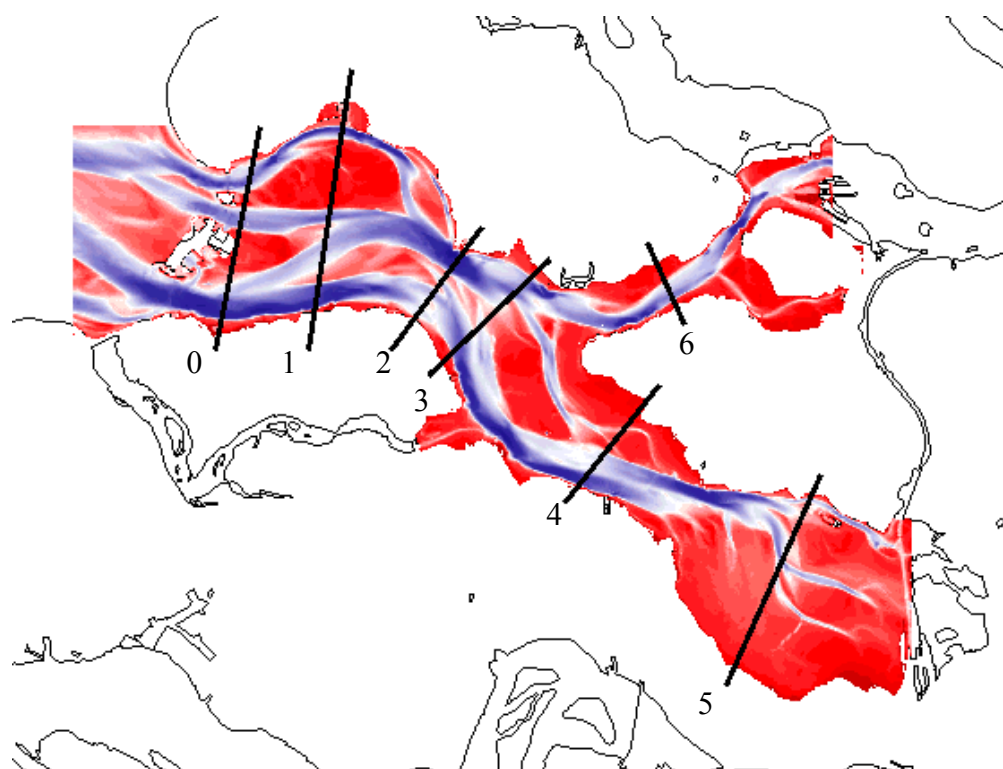


Figure E2.1: The locations of the cross-sections in the basin.

Table E2.1: The coordinates of the cross-section locations shown in figure E2.1.

	x	y
profiel 0	41530	412041
	39217	400702
profiel 1	46159	414934
	43961	400702
profiel 2	52740	407000
	48126	400702
profiel 3	56201	405339
	50000	399430
profiel 4	61664	398967
	56920	393066
profiel 5	69880	394454
	65020	383809
profiel 6	61085	406140
	62936	401975

Appendix E3: Sedimentation and erosion maps of the basin

Sedimentation and erosion map between 1968 and 1983.

Sedimentation and erosion map between 1983 and 1994.

Appendix E4: Vertical sedimentation and erosion profiles

Figure E4.1: The calculation sections of the basin

Vertical sedimentation and erosion profile of calculation section 5

Vertical sedimentation and erosion profile of calculation section 6

Vertical sedimentation and erosion profile of calculation section 7

Vertical sedimentation and erosion profile of calculation section 8

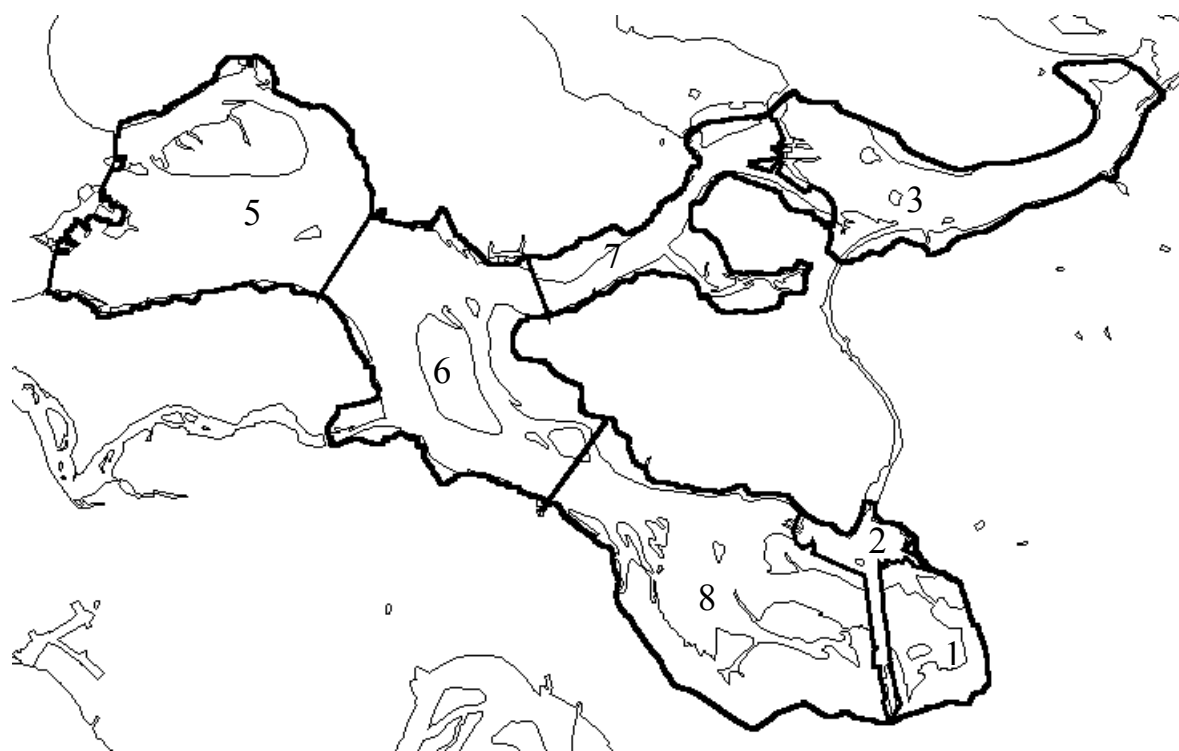


Figure E4.1: The calculation sections of the basin.

Appendix D: Inlet

Appendix D1: Cross-section profiles

Appendix D1: Cross-section profiles

Figure D1.1: The locations of the cross-sections

Cross-section profile of location 0.

Cross-section profile of location 1.

Cross-section profile of location 2.

Cross-section profile of location 3.

Cross-section profile of location 4.

Cross-section profile of location 5.

Cross-section profile of location 6.

Cross-section profile of location 7.

Cross-section profile of location 8.

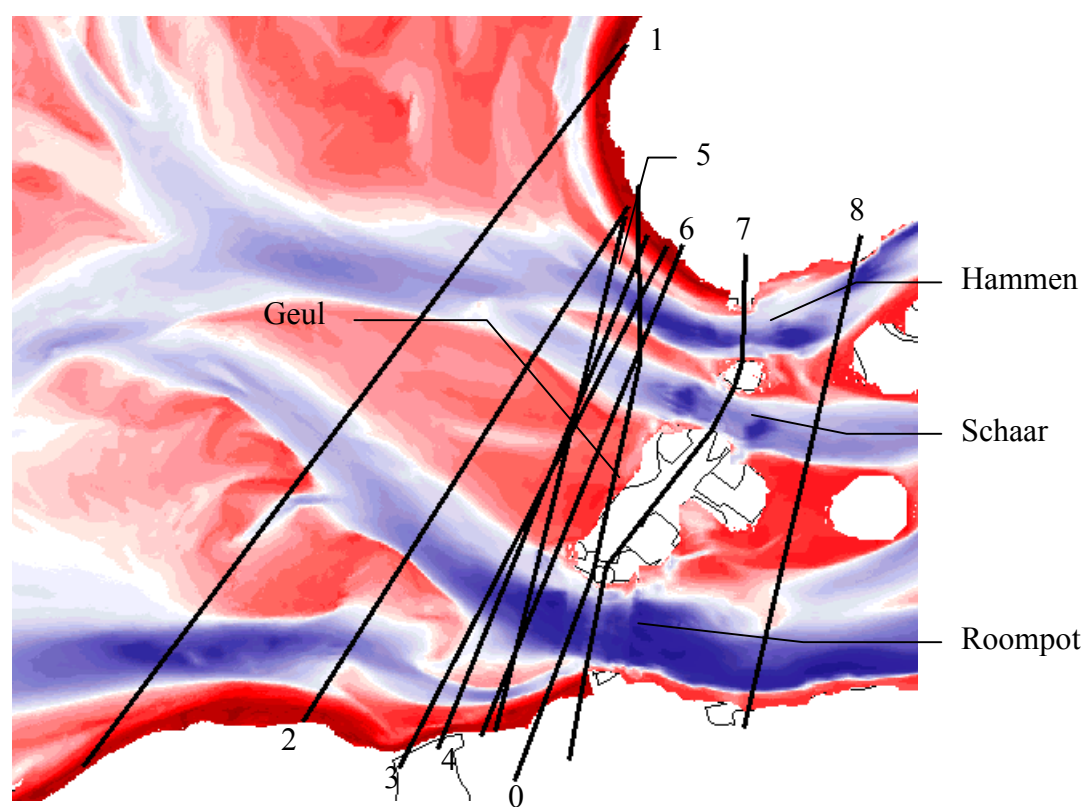


Figure D1.1: The locations of the cross-sections

